USGS
science for a changing world

Geology, Geochronology, Geochemistry, and Pb-Isotopic Compositions of Proterozoic Rocks, Poachie Region, West-Central Arizona—A Study of the East Boundary of the Proterozoic Mojave Crustal Province

U.S. Geological Survey Professional Paper 1639

U.S. Department of the Interior
U.S. Geological Survey

Availability of Publications of the U.S. Geological Survey

Order U.S. Geological Survey (USGS) publications from the offices listed below. Detailed ordering instructions, along with prices of the last offerings, are given in the current-year issues of the catalog "New Publications of the U.S. Geological Survey."

Books, Maps, and Other Publications

By Mail

Books, maps, and other publications are available by mail from—

USGS Information Services
Box 25286, Federal Center
Denver, CO 80225

Publications include Professional Papers, Bulletins, Water-Supply Papers, Techniques of Water-Resources Investigations, Circulars, Fact Sheets, publications of general interest, single copies of permanent USGS catalogs, and topographic and thematic maps.

Over the Counter

Books, maps, and other publications of the U.S. Geological Survey are available over the counter at the following USGS Earth Science Information Centers (ESIC's), all of which are authorized agents of the Superintendent of Documents.

- Anchorage, Alaska—Rm. 101, 4230 University Dr.
- Denver, Colorado—Bldg. 810, Federal Center
- Menlo Park, California—Rm. 3128, Bldg. 3, 345 Middlefield Rd.
- Reston, Virginia—Rm. 1C402, USGS National Center, 12201 Sunrise Valley Dr.
- Spokane, Washington—Rm. 135, U.S. Post Office Bldg., 904 West Riverside Ave.
- Washington, D.C.—Rm. 2650, Main Interior Bldg., 18th and C Sts., NW.

Maps only may be purchased over the counter at the following USGS office:

- Rolla, Missouri—1400 Independence Rd.

Electronically

Some USGS publications, including the catalog "New Publications of the U.S. Geological Survey," are also available electronically on the USGS's World Wide Web home page at **http://www.usgs.gov**

Preliminary Determination of Epicenters

Subscriptions to the periodical "Preliminary Determination of Epicenters" can be obtained only from the Superintendent of Documents. Check or money order must be payable to the Superintendent of Documents. Order by mail from—

Superintendent of Documents
Government Printing Office
Washington, D.C. 20402

Information Periodicals

Many Information Periodicals products are available through the systems or formats listed below:

Printed Products

Printed copies of the Minerals Yearbook and the Mineral Commodity Summaries can be ordered from the Superintendent of Documents, Government Printing Office (address above). Printed copies of Metal Industry Indicators and Mineral Industry Surveys can be ordered from the Center for Disease Control and Prevention, National Institute for Occupational Safety and Health, Pittsburgh Research Center, P.O. Box 18070, Pittsburgh, PA 15236-0070.

Mines FaxBack: Return Fax Service

1. Use the touch-tone handset attached to your fax machine's telephone jack. (ISDN [digital] telephones cannot be used with fax machines.)
2. Dial (703) 648-4999.
3. Listen to the menu options and punch in the number of your selection, using the touch-tone telephone.
4. After completing your selection, press the start button on your fax machine.

CD-ROM

A disc containing chapters of the Minerals Yearbook (1933–95), the Mineral Commodity Summaries (1995–97), a statistical compendium (1970–90), and other publications is updated three times a year and sold by the Superintendent of Documents, Government Printing Office (address above).

World Wide Web

Minerals information is available electronically at **http://minerals.er.usgs.gov/minerals/**

Subscription to the Catalog "New Publications of the U.S. Geological Survey"

Those wishing to be placed on a free subscription list for the catalog "New Publications of the U.S. Geological Survey" should write to—

U.S. Geological Survey
903 National Center
Reston, VA 20192

Geology, Geochronology, Geochemistry, and Pb-Isotopic Compositions of Proterozoic Rocks, Poachie Region, West-Central Arizona— A Study of the East Boundary of the Proterozoic Mojave Crustal Province

By **Bruce Bryant, J.L. Wooden, *and* L. David Nealey**

U.S. Geological Survey Professional Paper 1639

U.S. Department of the Interior
U.S. Geological Survey

U.S. Department of the Interior
Gale A. Norton, Secretary

U.S. Geological Survey
Charles G. Groat, Director

Version 1.0
First printing 2001

For sale by U.S. Geological Survey, Information Services
Box 25286, Federal Center
Denver, CO 80225

This publication is also available online at:
http://geology.cr.usgs.gov/pub/ppapers/p1639/

Library of Congress Cataloging-in-Publication Data

Bryant, Bruce, 1930–.
Geology, geochronology, geochemistry, and Pb-isotopic compositions of Proterozoic rocks, Poachie region, west-central Arizona : a study of the east boundary of the Proterozoic Mojave crustal province / by Bruce Bryant, J.L. Wooden, and L. David Nealey.
p. cm.—(U.S. Geological Survey professional paper ; 1639)
Includes bibliographical references.
1. Geology, Stratigraphic—Proterozoic. 2. Geology—Arizona—Poachie Range Region. I. Wooden, Joseph L. II. Nealey, L. David. III. Title IV. Series.
QE653.5.B79 2001
551.7'15'09791—dc21 2001016032

ISBN : 0-607-96229-1

Contents

Abstract 1
Introduction 2
Acknowledgments 3
Previous Work 3
Geology 4
Metamorphic Rocks 4
Plutonic Rocks 4
Early Proterozoic Plutonic Rocks 6
Mafic Gneiss 6
Coarse-Grained Granitic Rocks 6
Granite at Burro Creek 7
Fine-Grained Granite 7
Granite of Thorn Peak 8
Gneissic Tonalite 8
Granite, Aplite, Pegmatite, Mica Schist, and Gneiss 9
Middle Proterozoic Plutonic Rocks 9
Signal Granite 9
Mafic Granodiorite 10
Porphyritic Biotite Granite 10
Granite of Olea Ranch 10
Granite of Joshua Tree Parkway 12
Granite of Grayback Mountain 13
Diabase 14
Other Proterozoic Granitic Rocks 15
Geochronology 15
Metamorphic Rocks 15
Plutonic Rocks 16
Early Proterozoic Plutonic Rocks 16
Coarse-Grained Granitic Rocks 16
Granite of Thorn Peak 19
Gneissic Tonalite 20
Middle Proterozoic Plutonic Rocks 20
Signal Granite and Mafic Granodiorite 20
Granite of Olea Ranch 21
Granite of Joshua Tree Parkway and Granite of Grayback Mountain 21
Geochemistry 22
Analytical Methods 22
Metamorphic Rocks 23
Plutonic Rocks 23
Early Proterozoic Plutonic Rocks 23
Coarse-Grained Granitic Rocks 25
Granite of Thorn Peak 29
Gneissic Tonalite 29
Middle Proterozoic Plutonic Rocks 30
Signal Granite and Mafic Granodiorite 32
Granite of Olea Ranch 33
Granite of Joshua Tree Parkway 33
Granite of Grayback Mountain 33
Diabase 33

Comparison of Middle Proterozoic Plutonic Rocks with Early Proterozoic and Other Middle Proterozoic Plutonic Rocks in Region 34
Other Proterozoic Plutonic Rocks 42
Whole-Rock and Feldspar Pb-Isotopic Compositions 42
Summary and Interpretation 43
References Cited 44
Appendix. Location and Description of Chemically and (or) Isotopically Analyzed Samples 47

Figures

1. Map showing location of Proterozoic exposures and the Poachie region 2
2. Geologic map of Proterozoic rocks in the Poachie region 5
3. Photomicrograph of biotite-quartz-feldspar gneiss 6
4–8. Photographs showing:
4. Porphyritic granodiorite 7
5. Granite on Burro Creek 8
6. Granite of Thorn Peak 9
7. Diorite in gneissic tonalite unit 9
8. Signal Granite 11
9. Photomicrograph of mafic granodiorite 12
10. Photograph of fine-grained granite of Olea Ranch 13
11. Photographs of diabase 14
12–17. U-Pb concordia diagrams for:
12. Metamorphosed Dick Rhyolite 16
13. Coarse-grained granite 20
14. Granite at Burro Creek and granite of Thorn Peak 20
15. Gneissic tonalite 21
16. Signal Granite, mafic granodiorite, and granite of Olea Ranch 22
17. Granites of Joshua Tree Parkway and Grayback Mountain 22
18. SiO_2 vs. Na_2O+K_2O and Zr/TiO_2 vs. SiO_2 diagrams for Early Proterozoic metavolcanic rocks 23
19. Silica vs. alkalis diagrams for Early Proterozoic plutonic rocks 30
20. Chemical diagrams for Early Proterozoic rocks 31
21. Chondrite-normalized rare-earth element diagrams of Early Proterozoic rocks 32
22. Rb vs. Y+Nb discriminant diagram for Early Proterozoic granitic rocks 33
23. Silica vs. alkalis diagrams for Middle Proterozoic granitic rocks and diabase 38
24. Chemical diagrams for Middle Proterozoic granitic rocks and diabase 39
25. Chondrite-normalized rare-earth element diagrams of Middle Proterozoic granitic rocks 40
26. Chondrite-normalized rare-earth element diagram of diabase 41
27. Rb vs. Y+Nb discriminant diagram for Middle Proterozoic granitic rocks 41
28. Chemical diagrams showing comparison of Signal Granite with granite of Parker Dam and quartz monzodiorite of Bowmans Wash 41
29. Diagram showing Pb-isotopic whole-rock values for Early Proterozoic rocks of the Poachie region in regional context 42

Tables

1. U-Pb zircon ages of Proterozoic igneous rocks in the Poachie region 15
2. Analytical data and ages of zircons from the Proterozoic rocks of the Poachie region 17
3. Major-oxide and trace-element concentrations in some supracrustal rocks from the Bagdad metamorphic belt in the Poachie region and of one metasediment from cupola in the Signal batholith (sample 1166) 24
4. Major-oxide and trace-element concentrations in Early Proterozoic gabbro and coarse-grained granite from the Poachie region 26
5. Major-oxide and trace-element concentrations in Early Proterozoic fine-grained granite, granite of Thorn Peak, and gneissic tonalite and other Proterozoic granites of the Poachie region 28
6. Major-oxide and trace-element concentrations in Middle Proterozoic Signal Granite and associated mafic granodiorite 34
7. Major-oxide and trace-element concentrations in the Middle Proterozoic granites of Olea Range, of Joshua Tree Parkway, and of Grayback Mountain, and diabase 36
8. Pb-isotopic compositions of whole rocks and feldspars from the Poachie region 43

Geology, Geochronology, Geochemistry, and Pb-Isotopic Compositions of Proterozoic Rocks, Poachie Region, West-Central Arizona—A Study of the East Boundary of the Proterozoic Mojave Crustal Province

By **Bruce Bryant, J.L. Wooden, *and* L. David Nealey**

Abstract

Plutonic rocks dominate the Proterozoic geology of the Poachie region, west-central Arizona, and are about equally divided between Early and Middle Proterozoic age. Plutons are separated by screens and contain inclusions of amphibolite-facies metamorphosed sedimentary rocks and metamorphosed felsic and mafic volcanic rocks. Early Proterozoic plutonic rocks range in composition from gabbro to granite; gabbro forms only small intrusions, whereas granodiorite and granite form large plutons or plutonic suites. Middle Proterozoic plutonic rocks are mostly granite but range in composition from granite to mafic granodiorite. Textures of plutonic rocks of both ages range from coarse grained and porphyritic to fine grained. The Early Proterozoic rocks are variably foliated. The older ones commonly but not everywhere have a well-developed foliation; the younger ones have an apparently tectonic foliation only in local zones. The Middle Proterozoic rocks commonly have a well-developed flow foliation.

Ages of the Proterozoic stratified and plutonic rocks are generally well known. A principal belt of metamorphic rocks extends south from Bagdad across the area. Two samples of the Dick Rhyolite from the belt have a U-Pb zircon age of 1,720 Ma. Available data from other studies suggest that at least some of the metamorphic rocks in this belt are as old as 1,735 Ma. Ages determined for generally foliated plutonic rocks forming the east and central parts of the Poachie Range are 1,711±22 Ma for a gabbro and 1,706±4 Ma for gneissic diorite, a rock that cuts the gabbro. Granite at Burro Creek, possibly correlative with more silicic Early Proterozoic rocks in the Poachie Range, is 1,696±13 Ma. The mostly unfoliated granite of Thorn Peak has a U-Pb zircon age of 1,686±8 Ma. A pluton intruding the east side of the Bagdad metamorphic belt has a complex zircon population; the youngest grains are about 1,680 Ma and are interpreted to have formed during crystallization of the magma. The oldest xenocrystic grains are about 2,500 Ma and indicate the presence of Archean crustal material in the source region of the pluton.

Middle Proterozoic granitic rocks form several well-defined plutons. The Signal Granite forms a batholith in the Big Sandy River area. It and a closely associated mafic granodiorite have a U-Pb zircon age of 1,410±4 Ma. The Signal Granite is older than the granite of Parker Dam west of the Poachie region near the Colorado River, but the mafic granodiorite closely associated with the Signal Granite has an age similar to the quartz monzodiorite of Bowmans Wash, which is closely associated with the granite of Parker Dam. The granite of Olea Ranch is 1,418±2 Ma and is older than the well-studied Lawler Peak Granite 20 km to the north. The granites of Joshua Tree Parkway and of Grayback Mountain are 1,414.3±5 Ma, the same age within analytical uncertainty as the granite of Olea Ranch.

Chemically, Early Proterozoic plutonic rocks range from calcic to alkalic. No progression with time is noted, except that some of the gabbroic rocks, which are early in the sequence, are calcic. The rocks range from aluminous to peraluminous. Some peraluminous rocks have field relations and Pb-isotopic ratios indicating that metasedimentary rock was incorporated in their magmas. Middle Proterozoic plutonic rocks are alkali-calcic and peraluminous and metaluminous.

Whole-rock samples have high $^{207}Pb/^{204}Pb$ ratios characteristic of the Mojave crustal province, which both includes and extends west of the Poachie region. The highest ratios are from mica gneiss, tonalite adjacent to the gneiss, and the peraluminous granite of Thorn Peak. Older zircons from the tonalite were probably inherited from a fragmented crust that served as basement to the 1,700 Ma events, and the pluton was derived to a large extent by melting of that crust. Other Early Proterozoic plutonic rocks have Pb-isotopic ratios that in overall aspect are characteristic of the Mojave province; some $^{207}Pb/^{204}Pb$ ratios are lower but not as low as those in the Central Arizona crustal province to the east.

The Poachie region is underlain by rocks belonging to the Mojave crustal province, which has a complex history and includes some crustal material that formed in the Late Archean. Volcanic arcs and associated basins formed on this crust during west- or northwest-vergent subduction of oceanic crust at 1,730–1,710 Ma. This process involved addition of mantle material, extensive melting of the crust, magma generation and ascent, crustal deformation, and regional metamorphism at 1,710–1,690 Ma, about coeval with the Ivanpah orogeny in the Mojave crustal province. The basement on which the sedimentary and volcanic rocks were deposited was removed at the level presently exposed by this intense plutonic event. At 1,420–1,410 Ma crustal melting again occurred and large granitic plutons were emplaced. No regional deformation accompanied this event, although deformation in restricted zones did. At about 1,150 Ma, mantle-derived melts passively intruded along fracture systems to form sheets and dikes of diabase.

Introduction

Before this study Proterozoic rocks exposed in the Basin and Range–Colorado Plateau transition zone west of the Prescott-Jerome, Arizona, area had not been studied or mapped in detail except in a few small areas, such as at Bagdad. In connection with a study of the metamorphic and thermal relations between the basement rock of the Colorado Plateau and the core complexes of the Basin and Range, the senior author and several junior geologists mapped the Poachie Range at 1:50,000 (Bryant, 1992). This mapping was extended eastward to the edge of the Alamo Lake 1:100,000 quadrangle (Bryant, 1995), one of the quadrangles along the Pacific-Arizona Crustal Experiment (PACE) transect of the U.S. Geological Survey. The second author is conducting a regional study of the Pb-isotopic composition and U-Pb geochronology of the crust in the southwestern United States. His geochronologic results have greatly aided the geologic mapping, and our joint results have been presented only in preliminary and partial summary forms (Bryant and Wooden, 1986; Bryant and Wooden, 1991a and b). The third author joined us to help interpret the chemical data. Some of the whole-rock Pb-isotopic data have been summarized as part of a regional study (Wooden and DeWitt, 1991). Here we present the data and conclusions of our work in the Poachie Range and part of the Alamo Lake quadrangle to the east, here referred to as the Poachie region. Earlier U-Pb geochronologic investigations in this region have never been presented in a form usable by future workers; precise locations, analytical data, and isochron diagrams are essential tools to allow our work to be integrated with future studies.

The area of this study is in the Colorado Plateau transition zone about 150 km northwest of Phoenix (fig. 1). The Proterozoic rocks of the transition zone are divided into a number of north-northeast- to northeast-trending tectonic blocks (Karlstrom and Bowring, 1993). The Poachie region lies entirely within the Hualapai-Bagdad block of Karlstrom and Bowring (1988), or Hualapai block of Karlstrom and Bowring (1993) of the Yavapai province, or the northwest gneiss belt of P. Anderson (1989a). These blocks or belts are based on surface geology. The Yavapai geologic province is characterized overall by supracrustal volcanic sequences, whereas the Mojave geologic province to the west has supracrustal sequences rich in graywacke and quartzite and relatively poor in volcanic rock. Also, migmatite is common in the Mojave province and is lacking in the Yavapai province. The Mojave *geologic province* based on rock types should not be confused with the Mojave *crustal province* characterized by Pb-isotopic compositions of the rocks.

The Poachie region is in the eastern part of the Mojave crustal province (fig. 1), where rocks formed at about 1,700 Ma from an average source more radiogenic than the average crust model of Stacey and Kramers (1975): they have an average Th/U much greater than the crustal average and a depleted mantle model age (TDM) signature of 2,000–2,300 Ma. In contrast, the Central Arizona province to the east is characterized by a mid-ocean ridge basalt (MORB)-like mantle Pb-isotopic signature and an average Th/U less than the crustal average, crystallization ages of 1,760–1,690 Ma, and a TDM <1,800 Ma (Wooden and others, 1988; Wooden and Miller, 1990; Wooden and DeWitt, 1991; Bennett and De Paolo, 1987). The boundaries of the Nd-isotopic provinces are as yet poorly controlled due to the reconnaissance nature of the studies, but in this region the Pb-isotopic data are numerous, and the boundaries of the Mojave and Central Arizona Pb-isotopic provinces are quite accurately located. Also, the Poachie region spans the boundary between two types of Middle Proterozoic granite: metaluminous to the west and peraluminous to the east (J.L. Anderson, 1989).

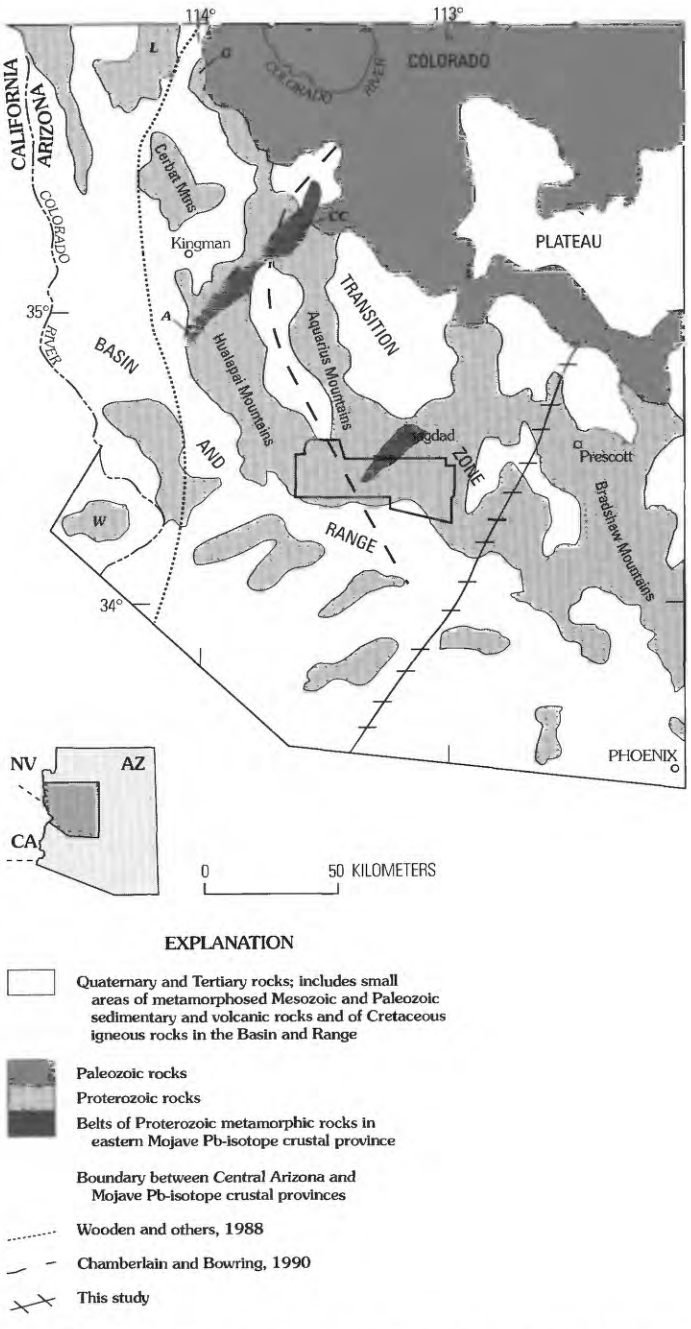

Figure 1. Location of exposures of Proterozoic rocks in west-central and northwest Arizona showing boundary between Mojave and Central Arizona crustal provinces based on earlier work and this study, and outline of Poachie region (fig. 2). A, Antler-Valentine metamorphic belt; W, Whipple Mountains; L, Lost Basin Range; G, Garnet Mountain; CC, Cottonwood Cliffs. Map generalized from Reynolds (1988).

Acknowledgments

This research was supported by the Geologic Framework, National Geologic Mapping, Pacific-Arizona Crustal Experiment (PACE), Basin and Range-Colorado Plateau Project (BARCO), and COGEOMAP programs of the U.S. Geological Survey. We thank Clay Conway, Ed DeWitt, and Phil Blacet for much advice on Proterozoic geology of the region. The conventional U-Pb zircon geochronology was accomplished with the assistance of Geoff Elliot, Cindy Brown, and Michele Hornberger. Single zircon analyses were determined on the SHRIMP ion probe at Australian National University. JLW thanks Dr. W. Compston for making these facilities available and Allen Nutman and colleagues for help with analytical determinations, data reduction, and making his visits to Canberra pleasant and productive. We appreciate the thoughtful reviews of this manuscript by Ed DeWitt and Dan Shawe.

Previous Work

Detailed geologic mapping of about 100 km^2 around Bagdad (Anderson and others, 1955) has furnished a benchmark for the geology of this part of the transition zone (fig. 1). The Bagdad area is dominated by a supracrustal sequence of metavolcanic and metasedimentary rocks, and it contains a variety of Proterozoic plutonic rocks. Conway and others (1986) extended that mapping 4 km southwest along the Bagdad metamorphic belt (fig. 1). Outside the Bagdad area reconnaissance mapping by Wilson and others (1969) divided the Proterozoic rocks into schist, gneiss, and granite. Immediately to the west detailed mapping by Lucchitta and Suneson (1982, 1994) contributed further to knowledge of the Proterozoic geology. The Geologic Map of Arizona (Reynolds, 1988) incorporates the published and unpublished mapping through 1986, including that in the Poachie Range (Bryant, 1992).

Early geochronologic studies of rocks from the region using K-Ar and Rb-Sr methods produced a variety of results (Aldrich and others, 1957; Wasserberg and Lanphere, 1965; Shafiqullah and others, 1980). These early data were of reconnaissance nature and were made before we knew about the complex thermal history of the region (Bryant and others, 1991). The U-Pb isotopic system has proven much more useful than the K-Ar and Rb-Sr systems for determining crystallization ages for older plutonic or metavolcanic rocks or rocks with complex thermal histories. The first such determinations were made for rocks from the Bagdad area as part of pioneering regional geochronological studies by Silver (1968). Recent references to these data subtract 1–2 percent, depending on the ratios used (Reynolds and others, 1986), or 25 m.y. (Conway and others, 1986), in order to make all the data consistent with presently accepted decay constants. The only zircon date from the Bagdad area for which the exact location and analytical data have been published is 1,411±3 Ma from the Lawler Peak Granite (Silver and others, 1980).

Ages of Proterozoic rocks elsewhere in central and western Arizona northwest and northeast of the Poachie region have been published by several workers. In the Prescott-Jerome region, about 50 km to the east, metamorphic rocks are about 1,760 to 1,720 Ma, and plutonic rocks that intrude them range from 1,750 to 1,700 Ma (Anderson and others, 1971; Karlstrom and others, 1987; Karlstrom and Bowring, 1993). In the northeast-trending belt of metamorphic rocks known as the Antler-Valentine belt (fig. 1), located 60 km northwest to 100 km north of the Poachie region, Chamberlain and Bowring (1990) obtained data that led them to revise the boundary between the Mojave and Central Arizona Pb-isotopic provinces of Wooden and others (1988) and to place it 50–100 km farther east (fig. 1). East of their boundary, at Cottonwood Cliffs at the northeast end of exposures of the Antler-Valentine belt, the metamorphic rocks are older than 1,730 Ma and are intruded by 1,730- and 1,710-Ma granites. The younger granite is interpreted to be late-kinematic in relation to the major regional deformation and metamorphism (Chamberlain and Bowring, 1990). Rocks west of the boundary, in the Hualapai Mountains and in the Lost Basin Range–Garnet Mountain area, show complex U-Pb zircon systematics that indicate an inherited 2.3-1.8 Ga zircon component. These rocks also have higher $^{207}Pb/^{204}Pb$ ratios relative to $^{206}Pb/^{204}Pb$ ratios than rocks to the east. The metamorphic rocks are interpreted to be about 1.73 Ga and are intruded by plutonic rocks dated as about 1.70 Ga. Chamberlain and Bowring (1990) projected the boundary between the two crustal provinces south through the Poachie region southwest of U.S. Highway 93 (figs. 1 and 2), and interpreted it to be a suture related to the convergence of the two terranes about 1.68–1.70 Ga. Wooden and DeWitt (1991) placed the boundary about 25 km east of Bagdad but did not have the information to extend it south of U.S. Highway 93.

Lead-isotopic systematics of Proterozoic rocks in central and western Arizona provide a way to reconstruct both the Proterozoic tectonic and magmatic evolution of the region. Wooden and DeWitt (1991) interpreted the whole-rock Pb-isotopic data of these rocks to indicate that volcanic arcs and sedimentary basins like those in central Arizona were built on Mojave crust in the area between the Central Arizona province and the Mojave province proper. Volcanic arcs and sedimentary basins formed on older crust in the boundary zone 1,730–1,710 Ma, and plutonism at 1,730–1,690 Ma tapped both Mojave and central Arizona mantle and crust (Wooden and DeWitt, 1991). Although the Poachie region is situated within the boundary zone between these provinces, the surface geology more closely resembles that of the Yavapai province than that of the Mojave province. Because of this resemblance, the area of the boundary zone was included in the Yavapai geologic province by Karlstrom and Bowring (1993).

The Antler-Valentine belt is the westernmost volcanic arc and sedimentary basin like those of the Central Arizona province, and aesthenosphere and (or) subducted Central Arizona mantle as well as Mojave crust contributed to the formation of the igneous rocks there. Preliminary results of studies in the Cerbat Mountains, north of the Antler-Valentine belt, suggest that the remains of a ≈1.73 Ga metamorphic belt similar to the Antler-Valentine belt is preserved among 1.72–1.68 Ga gneissose granitic rock (Duebendorfer and Chamberlain, 1994).

In northern Arizona in the Upper Granite Gorge of the Grand Canyon, U-Pb geochronologic and isotopic study places the east margin of Mojave crust between 154 and 159 km downstream from Lee's Ferry near the Crystal shear zone (Hawkins and others, 1996).

Geology

Metamorphic and plutonic rocks underlying Paleozoic, Mesozoic, and Tertiary supracrustal rocks form the basement in west-central Arizona.

Metamorphic Rocks

Our study area is underlain by plutonic rocks separated by north- to northeast-trending screens of amphibolite-facies metamorphic rocks (Xm, fig. 2). The principal screen extends south from Bagdad about 20 km south-southwest into the Poachie region where it separates Early Proterozoic gneissic tonalite (Xgt) from Middle Proterozoic granite of Olea Ranch (Yo) and, farther south, is within the granite of Olea Ranch, and the Early Proterozoic coarse-grained granite (Xcg). Near Bagdad the preservation of some primary textures and structures in the rocks reveals a stratigraphic sequence despite amphibolite-facies regional metamorphism of the rocks (Anderson and others, 1955). The stratigraphic sequence from oldest to youngest is (1) Bridle Formation (mafic volcanic rocks), (2) Butte Falls Tuff (felsic volcanic rocks), and (3) Hillside Mica Schist (shale and siltstone). According to Anderson and others (1955), Dick Rhyolite intrudes the sequence in the Bagdad area. More recent work by Conway and others (1986) south of Bagdad indicates that the Dick Rhyolite is extrusive and overlies the Bridle Formation (Conway and others, 1986).

The Dick Rhyolite, the only formally named formation from the Bagdad area shown on the map of the Poachie Range (Bryant, 1992), is a fine-grained biotite-quartz-feldspar gneiss containing scattered quartz and less common feldspar grains and aggregates as much as 1 mm in diameter, which probably were phenocrysts or crystal fragments (fig. 3). If we project the tops-to-the-east relationships from near Bagdad to the south, the unit is overlain by interlayered amphibolite and biotite-quartz-feldspar gneiss containing a few layers of schist, which is in turn overlain by muscovite-biotite schist and gneiss containing sillimanite and andalusite in many places. The muscovite-biotite schist and gneiss are probably correlative with the Hillside Mica Schist near Bagdad. South of U.S. Highway 93 all the metamorphic rocks are extensively intruded by granite and pegmatite. Farther south, increased intrusion and recrystallization tends to obscure any certain correlations with map units in the Bagdad metamorphic belt (fig. 2), although the rocks appear to be a continuation of the unit that is correlative with the Hillside Mica Schist. Metamorphic rocks in the southern part of the belt are muscovite-biotite schist and gneiss, locally containing sillimanite±garnet. They contain some layers of amphibolite, biotite-hornblende gneiss, and biotite-quartz-plagioclase gneiss. The latter megascopically resemble quartzite.

In the western part of the area, a second major screen of metamorphic rock (Xm) separates the Middle Proterozoic Signal Granite (Ys) on the west from the Early Proterozoic coarse-grained granite (Xcg) on the east (fig. 2). This screen is composed of biotite and biotite-hornblende-plagioclase schist and gneiss containing a few layers of sillimanite-muscovite schist and gneiss. The rocks are migmatized in many places and intruded by gabbro, diorite, granodiorite, and granite. The proportions of muscovite-biotite schist and gneiss increase southward within the screen.

Metamorphic rocks within the Signal batholith south of the west end of the Poachie Range differ from those elsewhere in the area and consist of biotite-quartz-feldspar gneiss locally containing garnet, hornblende-diopside-plagioclase granofels, and amphibolite. Their compositions suggest that they were derived from siltstones or fine-grained sandstones and (or) felsic tuffs containing calcareous or marly layers.

On the Santa Maria River southeast of the Bagdad metamorphic belt is muscovite-biotite schist and gneiss, locally containing sillimanite, garnet, or cordierite and layers of muscovite-biotite quartzite and intruded by aplite, pegmatite, and the granite of Thorn Peak. East of the Bagdad belt, metamorphic rocks are sparse in the area, are mostly screens and inclusions in a map unit rich in pegmatite, aplite, and granite, and consist of muscovite-biotite and sillimanite-muscovite-biotite schist and gneiss.

Foliation in the metamorphic rocks has a complex pattern. Strikes range from north-northwest to east-southeast, and dips are predominantly steep to moderate to the east. North-northeast strikes and steep east-southeast dips are most common. Mineral alignments have a maximum that trends N. 66° E. and plunges 19° NE. Some lineations have steeper plunges and more easterly trends. Axes of minor folds range in plunge from 0° to 80° and trend in all directions except northwest. Axial planes of the minor folds strike north-northwest to northeast and dip gently to steeply northeast and southeast. A few folds have various trends that differ from most folds. The data suggest a complex polyphase history of folding for these rocks. No superposition of folds or foliations was observed that would furnish a basis for deciphering the history in this area. In the Cerbat and Hualapai Mountains (Duebendorfer and others, 1998) and elsewhere in the Proterozoic rocks of Arizona (Karlstrom and Bowring, 1991), complex tectonic histories commonly include formation of northwest-striking foliation followed by formation of northeast-striking foliation. Proterozoic rocks in the Poachie region may have a similar history, perhaps obscured by additional deformation accompanying the emplacement of numerous Early and Middle Proterozoic plutons.

Plutonic Rocks

Plutonic rocks dominate the Proterozoic geology of the Poachie region and are about equally divided between Early and Middle Proterozoic age (fig. 2). Some of the units mapped range from heterogeneous ones composed of gabbro to granite to relatively well defined plutons having smaller compositional variations.

Figure 2 (facing page). Proterozoic rocks in the Poachie region showing locality of analyzed samples. From Bryant (1995 and unpublished reconnaissance mapping).

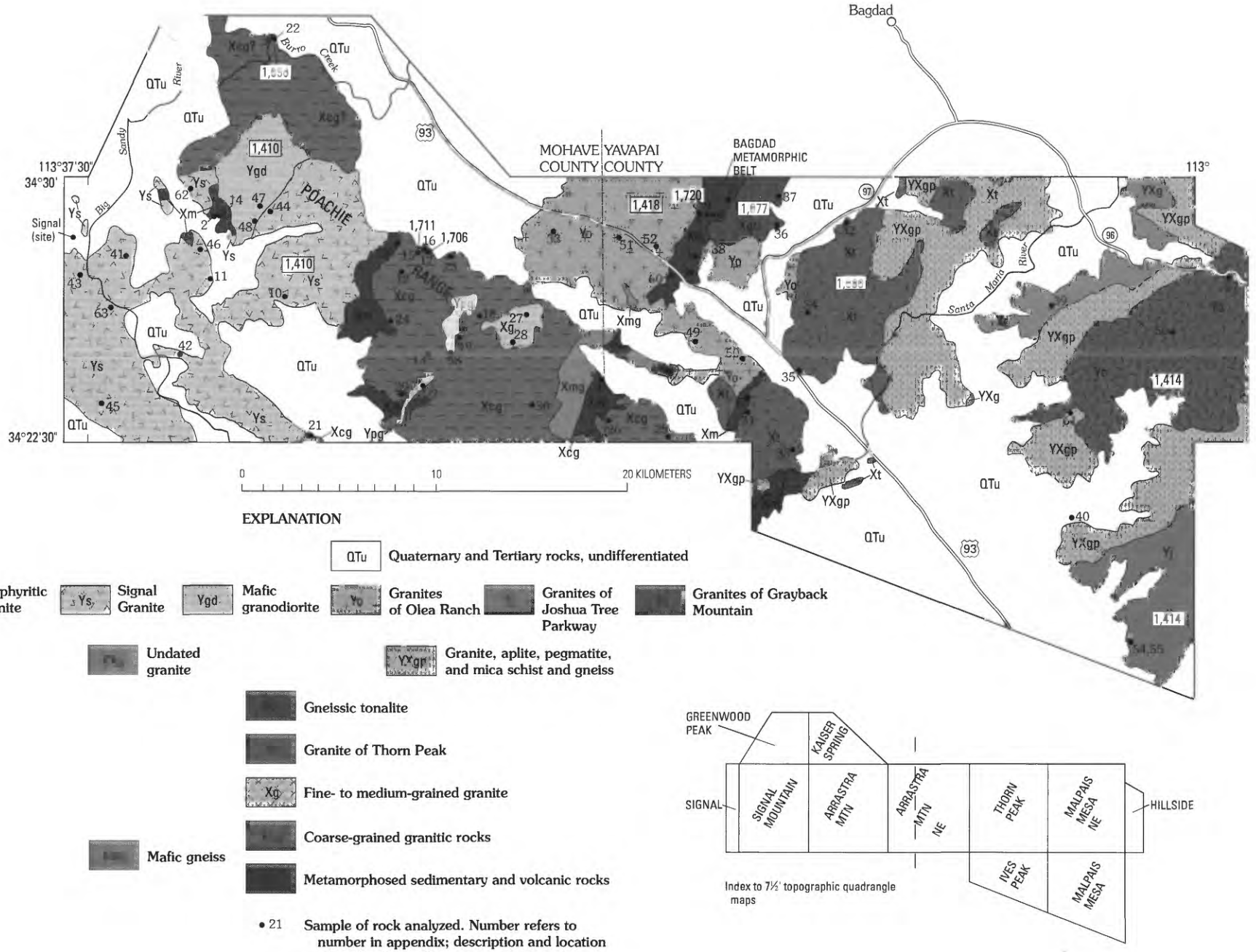
Bagdad
MOHAVE COUNTY
YAVAPAI COUNTY
BAGDAD METAMORPHIC BELT
113°37'30"
113°
34°30'
34°22'30"
Signal (site)
Big Sandy River
Burro Creek
Santa Maria River
POACHIE RANGE
1,410
1,418
1,720
1,877
1,711
1,706
1,414
QTu
Xcg
Xmg
Xm
Xg
Ygd
Ys
Ypg
Yo
YXgp
YXg
Xt
Yj
0
10
20 KILOMETERS
EXPLANATION
Quaternary and Tertiary rocks, undifferentiated
Porphyritic granite
Signal Granite
Mafic granodiorite
Granites of Olea Ranch
Granites of Joshua Tree Parkway
Granites of Grayback Mountain
Undated granite
Granite, aplite, pegmatite, and mica schist and gneiss
Gneissic tonalite
Granite of Thorn Peak
Fine- to medium-grained granite
Coarse-grained granitic rocks
Mafic gneiss
Metamorphosed sedimentary and volcanic rocks
• 21 Sample of rock analyzed. Number refers to number in appendix; description and location of analyzed samples
1,410 U-Pb zircon date in Ma. Where enclosed in rectangle represents a well-defined pluton
GREENWOOD PEAK
KAISER SPRING
SIGNAL
SIGNAL MOUNTAIN
ARRASTRA MTN
ARRASTRA MTN NE
THORN PEAK
MALPAIS MESA NE
HILLSIDE
IVES PEAK
MALPAIS MESA
Index to 7½' topographic quadrangle maps

Early Proterozoic Plutonic Rocks

Early Proterozoic plutonic rocks are mafic gneiss, coarse-grained granitic rocks, fine-grained granite, granite of Thorn Peak, gneissic tonalite, and a unit of mixed plutonic and metamorphic rocks that includes granite, aplite, pegmatite, schist, and gneiss. The granite at Burro Creek, probably part of the coarse-grained granitic rocks but not connected by mapping to them, is nonetheless described with those rocks.

Mafic Gneiss

West of the Bagdad metamorphic belt south of U.S. Highway 93 is a discontinuous belt of biotite-hornblende-plagioclase schist and gneiss (map unit Xmg, fig. 2). Rocks of this unit are abundantly intruded by adjacent Early and Middle Proterozoic granitic rocks and are characterized by plagioclase porphyroblasts. These intrusives produce a complex and gradational contact between the mafic gneiss and the bordering granitic rocks. The mafic gneiss does not resemble any of the rocks in the Bagdad metamorphic belt. The mafic rocks are not layered but are partly foliated, and they are tonalite, diorite, and gabbro. In one location the mafic gneiss cuts muscovite-biotite schist at the east contact of the unit. Where plagioclase porphyroblasts are absent, the gneiss has a grain size of 0.5–2 mm in contrast to most of the 1,700-Ma mafic plutonic rocks, which have a grain size of 5–15 mm.

The mafic gneiss consists of green, dark-green, and olive synkinematic to postkinematic anhedral hornblende as much as 2 mm long, anhedral synkinematic to postkinematic biotite as much as 1.5 mm long, plagioclase (An_{25-40}) as anhedral to subhedral grains as much as 2 mm in diameter and porphyroblasts as much as 1 cm in diameter. In some rocks 1–2-mm subhedral plagioclase grains are in a plagioclase-rich matrix having an average grain size of 0.2–0.4 mm. This texture suggests that the larger grains may be relict phenocrysts from an igneous protolith. Some rocks of the unit contain anhedral quartz generally 0.02–1 mm, but locally as much as 2 mm in diameter. Anhedral to euhedral epidote as much as 0.5 mm in diameter is partly contemporaneous with the biotite and partly secondary. Accessory minerals are sphene, apatite, opaque minerals, and minor allanite. Secondary chlorite replaces biotite and hornblende. Color index ranges from 20 to 62. Some of the rocks intruding the unit are hornblende-biotite tonalites, which are similar in composition to some of the mafic gneiss rather than the adjacent more felsic granites, which also intrude the unit. The composition and texture of the mafic gneiss suggest that its protoliths are intermediate to mafic hypabyssal or subvolcanic intrusions. Superficially these rocks resemble completely metamorphosed volcanic rocks.

Coarse-Grained Granitic Rocks

A heterogeneous group of mostly coarse grained and variably foliated plutonic rocks form the east and central parts of the Poachie Range (map unit Xcg, fig. 2). The rocks included in this unit form a suite ranging in composition from gabbro to granite. Hornblende-biotite and biotite granodiorite and granite are the dominant rock types, but rock types in the unit range to syenite and tonalite, and also include small bodies of gabbro and diorite. The unit generally has a complex and gradational contact with migmatitic schist and gneiss along its west contact.

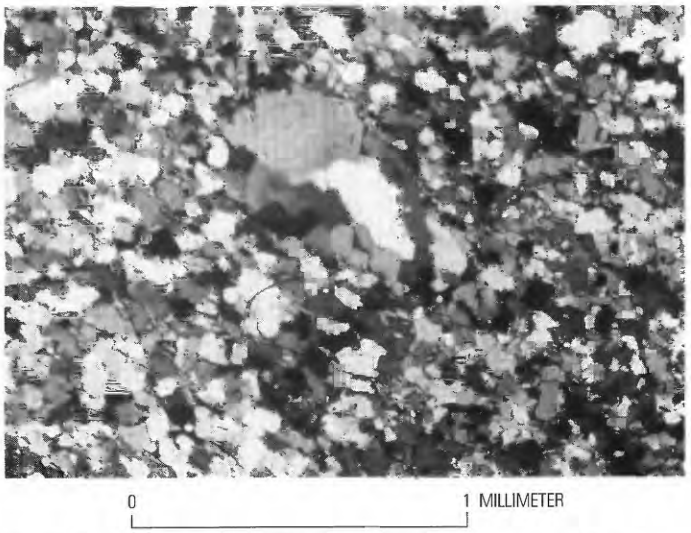

Figure 3. Photomicrograph of fine-grained biotite-quartz-feldspar gneiss of metamorphosed Dick Rhyolite. Lens of quartz grains probably represents recrystallized quartz phenocryst or crystal fragment. Appendix sample No. 8; U-Pb zircon age determination, figure 12; major-oxide and trace-element concentrations, table 3; whole-rock Pb-isotope analysis, table 8. Arrastra Mtn NE 7½' quadrangle.

The oldest plutonic rocks in this unit are gabbro and diorite. A few of these bodies are as much as 600 m long and were mapped separately (Bryant, 1992), but none are shown in figure 2. The mafic rocks are most numerous in the northwest part of the unit, and they also form small bodies in the metamorphic wallrock of the unit.

Roof pendants or large inclusions of possibly correlative gabbro are found in the Middle Proterozoic Signal Granite. Gabbro also intrudes metamorphic rocks of the Bagdad belt and roof pendants of metamorphic rock in the Signal Granite. The largest mafic intrusion among these is about 1.5 km long and 400 m wide.

The mafic rocks in the unit are generally medium grained, although some are coarse grained. Textures range from a thoroughly recrystallized mosaic to hypidiomorphic granular and diabasic, which is partly modified by recrystallization. The rocks are composed of plagioclase (An_{35-45} average; An_{60} maximum), green or olive-green hornblende, and, in many places, biotite. Monoclinic pyroxene is present in a few rocks, and orthorhombic pyroxene was found in one sample. Quartz is found in a few samples. Common accessory minerals are opaque minerals (locally a substantial component), sphene, and apatite. Some rocks have secondary chlorite and epidote. Color index is mostly 40–60 and is as much as 85. Modal compositions (IUGS classification, Streckeisen, 1973) range from melagabbro to quartz diorite.

The granitic part of the unit shows spatial compositional variations. These rocks are dominantly granodiorite in the north and granite in the south. In the northwest a distinctive porphyritic granodiorite and granite containing blocky feldspar phenocrysts as much as 3 cm in diameter is common (fig. 4). The various granitic rocks grade into each other in many places and were not

Figure 4. Foliated porphyritic granodiorite near west contact of coarse-grained granite. Blocky potassic feldspar phenocrysts are as much as 2.5 cm in diameter. Contains mafic inclusions aligned with foliation, and fracture-controlled aplite veinlet. Pen is 13 cm long. Appendix sample No. 20; major-oxide and trace-element concentrations, table 4; Arrastra Mtn 7 ½' quadrangle.

mappable as distinct plutons. Locally the granitic rocks contain scattered inclusions of metamorphic rock, migmatite, and more mafic phases of the plutonic unit, and these inclusions are more numerous near the western contact of the unit than elsewhere. The coarse-grained granitic rocks are cut by fine- to medium-grained and porphyritic granitic rocks, many of which could be either Early or Middle Proterozoic.

The felsic rocks (CI<40) range in modal composition from diorite to granite. In sec. 31, T. 13 N., R. 11 W. and sec. 5, T. 12 N., R. 11 W., parts of the unit are quartz-poor and are monzonite, monzodiorite, or quartz monzonite. No distinct contacts of those rock types were detected in fairly good exposures in washes in the area, but more detailed work may be needed to make sure that this variation cannot be mapped.

The variation in foliation seen megascopically is also apparent under the microscope. About a third of the samples examined show some biotite alignment, and between different samples the alignment ranges from poor to excellent. Some of the foliation measured in the field is on aggregates of mafic minerals, within which the individual grains are not aligned. Textures range from mosaic to hypidiomorphic granular. The latter texture is best developed where the rock contains subhedral phenocrysts of microcline.

Most of the felsic rocks contain biotite and lesser amounts of hornblende, except for the granites, which contain little or no hornblende. Opaque minerals, sphene, apatite, and zircon are found in almost all the rocks examined, and allanite occurs in some of them.

Quartz is as much as 4 mm in diameter and is interstitial to the feldspars in some rocks. Microcline is as much as 1.5 cm long and is locally perthitic and rarely interstitial to plagioclase. Plagioclase (oligoclase or sodic andesine) is anhedral to subhedral and as much as 8 mm long. Biotite as much as 2 mm long generally is in aggregates, many of which contain hornblende. Generally anhedral green hornblende as much as 3 mm long is in aggregates with biotite. Many of the larger grains have sieve texture with quartz.

Granite at Burro Creek. Granitic rocks on Burro Creek (unit Xcg in fig. 2) are not correlative with the Signal Granite, as suggested previously (Bryant and Wooden, 1986). These rocks are probably part of the plutonic complex that forms the east half of the Poachie Range, and it is treated as such here. In outcrop the differences between the Signal Granite and the granite at Burro Creek are as follows: (1) potassic feldspar megacrysts at Burro Creek tend to be equant compared to elongate in the Signal Granite, and (2) clots composed of mafic minerals at Burro Creek are larger and more irregular than those in the Signal Granite (fig. 5). The U-Pb date of a zircon for a sample from Burro Creek was erroneously reported as the age of the Signal Granite (Bryant and Wooden, 1986). We have not mapped the area between the sample site on Burro Creek and the Poachie Range area (Bryant, 1992), so we do not know whether it forms a mappable pluton in the coarse-grained granite unit or whether it is just another component of that heterogeneous unit.

Fine-Grained Granite

One 2-km-diameter pluton of fine- to medium-grained biotite granite (map unit Xg, fig. 2) locally containing muscovite forms the high summit at the east end of the Poachie Range. The pluton has a moderately sharp contact with the coarse-grained granite (unit Xcg) and contains inclusions of the wallrock. Adjacent to the pluton, dikes of fine-grained granite cut the coarse-grained granite. Pb-isotopic composition of a whole-rock sample from the pluton (appendix sample No. 28; table 8) shows that the granite of that pluton is Early Proterozoic. Other dikes and small plutons of fine-grained granite intruding the coarse-grained granite unit (Xcg) are also Early Proterozoic (appendix sample Nos. 29, 30; table 8), but some may be Middle Proterozoic age. Those plutons are mapped as YXg in the Poachie Range (Bryant, 1992).

On the east end of the Poachie Range, the fine-grained granite has an average grain size of about 2 mm, an allotriomorphic granular texture, and a color index ranging from 2 to 4. The granite contains <2 percent muscovite that mostly appears to be younger than the biotite, but locally some muscovite and some biotite crystallized at the same time. Biotite flakes are poorly to well aligned, but the foliation is not conspicuous in outcrop because of the small amount of biotite in the rock. Accessory minerals are zircon, allanite, sphene, apatite, and opaque minerals. Secondary minerals are chlorite, epidote, muscovite, and sericite.

Granite of Thorn Peak

In the central part of the area west of the Santa Maria River, moderately coarse grained muscovite-biotite and biotite granite (map unit Xt, fig. 2) forms a pluton 4–5 km wide and 15 km long and a few small satellitic plutons to the east. Contacts with metamorphic rocks (map unit Xm, fig. 2) along its southern margin are generally sharp. Contacts with a unit of mixed granite, aplite, pegmatite, and mica schist and gneiss (map unit YXgp, fig. 2) along the east part of the pluton and around the satellitic plutons range from sharp to gradational. Some of the granite in that mixed unit probably is the granite of Thorn Peak.

Potassic feldspar grains in the granite of Thorn Peak are as much as 1 cm in diameter, aggregates of biotite and muscovite 0.5–2 mm long, quartz and plagioclase crystals 2–5 mm in diameter. Accessory garnet is present locally. The granite of Thorn Peak has inclusions of mica schist, mica gneiss, and amphibolite, is cut by sparse dikes of pegmatite and aplite (fig. 6), and locally has a poorly developed to well-developed foliation parallel the trend of the pluton and the regional north-northeast structural trend. Some of the foliation is formed by aligned potassic feldspar grains and is interpreted to be due to flow, but other foliation appears to have formed by subsolidus recrystallization. Mapped with this unit is a pluton on Crosby Mountain northeast of the main pluton of the granite of Thorn Peak. That pluton consists of medium-grained and locally coarse grained granite containing accessory garnet. We have little information on the granite on Crosby Mountain, but according to Ed DeWitt (oral commun., 1990), granite of Thorn Peak cuts a granite resembling that on Crosby Mountain.

Quartz as interstitial grains as much as 2 mm in diameter and mosaic-textured aggregates having a grain size as large as 1 mm fill the space between the feldspars, as seen in thin section. Perthitic microcline forms subhedral to euhedral phenocrysts locally as much as 1 cm long and smaller anhedral to subhedral crystals. Generally subhedral but locally euhedral or anhedral plagioclase (An_{25-35}) is as much as 6 mm long, and also is found locally in mosaic-textured aggregates with quartz. Biotite is present as anhedral grains as much as 2 mm in diameter, and muscovite as much as 3 mm in diameter is intergrown and formed contemporaneously with biotite. Secondary muscovite formed by alteration of biotite. Common accessory minerals in the granite of Thorn Peak are zircon, apatite, and opaque minerals, and less common ones are sphene, tourmaline, garnet, and allanite. Epidote, chlorite, and sericite are secondary minerals in this unit. Modally the rocks are granite with color indices ranging from 2 to 8.

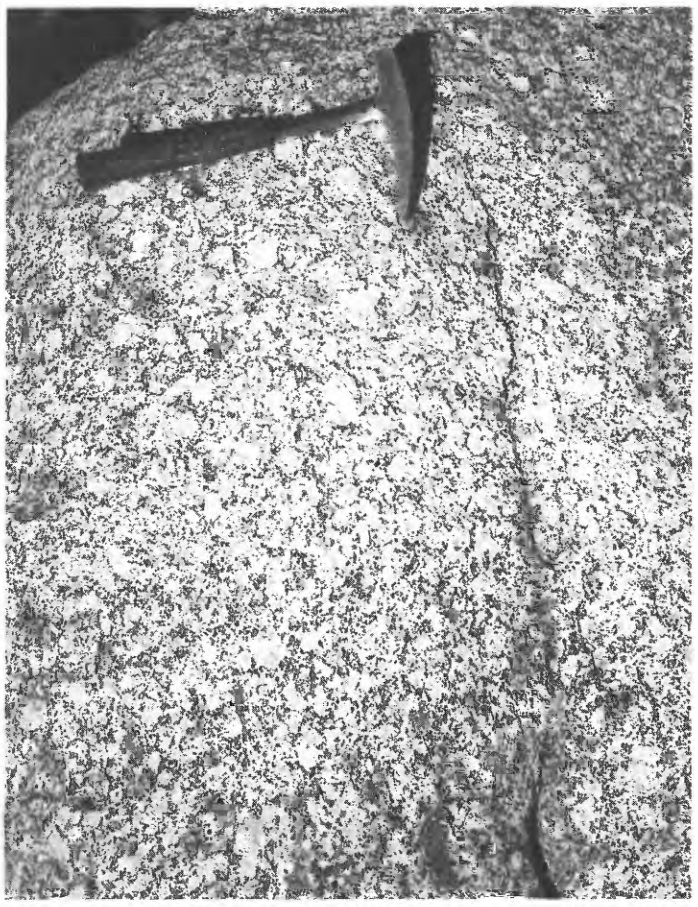

Figure 5. Coarse-grained granite at Burro Creek. Hammer is 33 cm long. Appendix sample No. 22; U-Pb zircon age determination, figure 14; major-oxide and trace-element concentrations, table 4; whole-rock and feldspar Pb-isotope analysis, table 8. Greenwood Peak 7 ½' quadrangle.

Gneissic Tonalite

Gneissic tonalite (map unit Xgt, fig. 2) crops out along the east flank of the Bagdad metamorphic belt. The northern part of this pluton has not been mapped, but reconnaissance indicates that parts of it extend only 3 km north of the Poachie map area. This unit was called gneissic granodiorite in earlier publications (Bryant, 1992, 1995; Bryant and Wooden, 1991b), but a review of available thin section and chemical data indicates that tonalite is a better name for this map unit. The south end of the gneissic tonalite is truncated by younger granite. In the Poachie region the unit intrudes mica schist and gneiss and contains many xenoliths of country rock within 2 km of its western contact. The eastern part of the pluton contains scattered inclusions of fine-grained diorite, tonalite, or granodiorite. Tourmaline-bearing leucogranite and pegmatite dikes intrude the unit. Much of the west contact in our map area is a shear zone, a southwestward extension of the Mountain Springs fault zone mapped by Anderson and others (1955) in the Bagdad area, and nearby tonalite has a partly healed cataclastic texture. On the east the contact is covered by Tertiary gravel. The gneissic tonalite unit contains rocks ranging in composition from biotite melagranite to hornblende tonalite and quartz diorite (fig. 7). Color index ranges from 25 to 65. In the Bagdad area the gneissic granodiorite and gabbro mapped south of Sanders Mesa (Anderson and others, 1955) are possibly correlative rocks.

Quartz is in anhedral grains as much as 4 mm in diameter and as mosaic-textured aggregates having a grain size of 0.1–0.3 mm. Some of the larger grains are strongly strained and are partly broken into subgrains and mosaic-textured aggregates. Plagioclase (An_{25-35}) is in anhedral to subhedral crystals as much as 8 mm long, which are locally bent and broken, and in mosaic-textured aggregates. Some plagioclase grains are normally zoned. Locally perthitic microcline in grains as much as 4 mm long are bent, broken, and healed by quartz and epidote. Microcline also forms mosaic-textured aggregates with quartz. Biotite forms

Figure 6. Granite of Thorn Peak near its west contact. Contains inclusions of fine-grained mica gneiss and xenocrysts of pegmatitic feldspar. Hammer is 33 cm long. Appendix sample No. 31; major-oxide and trace-element concentrations (sample without inclusions), table 5. Arrastra Mtn NE 7 ½' quadrangle.

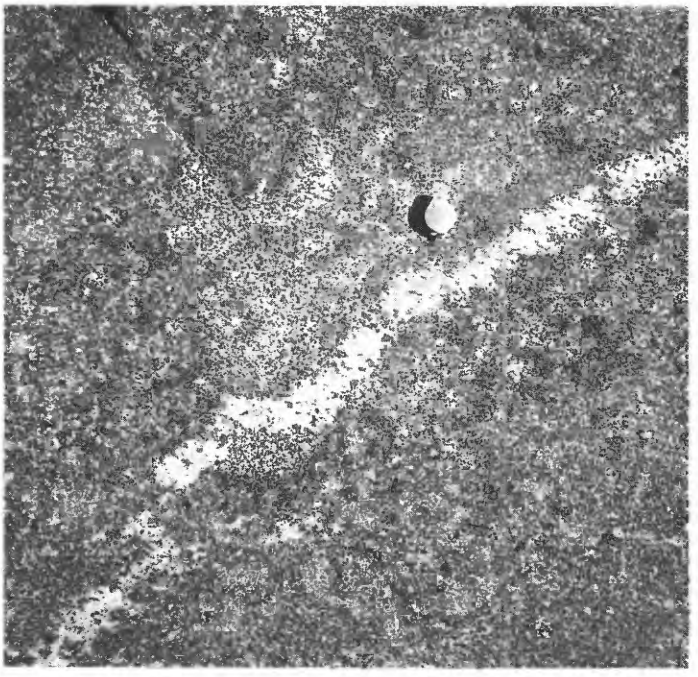

Figure 7. Biotite-hornblende diorite in gneissic tonalite unit. Cut by irregular pegmatitic segregations. Hand lens is 2 cm in diameter. Appendix sample No. 37; major-oxide and trace-element concentrations, table 5. Thorn Peak 7 ½' quadrangle.

flakes as much as 3.5 mm in diameter and aggregates of smaller grains. Some of the larger flakes are bent. Green to dark-green hornblende in anhedral to subhedral crystals as much as 2 mm long forms aggregates with or without biotite between blocky subhedral plagioclase. The hornblende is locally altered to light-green actinolite. Some rock containing numerous inclusions of mica schist and gneiss near the contact contains muscovite intergrown with biotite. Accessory minerals are sphene, apatite, zircon, allanite, and opaque minerals. Secondary minerals are chlorite, epidote, sericite, and carbonate group minerals.

Granite, Aplite, Pegmatite, Mica Schist, and Gneiss

In the eastern part of the area, rocks between the granite plutons are a mixture of muscovite-biotite schist and gneiss, locally containing sillimanite, intruded by pegmatite, alaskite, and granite in various proportions (map unit YXap, fig. 2). The schist and gneiss content of the unit ranges from as much as 50 percent to only a few percent. The pegmatite and alaskite contain small amounts of biotite, muscovite, and tourmaline, and in many places the pegmatite forms indistinct layers with gradational contacts in finer grained granite and aplite. Some of the granite is pegmatitic and contains potassic feldspar grains 10 cm in diameter, the grain size of many of the pegmatites. The granite is fine- to medium-grained biotite and muscovite-biotite granite like the granite of Thorn Peak, but some resembles the undated other Proterozoic rocks in the nearby part of the Poachie region. The granitic rocks are locally foliated.

Middle Proterozoic Plutonic Rocks

Middle Proterozoic rocks are Signal Granite, mafic granodiorite, porphyritic biotite granite, granite of Olea Ranch, granite of Joshua Tree Parkway, granite of Grayback Mountain, and diabase.

Signal Granite

The Signal Granite (Lucchitta and Suneson, 1982; map unit Ys, fig. 2) forms a batholith about 20 km long and 15 km wide in and west of the western part of the area and underlies the west end of the Poachie Range. The type locality, the ghost town of Signal, is at the west margin of our study area. The Signal Granite generally has well-defined contacts with country rock. However, inclusions or septa of metamorphic rock in the western part of the area are cut by numerous dikes and irregular intrusions of the granite. The granite is metamorphosed to augen gneiss and mylonite along its east contact. This zone of sheared granite is confined to the Signal batholith and might be related to movements within the intrusion during a late stage of its emplacement. It dips gently to moderately to the south or southeast parallel with the contact and has east- to northeast-trending lineation, which plunges gently to moderately. In the southern part of this contact zone the granite is locally brecciated along the zone of mylonite. According to Nyman and others (1994), kinematic indicators in this zone show that relative movements in the rock were to the northeast in a thrust sense during the formation of this fabric.

The body ranges in composition from granite to granodiorite and contains potassic feldspar phenocrysts generally 2–3 cm long, but locally as much as 6 cm long, and plagioclase and quartz grains as much as 1 cm in diameter (fig. 8*A*). Biotite and hornblende grains as much as 0.5 cm long form aggregates as much as 1 cm long. Some of the granodiorite is porphyritic: larger potassic feldspar crystals are scattered in a finer matrix (fig. 8*B*). Oriented lath-shaped, carlsbad-twinned, potassic feldspar crystals define flow foliation in most outcrops (fig. 8*C*). The Signal Granite contains widely scattered inclusions of a mafic facies, a closely associated mafic granodiorite, hornblende-biotite gneiss, and gabbro. A few quartz-microcline pegmatite pods, dikes, and lenses 0.1–1 m thick and dikes of medium-grained biotite granite cut the coarse-grained granite (fig. 8*D*).

The composition of the Signal Granite ranges considerably, as indicated by a range in the color index from 1 to 32. A leucocratic facies consisting of coarse- to fine-grained granite containing sparse biotite intrudes the main mass of the Signal Granite in bodies as much as 1.5 km long and 0.5 km wide (Bryant, 1992). A mafic facies composed of gray, medium-grained, locally porphyritic, biotite-hornblende tonalite to granite contains potassic feldspar phenocrysts as much as 4 cm in diameter. This facies is in mappable bodies as much as 3.5 km long and 1 km wide. The mafic phase is intruded by and grades to the main phase of the Signal Granite.

The Signal Granite contains anhedral quartz grains as much as 6 mm in diameter that are interstitial to the feldspar grains. Anhedral to subhedral microcline that is commonly perthitic and accompanied by myrmekitic intergrowths forms crystals more than a centimeter long. Anhedral to subhedral plagioclase (An_{17-33}) forms grains as much as a centimeter long in some samples. Anhedral biotite as much as 3 mm in diameter tends to be in aggregates between the feldspar grains. Anhedral green hornblende as much as 3 mm long usually occurs in aggregates with the biotite but locally is rimmed by biotite. Accessory minerals are zircon, apatite, allanite, sphene, and opaque minerals. Secondary minerals are sericite, carbonate minerals, chlorite, and epidote. Color index is generally between 10 and 20.

The coarse grain size of the Signal Granite makes modal compositions based on a standard thin section somewhat uncertain. Nevertheless it is obvious in the field that compositional variations exist. We conclude that composition of the main phase of the Signal Granite ranges from granite to granodiorite. Biotite is the principal mafic mineral, but many rocks have small amounts of hornblende, whereas a few rocks have subequal amounts of biotite and hornblende.

The mafic phase of the Signal Granite is commonly granodiorite and tonalite, and in it hornblende generally is as abundant as or more abundant than biotite. Grain size of the feldspars is smaller, usually in the range of 2–7 mm. Sphene is a more abundant accessory mineral than in the main phase of the Signal Granite. Color index is 20–35.

The leucocratic phase ranges in grain size from 2–3 mm to 5–10 mm. Finer grained rocks of the phase form dikes that cut the main phase of the Signal. Some of the rocks contain late porphyroblasts of quartz as much as 1.5 cm in diameter, and the quartz content of the rocks is higher than in the main phase of the Signal. Microcline tends to be more perthitic, and the plagioclase in some samples is sodic oligoclase. Color index is <1–10.

Mafic Granodiorite

A distinctive unit of dark-gray fine- to medium-grained locally porphyritic hornblende-biotite and augite-hornblende-biotite melagranodiorite, monzogranite, melagranite, and quartz monzodiorite closely associated with the Signal Granite on the south flank of the west end of the Poachie Range forms a pluton about 4 km in diameter (map unit Ygd, fig. 2). The rock is locally foliated parallel to dikes of Signal Granite and pegmatite that cut it. The foliation is interpreted to be due to flow while the rock was still at least partly in the liquid state because plagioclase phenocrysts and aggregates of mafic minerals are aligned, but the matrix lacks the distinctive textures typical of this pluton, which are described in the next paragraph. The body contains hornblende granite pegmatites a few centimeters thick and microcline-quartz pegmatites as much as 10 m thick. Contact relations with the Signal Granite are equivocal, for the mafic granodiorite contains inclusions of Signal Granite and is cut by dikes of Signal Granite, suggesting nearly simultaneous emplacement of the Signal Granite and the mafic granodiorite. However, no dikes of mafic granodiorite cut the Signal Granite, suggesting that the Signal Granite is slightly younger at the level of exposure. The color index of the mafic granodiorite is 20–30, similar to that of the more mafic phases of the Signal Granite.

The granodiorite contains quartz in granophyric intergrowths (fig. 9) 0.02–0.05 mm in diameter with potassic feldspar, as anhedral grains 0.1–0.5 mm in diameter and as xenocrysts several millimeters in diameter probably derived from the Signal Granite country rock. Plagioclase (An_{42-23}) forms euhedral to subhedral normally zoned phenocrysts as much as 2 mm long. Anhedral plagioclase grains in the matrix range from 0.04 mm to 1 mm in length in different rocks and are anhedral to euhedral and about 1 mm in equigranular rocks. Potassic feldspar occurs in some rocks of the unit as anhedral grains of cryptoperthite and microcline as much as 2.6 mm in diameter with or without granophyric intergrowths with quartz (fig. 9). Anhedral augite as much as 2 mm in diameter is partly altered to hornblende. Brown, greenish-brown, olive-green, and dark-green hornblende in anhedral crystals that are locally skeletal is generally about 0.5 mm long but locally as much as 1.5 mm long. Anhedral biotite is commonly 1 mm in diameter but locally 2 mm. The proportions of biotite, hornblende, and pyroxene range from rocks in which all three occur to ones in which either hornblende or biotite is the only mafic silicate mineral. Magnetite crystals, locally as much as 1.5 mm and commonly 0.2–0.8 mm in diameter, are volumetrically an important constituent in many samples of the unit. Accessory minerals are sphene, allanite, zircon, and apatite. Secondary minerals are chlorite, epidote, sericite, and sparse carbonate minerals.

Porphyritic Biotite Granite

A northeast-trending belt of porphyritic biotite granite (map unit Ypg, fig. 2) cuts the coarse-grained granite to granodiorite gneiss (unit Xcg) east of the Signal Granite. Plutons in that belt contain potassic feldspar phenocrysts as much as 1.5 mm in diameter in a fine- to medium-grained matrix of quartz, plagioclase, potassic feldspar, and biotite. The unit also has medium- to coarse-grained equigranular phases. One sample yielded a Middle Proterozoic whole-rock Pb-isotopic age (appendix sample No. 58; table 8).

Granite of Olea Ranch

Closely related coarse-grained granite, porphyritic granite, and fine-grained granite (map unit Yo, fig. 2) form mappable bodies (Bryant, 1992) and are here included in a unit designated the granite of Olea Ranch. Olea Ranch is located in SW¼ sec. 19, T. 13 N., R. 10 W., Arrastra Mtn 7½' quadrangle and is the only feature named on the 7½' topographic quadrangle in the area underlain by the unit other than Black Canyon, which was named for the basalt along it downstream from granite exposures.

A

C

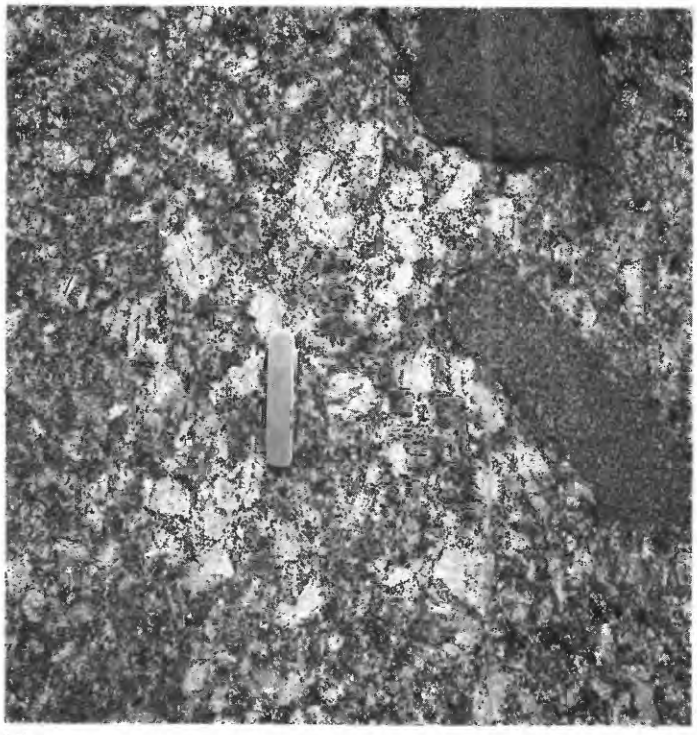

B

D

Figure 8. Outcrops of Signal Granite. *A*, Coarse-grained granite. Potassic feldspar crystals show some alignment at about 80° to pen. Pen is 13 cm long. Arrastra Mtn 7 ½' quadrangle. *B*, Coarse-grained porphyritic granite containing inclusions of hornblende-biotite granodiorite or potassic feldspar-bearing quartz diorite. Knife is 6 cm long. Signal Mountain 7 ½' quadrangle. *C*, Flow-aligned potassic feldspar crystals as much as 6 cm long and inclusions of fine-grained hornblende-biotite granodiorite or potassic feldspar-bearing quartz diorite. Hammer is 33 cm long. Signal Mountain 7 ½' quadrangle. *D*, Porphyritic granite containing scattered inclusions of fine-grained hornblende-biotite granodiorite or quartz diorite and cut by a quartz-microcline pegmatite. Feldspar phenocrysts and inclusions aligned in plane of flow. Hammer is 33 cm long. Signal Mountain 7 ½' quadrangle.

A 7-km-diameter pluton of coarse-grained biotite granite and granodiorite crops out north of Olea Ranch and along U.S. Highway 93 for about 3 km either side of the Mohave-Yavapai County line (Bryant, 1992). The rock ranges from equigranular to porphyritic and contains potassic feldspar crystals generally 1–2 cm and rarely as much as 3 cm long. Small amounts of primary muscovite are found in some of the coarse-grained granite. Dikes of pegmatite and fine- to medium-grained, locally porphyritic granite cut the coarse-grained granite. The coarse-grained granite contains scattered inclusions of biotite-quartz-feldspar gneiss, biotite-hornblende gneiss, biotite schist, amphibolite, and migmatite.

To the east, a pluton about 8 km long and 4 km wide (Bryant, 1992) consists of porphyritic biotite granite and granodiorite containing well-oriented tabular potassic feldspar phenocrysts generally 2–3 cm, but locally as much as 6 cm long that define a flow foliation in a medium-grained matrix. This rock is intruded by dikes of pegmatite and fine-grained granite and contains widely scattered inclusions of biotite-quartz-feldspar gneiss, biotite-hornblende-plagioclase gneiss, amphibolite, and fine-grained biotite granodiorite. Despite the distinctly different texture of the rock compared to the coarse-grained granite, our chemical and isotopic data show that the compositions and ages of the granite at Olea Ranch and the porphyritic granite to the east are identical.

Although not dated, a fine- to medium-grained, locally porphyritic granite that intrudes the coarse-grained granite appears to be closely related to the granites just described. The granite contains biotite and, in some places, muscovite. Locally the fine-grained granite is crowded with flow-aligned inclusions of biotitic rock (fig. 10), and rarely it contains inclusions of coarse-grained granite. In most places the fine-grained granite intrudes the coarse-grained granite, but in a few places textural gradations between those two rocks are found. The fine-grained granite forms plutons as much as 3 km long.

The coarse-grained granite contains anhedral quartz grains as much as 3 mm in diameter and mosaic-textured aggregates interstitial to the feldspars or in roundish masses. Generally perthitic microcline in anhedral to subhedral grains a centimeter or two long commonly includes quartz, plagioclase, biotite, and smaller grains of microcline. Plagioclase (An_{15-30}) is variously saussuritized and forms anhedral to subhedral grains as much as 7 mm long. Anhedral to subhedral biotite as much as 3 mm in diameter locally forms aggregates and is aligned. Accessory minerals are hornblende, muscovite intergrown with biotite, sphene locally as much as 1.5 mm in diameter, apatite, zircon, and allanite. Secondary minerals are muscovite, sericite, and epidote from plagioclase. Color index ranges from 2 to 28 and has a mean of 9.

The porphyritic granite contains quartz as anhedral grains as much as 3 mm in diameter and mosaic-textured aggregates between feldspar grains; anhedral to euhedral microcline and perthitic microcline as phenocrysts several centimeters long and matrix grains; subhedral to anhedral plagioclase (An_{15-30}) as much as 5 mm long; and anhedral to subhedral biotite as much as 1.3 mm in diameter usually as aggregates and locally weakly aligned parallel to the large microcline phenocrysts. The rock contains some myrmekite and accessory apatite, allanite, zircon, and opaque minerals. Chlorite from biotite and epidote from plagioclase are the secondary minerals. The matrix of the porphyritic granite generally has a grain size of 1–4 mm. Color index ranges from 6 to 19.

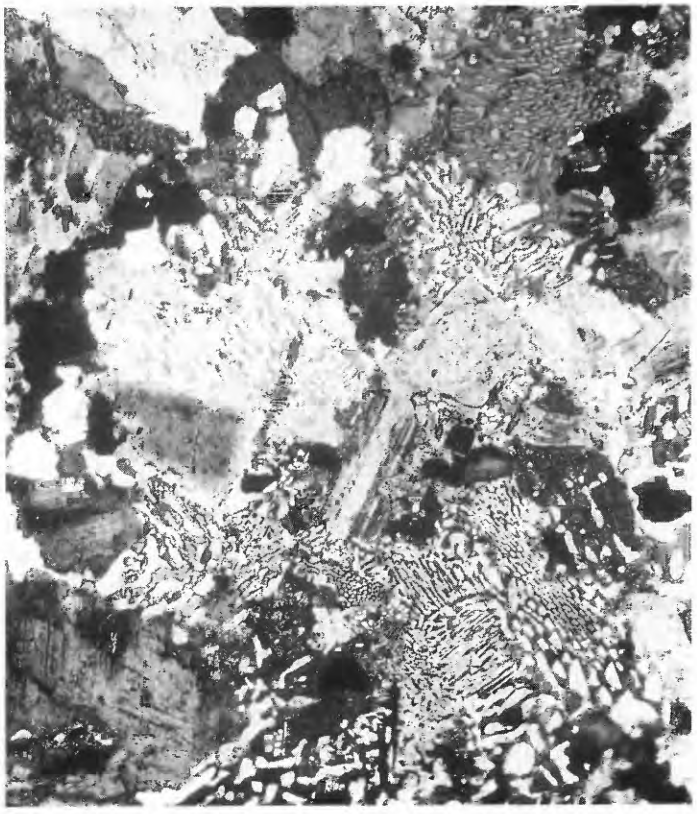

Figure 9. Photomicrograph of mafic granodiorite. Granophyric intergrowth in groundmass surrounds small euhedral phenocrysts of plagioclase, subhedral grains of augite and hornblende. Plagioclase in center is about 1 mm long. Appendix sample No. 47; U-Pb zircon age determination, figure 16; major-oxide and trace-element concentrations, table 6. Whole-rock and feldspar Pb-isotopic analysis, table 8. Signal Mountain 7 ½' quadrangle.

The medium- to fine-grained granite is locally porphyritic and contains anhedral quartz in grains as much as 2.5 mm in diameter and in mosaic-textured aggregates interstitial to plagioclase. Microcline and perthitic microcline are euhedral phenocrysts as much as 1 cm long in some rocks, but in others potassic feldspar is 0.3–1 mm in grain size. The larger microcline grains contain inclusions of quartz, plagioclase, and biotite. Euhedral to anhedral plagioclase (An_{28-39}) is in phenocrysts as much as 4.5 mm long but is mostly 1–2 mm in length. Anhedral biotite as much as 1.3 mm in diameter is locally in aggregates and locally aligned, probably due to flow in the crystallizing magma. Accessory minerals are muscovite, apatite, sphene, zircon, allanite, and opaque minerals. Secondary minerals are muscovite, sericite, carbonate minerals, and epidote from plagioclase and chlorite from biotite. Overall grain size of equigranular rocks and matrix of porphyritic rocks ranges from 0.1–0.5 mm to 1–1.5 mm. Color index ranges from 2 to 18 and has a mean of 10.

Granite of Joshua Tree Parkway

The eastern part of the Poachie region is underlain by two distinct but probably closely related rocks. These rocks crop out near the rest stop on U.S. Highway 93 about 6 km south of the area of figure 2, along a part of the highway designated the Joshua

Figure 10. Fine-grained granite of Olea Ranch containing mafic clots and inclusions. Hammer head is 19 cm long. Arrastra Mtn NE 7 ½' quadrangle.

Tree Parkway of Arizona, and they form hills to the north. There the rocks locally have some inclusions of fine-grained granite that appear to be older than the granite here discussed. Megacrystic granite and fine-grained granite are the two rock types included in this unit (map unit Yj, fig. 2).

The megacrystic granite is characterized by stout prisms of potassic feldspar as much as 6 cm long and 4 cm thick. The potassic feldspar grains are smaller in many places, and the texture of the granite is coarse-grained porphyritic having potassic feldspar phenocrysts 2–3 cm in length. This unit is cut by dikes of fine- to medium-grained granite and a few pegmatites. Contacts between megacrystic granite and fine-grained granite are difficult to locate precisely, because inclusions of megacrystic granite are numerous in the margins of the fine-grained granite plutons and dikes of fine-grained granite are numerous in the megacrystic granite.

The megacrystic granite consists of quartz in anhedral grains as much as 4 mm in diameter and mosaic-textured aggregates with a grain size of 1–3 mm; somewhat perthitic microcline containing inclusions of biotite, plagioclase, sphene, smaller microcline, and apatite; anhedral to subhedral plagioclase (An_{20-30}) as much as 6 mm long; anhedral to subhedral biotite as much as 3.5 mm in diameter, locally in aggregates as much as 1 cm long and weakly aligned; opaque minerals to 1.6 mm in diameter; and myrmekite. Accessory minerals are hornblende, sphene, apatite, zircon, and allanite. Muscovite, sericite, and epidote from plagioclase, and chlorite from biotite are secondary minerals. Color index is 8–12.

The fine-grained granite is locally foliated. It contains biotite and a few pegmatites, and in some places hornblende. In one area the rock is more mafic and consists of hornblende-biotite quartz monzodiorite, which contains numerous round to ellipsoidal inclusions of diorite, metagabbro, amphibolite, and porphyritic granodiorite as much as 1 m in diameter.

The fine-grained granite consists of anhedral quartz as much as 1.5 mm in diameter that is interstitial to plagioclase; anhedral, weakly perthitic microcline, locally interstitial to plagioclase; anhedral to subhedral variously saussuritized plagioclase (An_{32}) as much as 2 mm long; anhedral biotite as much as 3 mm in diameter; and myrmekite. Accessory minerals are hornblende in the more mafic varieties, sphene, allanite, apatite, zircon, and opaque minerals. Secondary minerals are chlorite from biotite and epidote and carbonate minerals from plagioclase. Color index ranges from 2 to 17.

Granite of Grayback Mountain

In the northeastern part of the area granite forms Grayback Mountain (map unit Yb, fig. 2) and extends several kilometers beyond the area mapped. This granite has three textural phases. Coarse-grained granite is the oldest phase. It contains stubby potassic feldspars 1–3 cm in length, quartz 0.5 cm in diameter, and biotite as much as 0.5 cm in diameter in clots. A few 0.2–0.3 m-thick dikes of quartz-feldspar and biotite-quartz-feldspar pegmatite cut the coarse-grained granite. A medium- to fine-grained, somewhat porphyritic biotite granite containing scattered 1–2 cm-diameter potassic feldspars cuts the coarse-grained granite and is locally cut by coarse-grained granite. The porphyritic granite is locally cut by quartz-feldspar pegmatites as much as 0.8 m thick. The porphyritic granite occupies a somewhat larger outcrop area than the coarse-grained granite. A third phase is found as small bodies near the margin and makes up a very small part of the pluton. This phase is a porphyry containing phenocrysts of quartz and potassic feldspar in a fine-grained matrix. The porphyry superficially resembles dikes of Cretaceous porphyry in the region. However, the porphyry locally grades into the medium- to fine-grained porphyritic granite.

The coarse-grained granite contains anhedral quartz as much as 3 mm in diameter and mosaic-textured aggregates that tend to fill in around the feldspar grains. Plagioclase is subhedral and as much as 4 mm long, has a composition of An_{20-25}, and is partly saussuritized. Anhedral to subhedral perthitic microcline is as much as 6 mm long. Anhedral to subhedral biotite as much as 2 mm in diameter locally forms aggregates. The rock contains myrmekite and accessory sphene, opaque minerals, allanite, apatite, and zircon. Chlorite and sericite are secondary. Color index is 10.

In the medium-grained porphyritic granite anhedral phenocrysts of quartz as much as 3 mm in diameter, subhedral to anhedral phenocrysts of perthitic microcline as much as 5 mm long, and subhedral to anhedral phenocrysts of plagioclase (An_{20}) are in a matrix of those minerals having a grain size of 0.2–0.8 mm. Biotite has the same size and form as in the coarse-grained granite. Myrmekite and muscovite intergrown with biotite are present; accessory minerals are opaque minerals, allanite, apatite, zircon, and sphene, and secondary minerals are muscovite and epidote. Color index is 6–8.

The fine-grained porphyritic phase contains euhedral phenocrysts of quartz as much as 5 mm in diameter, plagioclase (An_{15}) as much as 3 mm in diameter, and perthitic microcline as much as 6 mm in diameter in a matrix of quartz and feldspar with a grain size of 0.01–0.05 mm. Biotite, partly altered to

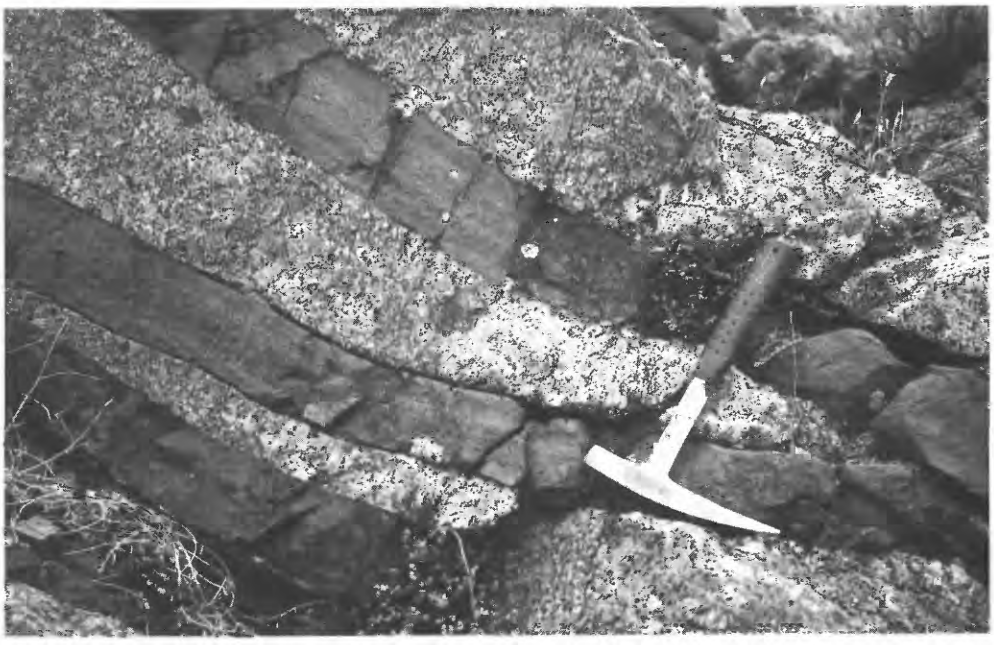

Figure 11. Outcrops of diabase. *A*, Thin sheets of diabase in Signal Granite. Sheets have a component of dip in direction of view and dip southwest about 40°. Thin sheets are locally numerous in the Signal Granite west of the Big Sandy River and are commonly associated with thicker sheets. Hammer is 33 cm long. Southwest part of Signal Mountain 7 ½' quadrangle. *B*, Chilled margin and layering in diabase sheet in coarse-grained granite in Arrastra Mtn 7 ½' quadrangle. Pencil is 13 cm long. Photograph by Karl Wirth.

A

muscovite, forms xenocrystic-appearing aggregates rimmed by opaque minerals. Sphene, opaque minerals, zircon, and apatite are accessory minerals, and epidote is a secondary mineral in the fine-grained porphyry. Color index is 2.

B

Diabase

Diabase sheets a few centimeters to a few tens of meters thick and 2 km in outcrop length and dikes 10 cm to 100 m thick and as much as 1.5 km long (not shown in fig. 2) intrude all the other Proterozoic rocks in the Poachie region (fig. 11*A*). Most of the sheets are gently dipping, but a few are nearly vertical (Bryant and Wooden, 1991b). These dikes are probably 1,150–900 Ma based on petrographic similarity to diabase in eastern and northwestern Arizona dated by various methods (Damon and others, 1962; Banks and others, 1972; Creasy, 1980; Elston and McKee, 1982; Silver, 1960, 1978). U-Pb dates of sphene from dikes in the Hualapai Mountains, Peacock Mountains, and the Cottonwood Cliffs area north and northwest of the Poachie region are about 1,080 Ma and are interpreted to be the crystallization age of the dikes (Shastri and others, 1991).

The diabase ranges from fine to coarse grained, and some bodies contain veinlets rich in plagioclase several millimeters thick. Textural variations are found within individual bodies. Locally chilled margins are present, and some sheets have a layered appearance (fig. 11*B*). In some rocks inclusion-like bodies of coarse-grained diabase have distinct but gradational contacts with surrounding medium-grained diabase. One sheet has veinlets of biotite-quartz diorite cutting it. Some of the dikes were emplaced along earlier shear or fracture zones, and those zones were reactivated. Many of the sheets are sheared along their contacts, especially in the western part of the area. Locally these shear zones contain quartz veins which were prospected for gold.

The bodies range from olivine-pyroxene diabase to pyroxene and hornblende diabase and have a mean color index of about 40 (CI=20–62). Some of the diabase bodies are partly to completely altered. One of the largest unaltered dikes contains euhedral laths of plagioclase (An_{70}) as much as 3 mm long surrounded by anhedral monoclinic pyroxene as much as 5 mm in diameter. Anhedral to subhedral olivine as much as 2 mm in diameter is also included in the pyroxene. Opaque minerals as much as 2 mm in diameter, accessory biotite, and secondary actinolite derived from the mafic minerals are present. Some rocks contain hornblende that has replaced primary pyroxene; in others the principal mafic mineral is acicular brown hornblende as

Table 1. U-Pb zircon ages of Proterozoic igneous rocks in the Poachie region.

Appendix sample No.	Unit	Field sample No.	Age, Ma	Comment
8	[1]Dick metarhyolite	1161	1,718±6	Data combined for age of ≈1,720 Ma
9	[1]Dick metarhyolite	P-93-1	1,721±6	
15	Gabbro	JW-84-11	1,711±22	
16	Coarse-grained granite	JW-84-12	1,706±4	
22	Granite on Burro Creek	JW-84-9	1,696±13	
35	Granite of Thorn Peak	1158	1,686±8	
38	Gneissic tonalite	JW-85-63	1,677±17	Younger zircon by ion microprobe
43	Signal Granite	1168	1,410±4	Based on discordia line from combined data of samples
44	Signal Granite	1164		
47	Mafic granodiorite	390		
50	Granite of Olea Ranch	JW-85-13	1,418±2	Based on composite discordia line
51		JW-85-15		
54	Granite of Joshua Parkway	A-151a	1,414±4	Ages of two plutons not statistically different; data combined
57	Granite of Grayback Mountain	A-153		

[1]An informal unit possibly correlative with the Dick Rhyolite.

much as 2 mm long. Some diabase contains small amounts of late-stage primary biotite. Opaque mineral and apatite are common accessory minerals.

Many of the diabase bodies are partly to completely altered. Plagioclase is saussuritized, and mafic minerals are altered to chlorite or actinolite. Secondary epidote, carbonate minerals, and, locally, sphene are found in altered diabase.

Other Proterozoic Granitic Rocks

Granites in the Poachie region that could not be correlated with dated granites are included in this unit (unit YXg, fig. 2). In the central part of the Poachie region, many of the rocks mapped in this unit (small bodies in Bryant, 1992; one body in fig. 2) are fine- to medium-grained biotite and muscovite-biotite granite. In the northeast part of the Poachie region, the granite in this unit is medium to coarse grained and equigranular to porphyritic. Locally it has a granodioritic composition. In some places the rock is weakly gneissose, and in a few other places aligned potassium feldspar crystals form a flow structure. The granite contains a few inclusions of gneiss and is cut by sparse pegmatite veins.

In thin section quartz ranges from anhedral to subhedral grains as much as 3 cm in diameter to granoblastic textured aggregates between the feldspar grains. Plagioclase (An_{26-32}) forms subhedral grains as much as 3 mm long. Potassic feldspar is perthitic microcline in grains as much as 1 cm long. Anhedral to subhedral biotite as much as 2 mm in diameter forms single grains or aggregates. Accessory muscovite is partly contemporaneous with the biotite and partly late. Accessory apatite, zircon, allanite, and opaque minerals and secondary epidote, chlorite, and sphene are present. Color index is 8–10.

Geochronology

The results of U-Pb zircon dating of Proterozoic rocks in the Poachie region indicate that Early Proterozoic igneous rocks were emplaced between approximately 1.72 Ga and 1.68 Ga (table 1). Metamorphic rocks interpreted to be metarhyolite were erupted at about 1.72 Ga, and plutonic rocks were emplaced from about 1.71 Ga to 1.68 Ga. Regional deformation and metamorphism were synchronous with the early part of plutonic activity but were completed by 1.69 Ga. A second major plutonic event took place in Middle Proterozoic time from about 1.42 to 1.41 Ga.

Metamorphic Rocks

The Bagdad metamorphic belt contains metamorphosed volcanic rocks from which zircons were separated. Two samples of biotite-quartz-feldspar gneiss or metarhyolite were examined. This unit was mapped as Dick Rhyolite (Bryant, 1992) because of its apparent continuity with that unit in and south of Bagdad (Anderson and others, 1955; Conway and others, 1986). Sample 1161 (appendix sample No. 8) is nonbedded but foliated metarhyolite, here referred to informally as the Dick metarhyolite. A U-Pb zircon age of 1,710±10 Ma was originally reported for this sample (Bryant and Wooden, 1991b). An age of 1,718±6 Ma is a better interpretation, however, based on further consideration of these data. The 1,718 Ma age is based on the regression of data for four of the six zircon fractions analyzed for this sample (table 2). One abraded fraction (NM63-102AB) appears to contain a small percentage of older, inherited zircon and was omitted from the preferred regression. A repeat analysis of additional material from this abraded fraction (NM63-102ABRP) indicated either

much less or no significant inheritance, so that its replotted position lies along the preferred regression. The second fraction omitted from the regression was composed of the larger magnetic zircons (M63-102). Omission of the second fraction was based primarily on its poor fit with the other four used in the regression.

Sample P-93-1 (appendix sample No. 9) represents a somewhat layered biotite-muscovite schist near the presumed top of the Dick metarhyolite (stratigraphic relations extrapolated from the work of Anderson and others, 1955, at Bagdad). The rock is richer in quartz and mica than typical samples of the metarhyolite, but it contains similar 1–2 mm equidimensional quartz grains and aggregates. Zircons from this sample are small well-formed crystals with 2:1 to 4:1 length:width ratios; there is no evidence of rounded or abraded grains or crystal terminations as would be characteristic of a detrital sedimentary rock. Four of the five zircon fractions analyzed from this sample define a discordia line with an upper intercept of 1,721±6 Ma. The remaining fraction (table 2, NM+100) plots well above this line and has an unusually low $^{206}Pb/^{204}Pb$ ratio indicating a high common lead component compared to other analyzed fractions. The ages of the two samples are the same within their 95 percent confidence level errors and the age of this unit is interpreted to be about 1,720 Ma.

The 1,720 Ma age of this metamorphosed volcanic rock raises the question whether the unit is actually correlative with the Dick Rhyolite as mapped at Bagdad. An alaskite porphyry, interpreted to intrude the base of the metavolcanic rocks west of Bagdad (Anderson and others, 1955), has a U-Pb zircon date of 1,730±12 Ma (J.L. Wooden and C.M. Conway, unpub. data, 1994). No zircons were found in a sample of Dick Rhyolite taken from its type locality about 2 km east of the aplite sample. An age of 1,730 Ma should be a minimum time for the emplacement of the lower part of the Bagdad metamorphic belt. Support for older ages in the Bagdad metamorphic belt is provided by Silver (1968), who gave undocumented dates of 1,715 to 1,735 Ma (corrected for modern decay constants; see Conway and others, 1986) for metamorphic rocks near Bagdad. A further complication is that Anderson and others (1955) interpreted the Dick Rhyolite to be intrusive, whereas Conway and others (1986) interpreted it to be extrusive. We interpret sample P-93-1 to be originally an extrusive or volcaniclastic rock. The 1,721 Ma date of P-93-1 is not statistically different from the 1,718 Ma date of sample 1161, a more massive rock. Both dates are significantly younger than the minimum age of 1,730 Ma established for the lower part of the Bagdad metamorphic belt west of Bagdad. We suggest that the age differences are real and reflect a composite section composed of metavolcanic rocks from two separate volcanic events. The metamorphic belt has been engulfed by younger intrusive complexes and deformed and recrystallized, making original stratigraphic relations impossible to determine. This interpretation is consistent with other modern U-Pb dating that has established that metamorphic packages in this region range in age from 1,750 to 1,710 Ma (Chamberlain and Bowring, 1990; Karlstrom and Bowring, 1993; Hawkins and others, 1996) and probably represent two or more discrete events.

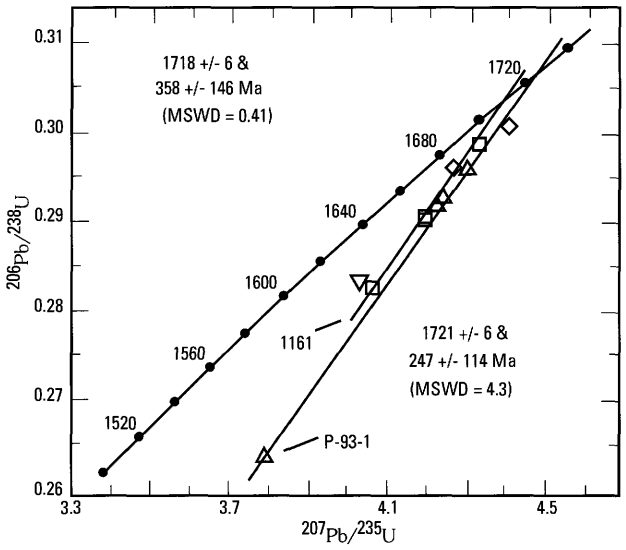

Figure 12. U-Pb concordia diagram for two samples from the Bagdad metamorphic belt. Samples 1161 (squares) and P-93-1 (triangles) are massive gneissic and schistose samples, respectively, from a metarhyolite unit possibly correlated with the Dick Rhyolite (appendix sample Nos. 8 and 9, respectively). Zircon fractions represented by diamonds (1161) and by inverted triangles (P-93-1) were not used in regressions. See text for complete discussion.

Plutonic Rocks

Plutonic rocks described following are Early Proterozoic and Middle Proterozoic in age.

Early Proterozoic Plutonic Rocks

Early Proterozoic rocks are coarse-grained granitic rocks and associated gabbro, granite of Thorn Peak, and gneissic tonalite.

Coarse-Grained Granitic Rocks

Three samples were taken from this unit for U-Pb zircon dating. They include gabbro, diorite, and the granite at Burro Creek. Sample 750 (appendix sample No. 15) is a gabbro from an area (shown on the map of the Poachie Range; Bryant, 1992) in the northwest part of the coarse-grained granite, where gabbro and diorite are more widespread than elsewhere in the unit. Gabbro bodies are the oldest components and make up only a minor part of the plutonic complex, which forms the east and central parts of the Poachie Range. These bodies are commonly metamorphosed to amphibolite at their margins and cut by younger members of the plutonic suite. Zircons separated from this sample were well-formed crystals of surprisingly large minimum diameters (>100 micrometers). Two zircon fractions from sample 750 indicate an age of 1,711±22 Ma (table 2 and fig. 13). The high uncertainty of this age reflects the limited spread of the two points and their distance from concordia.

Table 2. Analytical data and ages of zircons from the Proterozoic rocks of the Poachie region.

[App. no., appendix number; Field sam. no., field sample number (parentheses indicate J.L.W.'s number for sample from the site]

						Measured ratios		Corrected ratios						Age (Ma)		
App. no.	Field sam. no.	Fraction[1]	Sam. wt. (mg)	U (ppm)	Pb (ppm)	$^{206}Pb/^{204}Pb$	$^{208}Pb/^{206}Pb$	$^{206}Pb/^{238}U$	±%	$^{207}Pb/^{235}U$	±%	$^{207}Pb/^{208}Pb$	±%	$^{206}Pb/^{238}U$	$^{207}Pb/^{235}U$	$^{207}Pb/^{206}Pb$
						Early Proterozoic rocks										
8	1161	Dick metarhyolite[2] (biotite-quartz-feldspar gneiss)														
		NM+102	4.0	178	56	1420	0.1435	0.29064	0.5	4.1948	0.5	0.10467	0.1	1645	1673	1708
		NM63-102	5.6	199	61	6800	0.1239	0.29100	0.5	4.1942	0.5	0.10453	0.1	1647	1673	1706
		NM63-102AB	4.2	199	65	7000	0.1492	0.30105	0.4	4.3965	0.4	0.10582	0.1	1696	1712	1730
		NM63-102ABRP	2.6	201	65	6290	0.1543	0.29901	0.4	4.3259	0.4	0.10493	0.1	1686	1698	1713
		M63-102	4.5	264	83	5250	0.1282	0.29620	0.4	4.2651	0.4	0.10443	0.1	1672	1687	1704
		M63	4.2	256	76	8190	0.1216	0.28265	0.5	4.0618	0.5	0.10422	0.1	1605	1647	1701
9	P-93-1	Dick metarhyolite[2] (biotite-muscovite schist)														
		NM+100	1.9	164	53	680	0.1753	0.28342	0.1	4.0266	0.5	0.10304	0.4	1608	1640	1680
		NM80-100	3.3	154	49	4367	0.1365	0.29622	0.2	4.2970	0.2	0.10521	0.1	1672	1693	1718
		NM80	5.6	173	54	9524	0.1309	0.29282	0.1	4.2383	0.2	0.10498	0.2	1656	1681	1714
		M+100	2.4	223	63	4184	0.1415	0.26364	0.2	3.7847	0.3	0.10412	0.2	1508	1589	1699
		M80	4.6	191	60	7175	0.1350	0.29200	0.1	4.2246	0.1	0.10493	0.1	1651	1679	1713
15	750 (JW-84-11) Gabbro—coarse-grained granite suite															
		NM163	5.7	966	336	16680	0.2499	0.29810	0.5	4.3026	0.5	0.10468	0.1	1682	1694	1709
		NM63	3.0	1417	485	14416	0.2424	0.29476	0.5	4.2519	0.5	0.10462	0.1	1665	1684	1708
16	751 (JW-84-12) Quartz diorite—coarse-grained granite suite															
		NM+163	4.4	393	127	4100	0.1703	0.29315	0.5	4.2052	0.5	0.10404	0.1	1657	1675	1697
		NM102-163RP	6.0	363	116	8100	0.1622	0.29352	0.5	4.2090	0.5	0.10400	0.1	1659	1676	1697
		NM102-163AB	4.2	358	119	4320	0.1704	0.30286	0.4	4.3648	0.5	0.10452	0.1	1706	1706	1706
		NM63	7.1	378	122	11000	0.1703	0.29334	0.5	4.2231	0.5	0.10442	0.1	1658	1679	1704
		M+163RP	8.8	373	117	4420	0.1620	0.28663	1.4	4.1018	1.8	0.10379	1.0	1625	1655	1693
		M63-102	4.3	386	121	5070	0.1693	0.28464	1.1	4.0954	1.1	0.10435	0.1	1615	1553	1703
		M63RP	4.8	451	143	5360	0.1737	0.28786	0.4	4.1395	0.5	0.10430	0.1	1631	1662	1702
22	749 (JW-84-9) Granite of Burro Creek															
		NM+163	5.8	449	140	15000	0.1599	0.28742	0.5	4.0803	0.5	0.10296	0.1	1629	1650	1678
		NM+163AB	3.8	441	142	11550	0.1713	0.29264	0.4	4.1718	0.4	0.10339	0.1	1655	1668	1686
		NM102-163	9.6	499	157	15500	0.1713	0.28565	0.5	4.0544	0.5	0.10294	0.1	1620	1645	1678
		NM63-102	7.3	512	163	15000	0.1756	0.28859	0.5	4.1081	0.5	0.10324	0.1	1634	1656	1683
35	1158	Granite of Thorn Peak														
		NM63-102	4.3	442	108	2550	0.0852	0.23661	0.4	3.3791	0.5	0.10358	0.1	1369	1500	1689
		M102-163	2.5	433	104	1310	0.1153	0.22420	0.2	3.1929	0.2	0.10328	0.2	1304	1455	1684
		M+102	2.1	434	112	2620	0.0947	0.24651	0.2	3.5118	0.2	0.10351	0.1	1420	1531	1688
		M63	2.4	582	131	1675	0.0856	0.21605	0.2	3.0888	0.3	0.10369	0.2	1261	1430	1691

Table 2—Continued. Analytical data and ages of zircons from the Proterozoic rocks of the Poachie region.

App. no.	Field sam. no.	Fraction[1]	Sam. wt. (mg)	U (ppm)	Pb (ppm)	Measured ratios $^{206}Pb/^{204}Pb$	Measured ratios $^{208}Pb/^{206}Pb$	Corrected ratios $^{206}Pb/^{238}U$	±%	Corrected ratios $^{207}Pb/^{235}U$	±%	Corrected ratios $^{207}Pb/^{208}Pb$	±%	Age (Ma) $^{206}Pb/^{238}U$	Age (Ma) $^{207}Pb/^{235}U$	Age (Ma) $^{207}Pb/^{206}Pb$
						Early Proterozoic rocks—*Continued*										
38	1163 (JW-85-63) Gneissic tonalite															
		NM+163	0.5	1003	279	4160	0.1215	0.26114	0.4	4.0918	0.4	0.11364	0.1	1496	1653	1858
		NM102-163	3.4	758	181	8770	0.1263	0.22344	0.4	3.4120	0.4	0.11075	0.1	1300	1507	1812
		M102-163	2.0	500	159	11680	0.1178	0.29980	0.2	4.5536	0.2	0.11016	0.1	1690	1741	1802
		NM-102	3.6	548	175	10500	0.1344	0.29811	0.4	4.4013	0.4	0.10708	0.1	1682	1713	1750
		NM63	2.2	537	167	15860	0.1323	0.29133	0.2	4.2652	0.2	0.10618	0.1	1648	1687	1735
		M-63	2.4	546	168	24000	0.1318	0.28983	0.2	4.2252	0.2	0.10573	0.1	1641	1679	1727
38	1163 (JW-85-63) Ion probe data															
		1 (Grain #)		455	151		0.1135	0.31510	2.9	4.6807	3.1	0.1077	0.6	1766	1764	1762
		2		199	60		0.1078	0.28690	3.0	4.0527	3.3	0.1024	1.1	1626	1645	1669
		3		1018	330		0.1060	0.31090	2.9	4.4724	3.0	0.1043	0.4	1745	1726	1702
		4.1		178	86		0.1182	0.43600	3.0	9.8136	3.2	0.1632	0.8	2333	2417	2489
		4.2		286	90		0.0885	0.30560	1.9	4.3668	2.2	0.1037	1.0	1719	1706	1690
		5.1		172	84		0.1169	0.44570	3.0	9.8619	3.1	0.1605	0.7	2376	2422	2461
		5.2		567	167		0.1017	0.28470	2.9	3.9654	3.1	0.1010	0.7	1615	1627	1643
		6		331	105		0.1295	0.29890	2.9	4.2545	3.1	0.1032	0.7	1686	1685	1683
		7		398	198		0.0809	0.46270	2.9	10.9635	3.0	0.1719	0.5	2451	2520	2576
		7.2		440	144		0.1419	0.30500	1.8	4.4378	2.1	0.1055	0.8	1716	1719	1723
		8		163	49		0.0953	0.29170	3.0	4.1356	3.4	0.1028	1.4	1680	1661	1676
		9		228	71		0.0731	0.30820	1.9	4.3998	2.4	0.1036	1.3	1732	1712	1689
		10		199	61		0.0825	0.29960	1.9	4.4506	2.4	0.1077	1.2	1690	1722	1761
						Middle Proterozoic rocks										
43	1168	Signal Granite														
		NM+163	3.6	902	214	7375	0.1141	0.22864	0.4	2.8097	0.8	0.08913	0.6	1327	1358	1407
		M63-102	2.8	914	216	4975	0.1362	0.22314	0.4	2.7455	1.1	0.08924	0.9	1298	1341	1409
44	1164 (JW-85-64) Signal Granite															
		NM+163	3.2	1136	250	4485	0.1203	0.21051	0.4	2.5867	0.5	0.08912	0.1	1232	1297	1407
		NM102-163	2.1	939	213	3750	0.1398	0.21356	0.4	2.2644	0.4	0.08913	0.1	1248	1307	1407
47	390 (JW-84-10) Mafic granodiorite															
		NM102-163LT	5.6	264	75	1840	0.2777	0.23678	0.5	2.9130	0.5	0.08923	0.1	1370	1385	1409
		NM102-163DK	3.6	663	180	5900	0.2355	0.23751	0.5	2.9220	0.5	0.08923	0.1	1374	1388	1409
		NM-63	4.4	293	71	7550	0.1830	0.22066	0.4	2.7170	0.4	0.08930	0.1	1385	1333	1411
50	752 (JW-84-13) Porphyritic granite of Olea Ranch															
		NM63-102	8.0	1229	286	13500	0.1136	0.22457	0.5	2.7764	0.5	0.08967	0.1	1306	1349	1418
		NM-63	7.7	1336	309	14000	0.1232	0.22140	0.5	2.7392	0.5	0.08971	0.1	1289	1339	1419
51	753 (JW-84-15) Coarse-grained granite of Olea Ranch															
		NM+163	6.6	572	142	4735	0.1056	0.24109	0.5	2.9781	0.5	0.08959	0.1	1392	1402	1417
		NM102-163	8.5	633	155	4575	0.1257	0.23309	0.5	2.8808	0.5	0.08964	0.1	1351	1377	1418

Table 2—Continued. Analytical data and ages of zircons from the Proterozoic rocks of the Poachie region.

App. no.	Field sam. no.	Fraction[1]	Sam. wt. (mg)	U (ppm)	Pb (ppm)	Measured ratios				Corrected ratios				Age (Ma)		
						$^{206}Pb/^{204}Pb$	$^{208}Pb/^{206}Pb$	$^{206}Pb/^{238}U$	±%	$^{207}Pb/^{235}U$	±%	$^{207}Pb/^{208}Pb$	±%	$^{206}Pb/^{238}U$	$^{207}Pb/^{235}U$	$^{207}Pb/^{206}Pb$
						Middle Proterozoic rocks—*Continued*										
54	A-151a	Megacrystic granite of Joshua Parkway														
		NM102-163	5.5	262	61	3740	0.1153	0.22455	0.2	2.7632	0.5	0.08925	0.5	1306	1346	1409
		NM-63	4.3	321	74	6140	0.1106	0.22200	0.2	2.6978	0.5	0.08814	0.5	1292	1328	1385
		NM63-102	4.1	314	70	2040	0.1205	0.21991	0.2	2.6935	0.6	0.08883	0.6	1281	1327	1401
		M+163	3.4	298	70	1270	0.1272	0.21922	0.2	2.6935	0.3	0.08911	0.3	1278	1327	1407
57	A-153	Coarse-grained granite of Grayback Mountain														
		NM163	3.1	665	166	510	0.1633	0.21940	0.2	2.6962	0.3	0.08913	0.2	1279	1327	1406
		NM63-102	2.2	685	158	965	0.1349	0.21308	0.2	2.6262	0.7	0.08939	0.7	1245	1308	1413
		M102-63	2.3	792	167	1270	0.1188	0.19909	0.2	2.4376	0.4	0.08880	0.3	1170	1254	1400
		M-63	2.3	785	149	1111	0.1298	0.17704	0.2	2.1542	0.8	0.08825	0.7	1051	1166	1388

[1]Abbreviations: M, magnetic; NM, nonmagnetic; AB, abraded; ABRP, repeat analysis of abraded zircon fraction; RP, repeat analysis of fraction; LT, light; DK, dark. Numbers refer to size of grains of split in micrometers; +, greater than; -, less than or between two sizes.
[2]An informal unit possibly correlative with the Dick Rhyolite.

The second sample (751; appendix sample No. 16) examined from this plutonic complex is a gneissic biotite diorite from the northwestern part of the area of generally foliated plutonic rocks that form the eastern and central parts of the Poachie Range. Seven fractions of zircon were analyzed for this sample (table 2 and fig. 13). Six of these fractions fall along two separate discordia lines, both of which are anchored by a concordant fraction (NM102-163AB). The 1,706 Ma date of the concordant fraction, which was abraded, is the best estimate of the time of crystallization of this sample. The two discordia lines are interpreted tentatively to represent periods of Pb-loss that variably affected zircon grains. The discordia line with the older period of Pb-loss is defined by two of the three magnetic fractions and the smallest of the nonmagnetic fractions, a pattern roughly consistent with this interpretation. Uranium concentrations, however, show no particular correlation with the two discordia lines. Because the quartz diorite is older than the coarse-grained granite (most of unit Xcg), we interpret the peak of the regional metamorphism to be somewhat younger than 1,706 Ma, as the diorite has a well-developed superposed solid-state fabric.

Sample 749 (appendix sample No. 22) represents the granite at Burro Creek. This coarse-grained granite with equant feldspar megacrysts was originally thought to be part of the Signal Granite. Four zircon size fractions were analyzed and define a good discordia line (MSWD=0.6) with an upper intercept of 1,696±13 Ma, which is taken to be the crystallization age (table 2 and fig. 14). The relatively large error associated with this age in spite of the good fit is a result of the limited spread of the four points. The $^{207}Pb/^{206}Pb$ age of 1,686 Ma from the abraded fraction NM+163AB serves as a minimum estimate of the age of crystallization. This plutonic rock is interpreted to have been emplaced during the later stages of or after the main regional metamorphism because it lacks foliation.

Granite of Thorn Peak

Sample 1158 (appendix sample No. 35) represents muscovite-biotite and biotite granite that forms an elongate pluton west of the Santa Maria River. Four zircon fractions (table 2 and fig. 14) analyzed from this pluton are strongly discordant. $^{206}Pb/^{238}U$ ages range from 1,420 to 1,261 Ma despite moderate U concentrations of 430–580 ppm. A regression of the four fractions gives concordia intercepts of 1,681±32 and –30 ±206 Ma. This regression is rejected because the lower intercept age is negative, and the upper intercept date is less than any of the $^{207}Pb/^{206}Pb$ dates. A regression forced through 0 Ma and giving an upper intercept of 1,686±8 Ma (fig. 14) is preferred as the best estimate of a minimum crystallization age. This regression provides an average of the $^{207}Pb/^{206}Pb$ dates of the four fractions that range from 1,684 to 1,691 Ma. Three of the $^{207}Pb/^{206}Pb$ dates cluster between 1,688 and 1,691 Ma, and their average of 1,689±2 Ma probably provides a better minimum date. The presence of only local zones of foliated rock in this pluton indicates that it was emplaced after the main phase of regional deformation but before all deformation had ceased. Within statistical uncertainties this age is consistent with the 1,696 Ma age of the granite at Burro Creek, marking the declining stage of this deformation.

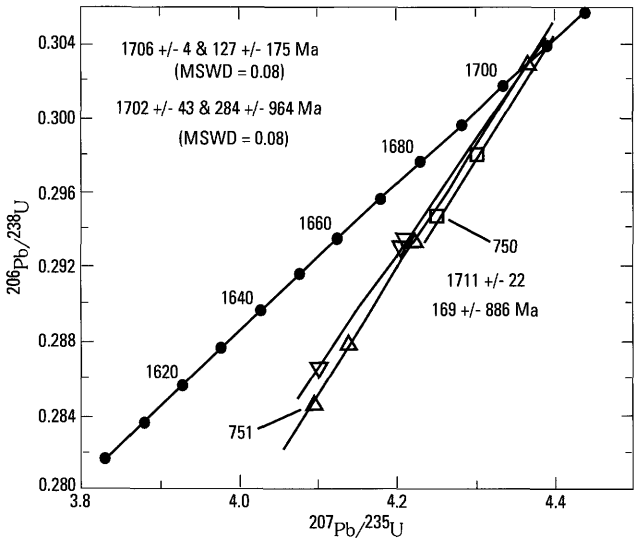

Figure 13. U-Pb concordia diagram for samples from the coarse-grained granite suite. Samples 750 (open squares) and 751 (open triangles) represent a gabbro and a quartz diorite, respectively (appendix sample Nos. 15 and 16). Age of the quartz diorite is best estimated by the one concordant zircon fraction at 1,706 Ma. The remaining six fractions appear to define two discordia lines (upright vs. inverted open triangles) having upper-intercept ages in agreement with the concordant fraction. The two discordia lines imply two distinct times of Pb-loss.

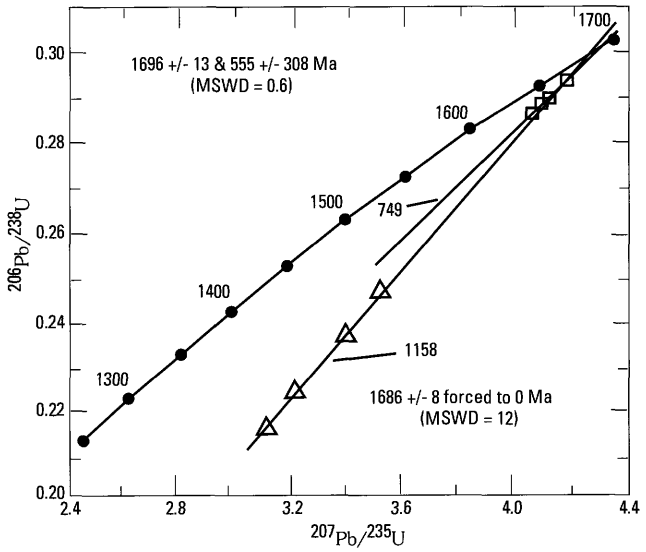

Figure 14. U-Pb concordia diagram for samples 749, the granite at Burro Creek (squares), and 1158, the granite of Thorn Peak (triangles) (appendix sample Nos. 22 and 35). Sample 749 is tentatively considered a member of the coarse-grained granite suite.

Gneissic Tonalite

Sample 1163 (appendix sample No. 38) represents a variably foliated pluton ranging in composition from melagranite to quartz diorite that intruded the mica schist and gneiss in the upper part of the Bagdad metamorphic belt, which are interpreted to be stratigraphically higher than the metarhyolite (as represented by samples 1161 and P-93-1 described previously). The gneissic structure in the unit is best developed near the Mountain Springs fault and was probably formed during movement along that zone during and after emplacement, perhaps as late as ≈1.4 Ga. The rock at the sample locality for sample 1163 has numerous small (<2 cm) xenoliths and a few as large as 10 cm in diameter. The six fractions analyzed by conventional U-Pb zircon technique (table 2) do not define a discordia line (fig. 15*A*). $^{207}Pb/^{206}Pb$ ages for these fractions range from 1,858 to 1,727 Ma and are perfectly correlated with the size range of the fractions; the oldest dates are from the largest and the youngest from the smallest fractions. This is a classic age pattern that results from the overgrowth of younger zircon over older cores. The only age information available from these data is that the pluton has a maximum age of 1,727 Ma and at least some of the inherited zircons are older than 1,858 Ma.

A limited number of grains from this sample were analyzed by the ion microprobe technique (table 2, ion probe data) using the SHRIMP I at the Research School of Earth Sciences, Australian National University. Three of ten grains analyzed (analyses 4.1, 5.1, 7) had cores with $^{207}Pb/^{206}Pb$ ages of 2,461, 2,489, and 2,576 Ma clearly identifying a latest Archean to earliest Proterozoic inherited component. The remaining grains analyzed had $^{207}Pb/^{206}Pb$ ages ranging from 1,762 to 1,643 Ma. Some of this age range is probably the result of analyzing areas of zircons that were part inherited and part younger zircon. Analyses 1, 7.2, and 10 giving $^{207}Pb/^{206}Pb$ dates of 1,762, 1,723, and 1,761 Ma, respectively, are interpreted to represent this circumstance. Alternatively, these three ages, especially the two at 1.76 Ga, might represent an additional, younger inherited component. At the time this work was done, we had no way to image the grains to be analyzed ahead of time to identify cores or zoning patterns and guide the positioning of the ion beam. Seven of the ten analyses giving younger dates define a discordia line with intercepts of 1,677±17 and 740±392 Ma (fig. 15*B*). These seven analyses include both normal and reversely discordant analyses; slightly reversely discordant analyses are not unusual with the ion microprobe technique because of the difficulty of determining highly accurate U concentrations. Note that errors associated with the U-Pb and Pb-Pb dates determined on the ion microprobe are much higher than those associated with conventionally determined U-Pb data. One grain (6) gave a concordant date of 1,685 Ma, and five of the seven analyses chosen for regression have $^{207}Pb/^{206}Pb$ dates from 1,669 to 1,690 Ma and average 1,681 Ma. Although it is obviously difficult to determine a precise crystallization age for sample 1163, an estimated age of 1,680±10 Ma seems probable from the ion microprobe analyses.

Middle Proterozoic Plutonic Rocks

Middle Proterozoic rocks discussed herein are Signal Granite, mafic granodiorite, granite of Olea Ranch, granite of Joshua Tree Parkway, and granite of Grayback Mountain.

Signal Granite and Mafic Granodiorite

Samples 1168 and 1164 (appendix sample Nos. 43 and 44) represent the Signal Granite, which forms a batholith-sized body of coarse-grained granite containing very large potassic feldspar

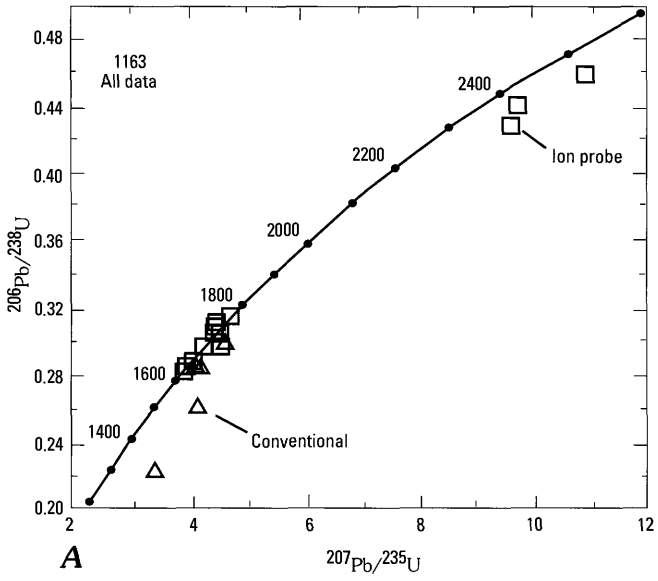

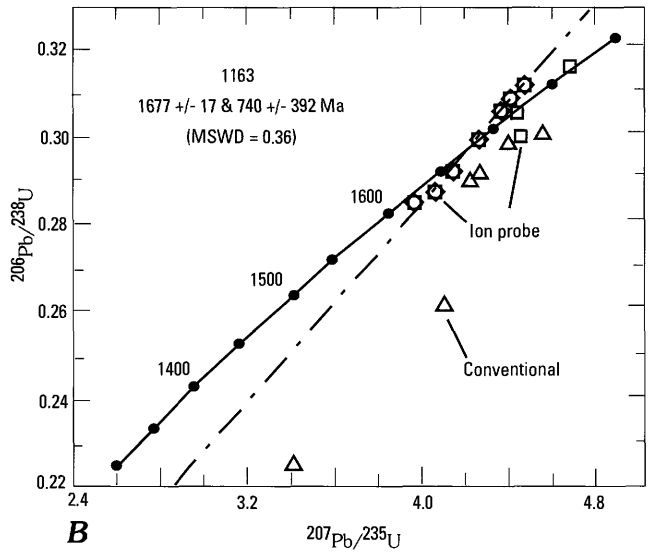

Figure 15. U-Pb concordia diagrams for sample 1163, a gneissic tonalite (appendix sample No. 38). Both conventionally determined (triangles) and ion microprobe (squares and octagons) data are shown for this sample. The conventionally determined U-Pb data do not define a discordia line but indicate inheritance of zircons older than 1,860 Ma by a magma younger than 1,730 Ma. All data are shown in figure 15*A*. The ion microprobe data indicate an inherited component of earliest Proterozoic to latest Archean age (fig. 15*A*). Seven of the ion microprobe data points (octagons, fig. 15*B*) can be interpreted to define a discordia line with an upper intercept of 1,677 Ma, which may provide an estimate of the crystallization age of the gneissic tonalite. See text for a more detailed discussion.

megacrysts. Sample 1164 was taken from near the old town site of Signal, the type locality for the unit. Sample 390 (appendix sample No. 47) is from a pluton 7 km long and 4 km wide of mafic granodiorite that is the same age to slightly older than the Signal Granite, based on field relations. Three zircon fractions from 390 define a discordia line with intercepts of 1,408±4 and –36±101. The negative lower intercept is unreasonable, so a discordia line forced through 0 Ma with an intercept of 1,410±3 Ma, the same as the average $^{207}Pb/^{206}Pb$ date of the three fractions, is preferred (table 2 and fig.16). Only two fractions each were analyzed for samples 1168 and 1164 of the Signal Granite (table 2). U-Pb data are moderately discordant but give a tight grouping of $^{207}Pb/^{206}Pb$ dates (1,407–1,409 Ma). A discordia line defined by all four fractions has intercepts of 1,408±15 and 12±169 Ma. Data for all three samples indicate that their crystallization ages are not resolvable; therefore, a combined discordia with intercepts of 1,410±4 and 26±54 Ma, defined by all seven fractions, is considered to provide the best estimate of the age of this batholith (fig. 16).

Granite of Olea Ranch

Sample 752 (appendix sample No. 50) represents a pluton of porphyritic granite and granodiorite containing oriented phenocrysts of potassic feldspar and located east of the Bagdad metamorphic belt. Sample 753 (appendix sample No. 51) comes from a pluton of coarse-grained biotite granite and granodiorite located along U.S. Highway 93 west of the Bagdad metamorphic belt. These plutons and other granitic bodies are grouped as the granite of Olea Ranch. They have no intrusive relations with the Signal Granite, which is 7 km to the west, but they are clearly intrusive into Early Proterozoic metamorphic and plutonic rocks. Only two zircon fractions were analyzed from each of these samples (table 2). The data from sample 752 are moderately discordant but have little spread in Pb/U ratios; data from sample 753 are less discordant but also have limited spread in Pb/U (fig. 16). $^{207}Pb/^{206}Pb$ dates for all fractions range only from 1,417 to 1,419 Ma. A composite discordia line defines an age of 1,416±5 and –51±103 Ma. The negative lower intercept is unacceptable so that a regression forced through 0 Ma and giving an upper intercept of 1,418±2 Ma is preferred. The analytical data, particularly the $^{207}Pb/^{206}Pb$ groupings of 1,407–1,411 Ma vs. 1,417–1,419 Ma, strongly indicate that the granite of Olea Ranch is slightly older than that of the Signal batholith.

Granite of Joshua Tree Parkway and Granite of Grayback Mountain

The eastern part of the map area contains two separate Middle Proterozoic granitic complexes. Sample A-151a (appendix sample No. 54) represents the megacrystic phase of the granite of Joshua Tree Parkway. The four zircon fractions from this sample are moderately discordant and have a very limited spread in Pb/U ratios; one fraction (NM-63) plots to the left of the other three (fig. 17). No discordia line can be fitted to these data. $^{207}Pb/^{206}Pb$ ages of 1,407 and 1,409 Ma for two of the fractions provide an estimate of the crystallization age. Sample A-153 (appendix sample No. 57) is from the coarse-grained phase of the granite of Grayback Mountain. The four zircon fractions from this sample are also moderately discordant but have an adequate spread in Pb/U ratios to define a discordia line with intercepts of 1,415±6 and 110±52 Ma. The oldest $^{207}Pb/^{206}Pb$ age from these fractions is 1,413 Ma and is consistent with the upper intercept age of 1,415 Ma being a reasonable estimate of the crystallization age of this sample. The ages of these two granitic complexes are not statistically different; the granite of Joshua Tree Parkway might be slightly younger, based on the $^{207}Pb/^{206}Pb$ ages.

The combined U-Pb ages for the Signal batholith, the granite of Olea Ranch, and the granites of Joshua Tree Parkway and Grayback Mountain range from only 1,407 to 1,418 Ma. The ages of the Signal batholith and the granite of Olea Ranch show that the intrusion of these Middle Proterozoic complexes did occur at distinct times. Other Middle Proterozoic intrusives in the region have similar ages. The Lawler Peak Granite north of Bagdad has an age of 1,413±3 Ma (Silver and others, 1980). Along the Colorado River east of the Whipple Mountains, about 60 km west of the Poachie region, the Parker Dam granite of Anderson (1983) and Anderson and Bender (1989), which texturally resembles the Signal Granite, has an age of 1,401±3 Ma; and the Bowmans Wash quartz monzodiorite of Anderson (1983) and Anderson and Bender (1989), which resembles the mafic granodiorite, has an age of 1,407±5 Ma (Anderson and Bender, 1989). In the Buckskin Mountains 20 km southwest of the Poachie region, one intrusive body has an age of about 1,400 Ma, and inclusions of coarse-grained granitic rock in the Miocene Swansea Plutonic Suite have an age of about 1,410 Ma (Wooden and Bryant, unpub. data, 1995; Bryant and others, 1996). About 30 km southeast of the Poachie region, granodiorite near Yarnell, Ariz., has an age of about 1,421 Ma (Wooden and Ed DeWitt, unpub. data, 1995). In the Poachie region map area (fig. 1), dated Middle Proterozoic intrusives compose about half of the exposed area of Proterozoic basement. If the undated granitic rocks are of Middle Proterozoic age, about two-thirds of the exposed basement would be that age. In this region, then, the Middle Proterozoic intrusive event is characterized by the episodic emplacement of discrete bodies ranging in size from batholiths to smaller plutons over a 20–30 m.y. interval. These intrusive bodies composed a large composite batholith comparable in size to the composite Mesozoic batholiths of the Western United States.

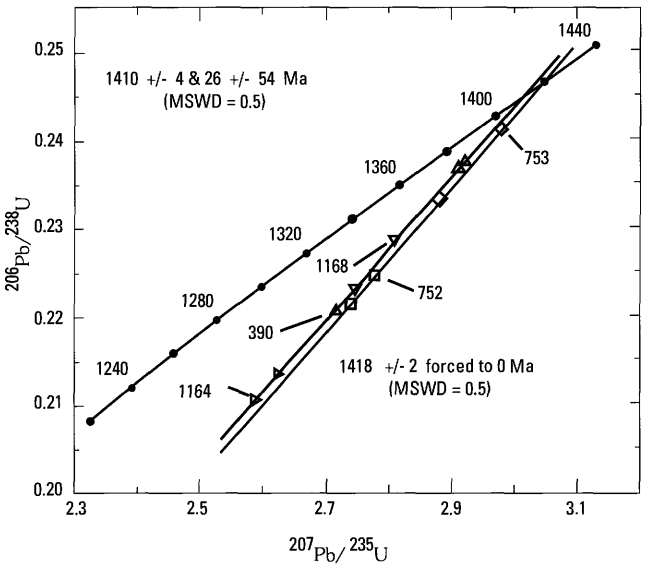

Figure 16. U-Pb concordia diagram for the Signal Granite (sample 1168, inverted triangles, and sample 1164, rotated triangles; appendix sample Nos. 43 and 44), the mafic granodiorite (sample 390, upright triangles; appendix sample No. 47), and the granite of Olea Ranch (sample 752, squares, and sample 753, diamonds; appendix sample Nos. 50 and 51). Ages of the Signal Granite and the mafic granodiorite are not resolvable from each other at 1,410 Ma. Combined data for the granite of Olea Ranch define an age of 1,418 Ma, which is resolvable from that of the Signal Granite and mafic granodiorite.

Geochemistry

Analytical Methods

Ten major elements were determined by wavelength dispersive X-ray fluorescence spectrometry (Taggart and others, 1990). In most samples Rb, Sr, Y, Zr, and Nb and, in some samples, Cr, Ni, Cu, Zn, Ba, La, and Ce were determined by energy-dispersive XRF using a Kevex 700 EDXRF spectrometer with a Kevex 7000 analyzer (King, 1990). Rare-earth elements were determined by inductively coupled plasma-mass spectrometry using an internal standard for drift correction, matrix effects, and oxide formation calculation (Lichte and others, 1987). Uranium and thorium were determined by delayed neutron counting following neutron irradiation of the sample (McKown and Knight, 1990). Fluorine and FeO were determined by ion-selective electrode potentiometry (Pribble, 1990) and potentiometric titration (Papp and others, 1990), respectively. In a few samples some rare earths and other minor elements were determined by instrumental neutron activation analysis (Baedecker and McKown, 1987). Rare-earth elements shown in diagrams are normalized to chondrite values from Hanson (1980).

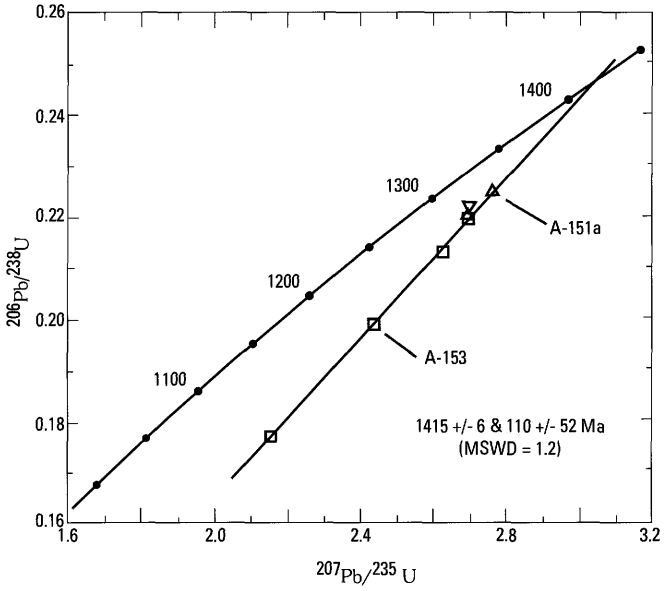

Figure 17. U-Pb concordia diagram for the granites of Joshua Tree Parkway (sample A-151a; appendix sample No. 54; triangles) and of Grayback Mountain (sample A-153; appendix sample No. 57; squares). The data for sample A-151a do not define a discordia line, and one of the fractions (inverted triangle) plots to the left of the others. A minimum age of about 1,408 Ma is indicated by the Pb-Pb ages of the zircons. The data for sample A-153 define a discordia line having an upper intercept at 1,415 Ma, which is taken to be the crystallization age.

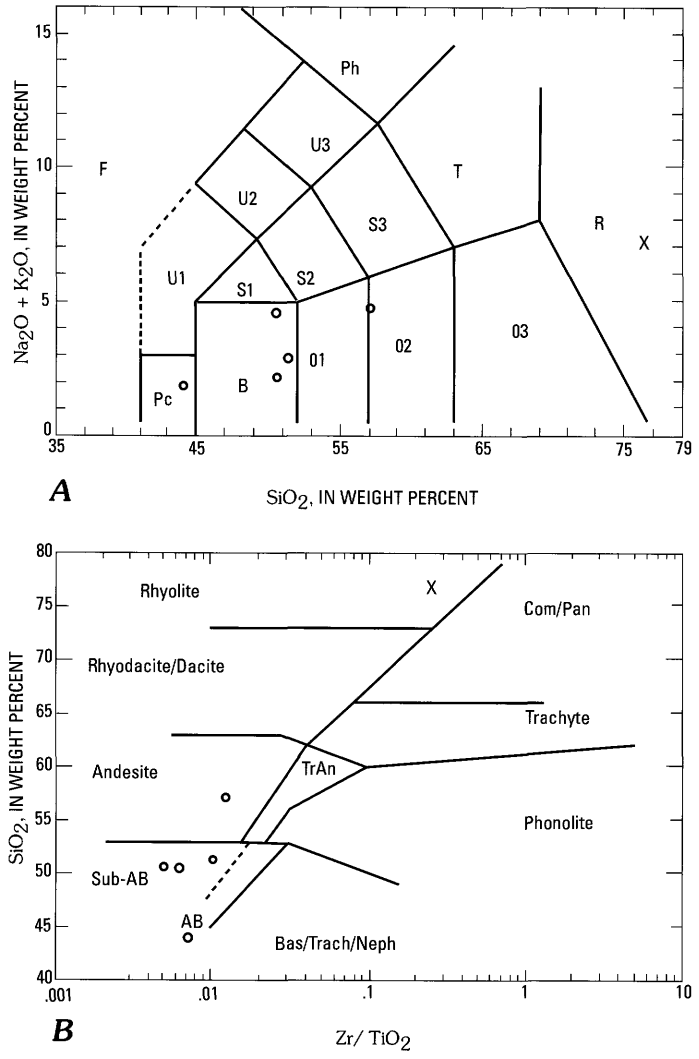

Figure 18. Early Proterozoic metavolcanic rocks. Circle, amphibolite; cross, rhyolite. *A*, SiO_2 vs. Na_2O+K_2O. Fields of interest: Pc, picrobasalt; B, basalt; AB, alkali basalt; 01, basaltic andesite; 02, andesite; R, rhyolite (LeBas and others, 1986). *B*, Zr/TiO_2 vs. SiO_2 (Floyd and Winchester, 1978).

Metamorphic Rocks

All but one of the samples of metamorphic rocks analyzed are of the Bagdad metamorphic belt. Analyses are from two samples of metasedimentary rock, one of which is from a cupola in the Signal batholith, from which we attempted to obtain zircon for dating, the massive metarhyolite we dated, and five samples of amphibolite (table 3).

The samples of metasedimentary rock are mica gneisses derived from shale (appendix sample No. 1) and sandstone (appendix sample No. 2), and they have Th/U ratios of 8.3 and 6.4, respectively. These ratios are characteristic of rocks of or derived from the Mojave crustal province (Wooden and DeWitt, 1991). The metashale shows strong light-rare-earth element vs. heavy-rare-earth element (LREE/HREE) enrichment [(La/Yb)CN=35.8], and the metasandstone shows moderate enrichment [(La/Yb)CN=10.0]. Both rock types have small negative Eu anomalies. The REE pattern for sample 2 resembles that of average upper crust (Taylor and McLennan, 1981), except that it falls below the average upper crustal curve. It also resembles the pattern of many post-Archean shales. This sample shows a flat LREE-HREE pattern compared to sample 1, which shows an overall negative slope.

The amphibolites generally have the composition of basalts based on both their alkali:silica ratios and the ratio of the less mobile elements of zirconium divided by TiO_2 plotted against SiO_2 (fig. 18*A*, *B*). Sample 1159a (appendix sample No. 3) from an interlayer in the metasedimentary rocks plots in the picrobasalt field in fig. 18*A* and the alkali basalt field in fig. 18*B*. The latter name is invalid because the sample has a low alkali content. This rock is iron-rich (fig. 20*B*). Sample 633 (appendix sample No. 5), a metabasalt from a sliver of the Bagdad metamorphic belt included in the granite of Thorn Peak, is also iron-rich. Sample M-81 (appendix sample No. 7) from the quartz-bearing amphibolite marker layer at the top of the Dick metarhyolite is derived from andesite (fig. 18). The amphibolites are generally calcic but range to alkali calcic (fig. 19*A*) and have average K_2O concentrations (fig. 19*B*) and low Rb and moderate Sr contents (fig. 20*C*). Th/U ratios range from 2 to 4 and average 2.5 (fig. 20*D*). These rocks have a small light-rare-earth vs. heavy-rare-earth element (LREE/HREE) enrichment [(La/Yb)CN=1.3–4.7]. The sample (633; appendix sample No. 5) having the very low enrichment has a small negative europium anomaly (fig. 21*A*).

The metarhyolite sample (appendix sample No. 8) is a calc-alkalic rhyolite and is very sodic (fig. 19*A*, *B*). It has lower Rb and Sr concentrations and a lower Th/U ratio (2.5) than most of the plutonic rocks in the Poachie region (figs. 19*A*, 20*C*, *D*). It is more zircon-rich than the plutonic rocks of similar high SiO_2 concentrations. These chemical characteristics are similar to those of both the Dick Rhyolite and the King Peak Rhyolite in the Bagdad area (C.M. Conway, oral commun., 1995). The metarhyolite shows a small light-rare-earth element vs. heavy-rare-earth element (LREE/HREE) enrichment [(La/Yb) CN=5.1], and a moderate negative Eu anomaly (fig. 21*A*). The total REE concentration of the rock is high (REE=332 ppm).

Plutonic Rocks

Early and Middle Proterozoic plutonic rocks from the Poachie region have many chemical similarities consistent with derivation from the same source regions under similar conditions. Early Proterozoic (1,710–1,680 Ma) plutonic rocks were emplaced over a period that spanned the main episode of orogeny, plutonism, and metamorphism (tables 4 and 5). Middle Proterozoic (1,418–1,410 Ma) rocks from several plutons were emplaced in a shorter period during a second episode of widespread plutonism (tables 6 and 7).

Early Proterozoic Plutonic Rocks

Early Proterozoic plutonic rocks described here are coarse-grained granitic rocks and associated diorite and gabbro, granite of Thorn Peak, and gneissic tonalite.

Table 3. Major-oxide and trace-element concentrations in some supracrustal rocks from the Bagdad metamorphic belt in the Poachie region and of one metasediment from cupola in the Signal batholith (sample 1166).

[App., appendix; nd, not determined; LOI, loss on ignition; FeTO3, total Fe as Fe_2O_3]

Unit	Metasedimentary rocks		Metavolcanic rocks Amphibolites					Metarhyolite
App. No.	1	2	3	4	5	6	7	8
Field No.	1154	1166	1159a	W-419	633	M-96	M-81	1161
Lab No.	D-266709	D-278413	D-568687	D-568689	D-568688	D-568690	D-568687	D-266707
Job No.	RV13	SD65	WB23	WB23	WB23	WB23	WB23	RV13
Major-oxide concentration, in weight percent[1]								
SiO_2	61.1	71.5	43.6	50.0	50.3	50.6	56.8	75.2
Al_2O_3	17.9	13.8	14.7	12.7	13.8	15.9	15.0	11. 4
FeTO3	8.89	3.43	18.0	12.2	15.7	9.93	8.95	3.49
MgO	2.15	.98	6.63	10.1	4.09	5.98	4.06	.77
CaO	.41	2.13	9.84	9.61	8.74	11.4	8.31	.32
Na_2O	1.17	2.67	1.35	2.00	4.27	2.29	4.16	3.53
K_2O	3.50	3.58	0.49	0.17	0.29	0.60	0.57	3.39
TiO_2	.79	.41	2.73	1.31	1.90	1.33	1.12	.23
P_2O_5	.11	.07	0.53	0.39	0.25	0.31	0.26	.05
MnO	.46	.06	0.97	0.24	0.23	0.16	0.16	.04
LOI	2.87	.59	0.60	0.43	0.38	0.55	0.35	.76
Total	96.48	98.63	98.84	99.15	99.95	99.05	99.75	98.42
[2]FeO	1.24	2.66	nd	nd	nd	nd	nd	2.28
[2]F	.08	.04	nd	nd	nd	nd	nd	.08
Trace-element concentration, in parts per million[3]								
Nb	12	16	11	10	<10	11	16	31
Rb	196	152	22	10	>10	20	<10	67
Sr	108	234	93	360	178	340	198	31
Zr	200	234	180	120	116	124	162	579
Y	39	38	37	14	34	18	28	161
Ba	nd	nd	108	66	48	116	100	nd
Ce	nd	nd	35	<30	40	34	<30	nd
La	nd	nd	<30	<30	<30	<30	<30	nd
Cu	nd	nd	33	54	10	43	25	nd
Ni	nd	nd	118	275	49	62	26	nd
Zn	nd	nd	138	92	91	102	56	nd
Cr	nd	nd	116	690	60	158	79	nd
Trace-element concentration, in parts per million[4, 5]								
Ba	770	890	130	96	66	130	110	780
Y	9.9	nd	nd	nd	nd	nd	nd	71.5
La	53.7	60.4	15.9	12.7	7.3	14.6	16.7	55.2
Co	nd	nd	52.7	52.0	38.1	36.4	24.2	nd
Sc	nd	nd	35.0	23.8	36.4	32.0	22.5	nd
Cs	nd	nd	2.8	1.1	0.41	3.13	0.43	nd
Sb	nd	nd	0.54	0.26	0.97	0.97	0.41	nd
Ta	nd	nd	0.796	0.86	0.42	0.71	0.819	nd
Hf	nd	nd	3.72	2.6	2.92	2.64	3.59	nd
Ce	112	119	37.7	31.1	19.1	32.6	34.7	115
Pr	13.6	13.4	nd	nd	nd	nd	nd	15.0
Nd	47.0	46.1	24	16	14	17	18	67.6
Sm	8.90	9.04	6.85	4.19	4.41	4.17	4.42	17.4
Eu	1.67	1.40	2.16	1.1	1.30	1.27	1.24	2.94
Gd	8.40	5.85	nd	nd	nd	nd	nd	19.00
Tb	1.00	.92	1.14	0.65	0.961	0.59	0.68	3.00
Dy	4.60	5.88	nd	nd	nd	nd	nd	16.60
Ho	.72	1.21	nd	nd	nd	nd	nd	3.10

Table 3—Continued. Major-oxide and trace-element concentrations in some supracrustal rocks from the Bagdad metamorphic belt in the Poachie region and of one metasediment from cupola in the Signal batholith (sample 1166).

Unit	Metasedimentary rocks		Metavolcanic rocks Amphibolites					Metarhyolite
App. No.	1	2	3	4	5	6	7	8
Field No.	1154	1166	1159a	W-419	633	M-96	M-81	1161
Lab No.	D-266709	D-278413	D-568687	D-568689	D-568688	D-568690	D-568687	D-266707
Job No.	RV13	SD65	WB23	WB23	WB23	WB23	WB23	RV13
Trace-element concentration, in parts per million[4, 5]—*Continued*								
Er	2.30	3.89	nd	nd	nd	nd	nd	8.30
Tm	.23	.62	nd	nd	nd	nd	nd	1.10
Yb	1.00	4.02	3.51	2.1	3.82	2.2	2.4	7.20
As	nd	nd	0.92	1.0	1.5	<0.700	1.3	
Lu	.22	.59	0.49	0.29	0.52	0.30	0.34	1.04
[6]Th	21.3	26.2	1.5	1.9	1.6	2.2	4.36	12.1
[6]U	2.58	4.8	0.5	0.96	0.60	0.55	1.3	4.76

[1] Major oxides determined by wavelength dispersive X-ray fluorescence: A.J. Bartel, K. Stewart, J.E. Taggart, E. Robb, analysts.
[2] FeO determined by potentiometric titration and F by ion-selective electrode potentiometry: E. Brandt, S. Roof, G. Mason, J.H. Christie, analysts.
[3] Trace elements determined by energy dispersive X-ray fluorescence: L. Evans, R.R. Larson, B.W. King, analysts.
[4] Rare earths determined by inductively coupled plasma–mass spectrometry in Nos. 1, 2, 8: A. Meier, D. Fey, P.H. Briggs, J.G. Crock, analysts.
[5] Rare earth and trace elements determined by instrumental neutron activation analysis in Nos. 3–7: G.A. Wandless, analyst.
[6] Th and U determined by delayed neutron activation analysis in Nos.1, 2, 8: R.B. Vaughn, D.M. McKown, analysts.

Coarse-Grained Granitic Rocks

Rocks included in the suite mapped as the coarse-grained granite unit have silica concentrations ranging from 46 to 70 percent SiO_2 (table 4). They range from calcic for the mafic rocks to alkalic in some intermediate rocks. Most of the analyzed rocks having a SiO_2 content >60 percent are mostly alkali-calcic but range into the alkalic and calc-alkalic fields (fig. 19*A*). They have normal SiO_2 vs. K_2O/Na_2O+K_2O ratios (fig. 19*B*).

The coarse-grained granitic rocks of the Poachie region have the same degree of alkalinity as suites 1, 2, and 4 (pretectonic biotite granodiorite and granite, pre- to syntectonic hornblende-biotite tonalite and granodiorite, and syn- to posttectonic granodiorite to granite, respectively) in the Prescott region (DeWitt, 1989). Calcic rocks in the Poachie region are few and have silica concentrations <55 weight percent SiO_2, whereas in the Prescott region suite 3 (pre- to late tectonic biotite-hornblende granodiorite), particularly, has calcic rocks at higher SiO_2 concentrations. Many of the plutons in the Prescott region are older than 1.7 Ga and older than any dated in the Poachie region. According to Anderson and others (1993) 1.7 Ga granitic rocks in the Mojave province are alkali-calcic in contrast to the alkalic, alkali-calcic, and calc-alkalic nature of those in the Poachie region. In the SiO_2 vs. Na_2O+K_2O diagram (fig. 19*A*) the Early Proterozoic rocks of the Poachie region form a field that overlaps that of the syn- and posttectonic plutons of the Prescott belt and the syntectonic plutons northwest of the Prescott belt of P. Anderson (1989b) but extends to more alkalic and potassic compositions than any rocks shown in those diagrams.

The coarse-grained silicic granitic rocks have Rb/Sr ratios and Rb concentrations (fig. 20*C*; table 4) similar to syn- and posttectonic plutons of suite 4 in the Prescott region (DeWitt, 1989), and they are especially similar to the granite of Iron Springs and the Crazy Basin Quartz Monzonite. Some rocks of the coarse-grained granite unit are more mafic than those plutons and have higher Sr concentrations.

However, the coarse-grained granitic unit of the Poachie area has higher Zr, Ba, and Ce concentrations but similar La concentrations compared to the Crazy Basin, and Iron Springs plutons (table 4; DeWitt, 1989). Our data agree with a trend of increasing incompatible minor element concentrations, increasing K concentration, and alkalinity of plutonic rocks in a westward direction during the ≈1,700 Ma episode of plutonic activity (fig. 19; DeWitt, 1989). We do not have enough information to allow us to divide the Early Proterozoic plutonic rocks of the Poachie region into suites, as has been done in the Prescott region (DeWitt, 1989), although our geochronological data indicate that the plutonic rocks were emplaced over a time ranging from 1,710 to 1,680 Ma, a time span that is shorter than the 1,750–1,700 Ma time span of pluton emplacement in the Prescott region (DeWitt, 1989; Karlstrom and others, 1987). Our chemical data indicate no simple chemical progression with time in the Early Proterozoic rocks of the Poachie region; the younger rocks range from alkalic to calc-alkalic (fig. 19*A*).

Chondrite-normalized REE patterns for the rocks of the coarse-grained granite suite (table 4) suggest that the four analyzed gabbros (appendix samples 10–15) may have been derived by a small amount of partial melting of a mantle peridotite. In the gabbros LREE/HREE enrichment (La/Yb)CN ranges from 4.5 to 7.1 (fig. 21*B*), and in the more silicic rocks of the suite that value ranges from 9.5 to 24 (fig. 21*C*). Some of the more silicic rocks have small negative europium anomalies (fig. 21*C*), perhaps due to fractionation of plagioclase from a parent magma. Sample W-301 (appendix sample No. 19), a feldspar-rich and quartz-poor rock, has a prominent positive europium anomaly, probably due to accumulation of plagioclase in its magma. These variations probably indicate the range of starting materials and processes of differentiation in the development of this complex suite of rocks. Total rare-earth element concentrations range from 61–77 ppm in the gabbros to 319–421 ppm in the granitic rocks of the suite.

Table 4. Major-oxide and trace-element concentrations in Early Proterozoic gabbro and coarse-grained granite from the Poachie region.

[nd, not determined; LOI, loss on ignition; FeTO3, total Fe as Fe_2O_3]

	Small bodies of gabbro in coarse-grained granite, and Signal Granite						Coarse-grained granitic rocks									
Appendix No	10	11	12	13	14	15	17	18	19	20	21	22	23	24	25	26
Field No.	450	907	W-61	W-307	1165	750	192	1137	W-301	1167	552a	749	1132a	212	713	680
Lab No.	D-3637772	D-568685	D-363771	D-363773	D-78412	D-259526	D-259527	D-363778	D-363777	D-278414	D-363781	D-259524	D-363779	D-363780	D-363784	D-363776
Job No.	UD76 WB47	WB23	UD76	UD76	SD65 WB47	SC97 RP40 WB47	RP40 SC97 WB47	UD76	UD76	SD65	UD76	RP40	UD76	UD76	UD76	UD76
Major oxide concentration, in weight percent[1]																
SiO_2	45.9	46.5	49.5	49.8	51.3	52.0	55.2	56.4	60.8	62.0	62.3	62.4	63.8	65.5	67.8	70.6
Al_2O_3	17.5	16.4	14.9	16.2	16.0	16.1	18.3	18.1	18.2	16.0	18.0	16.1	16.4	15.0	14.0	14.7
FeTO3	10.6	12.2	11.4	11.1	7.83	8.75	7.78	6.85	4.06	6.37	3.83	5.22	4.64	5.17	4.90	1.99
MgO	7.80	7.93	7.58	6.39	7.95	7.83	2.64	2.39	0.85	2.41	0.70	1.89	1.73	1.89	1.12	0.24
CaO	13.50	9.49	9.00	10.0	10.8	10.3	6.18	5.02	2.67	3.52	2.89	4.06	3.68	3.43	2.20	0.77
Na_2O	1.58	2.57	2.6	3.14	2.99	2.6	4.39	4.15	4.65	2.97	4.4	3.58	4.55	3.29	2.75	3.45
K_2O	0.34	0.36	1.9	0.29	1.26	0.64	2.12	3.31	5.36	3.43	5.48	3.73	3.09	3.42	4.52	6.49
TiO_2	0.66	1.65	1.11	1.7	0.51	0.68	1.45	1.19	0.74	0.93	0.71	0.83	0.66	0.76	0.76	0.19
P_2O_5	0.12	0.50	0.32	0.6	0.11	0.1	0.52	0.39	0.21	0.37	0.18	0.35	0.18	0.27	0.29	<.05
MnO	0.19	0.17	0.20	0.18	0.13	0.15	0.11	0.09	0.11	0.09	0.09	0.07	0.11	0.08	0.10	0.05
LOI	0.88	1.39	0.97	0.85	0.93	0.99	0.81	0.81	0.47	0.77	0.40	0.68	0.71	0.54	0.87	0.45
Total	98.19	99.16	98.41	99.4	98.88	91.15	98.69	97.7	98.12	98.08	98.58	98.23	98.84	98.81	98.44	98.53
[2]FeO	nd	nd	nd	nd	6.56	5.84	4.3	nd	nd	4.08	nd	2.7	nd	nd	nd	nd
[2]F	nd	nd	nd	nd	.05	.15	.12	nd	nd	.05	nd	.12	nd	nd	nd	nd
Trace-element concentration, in parts per million[3]																
Nb	<10	<10	<10	15	<10	9	12	12	<10	<10	12	24	11	<10	17	18
Rb	12	15	88	10	99	28	93	146	190	138	147	149	106	145	191	324
Sr	267	385	636	546	232	317	640	697	377	559	368	648	306	481	254	63
Zr	43	67	95	135	69	85	450	398	568	245	592	259	243	210	318	245
Y	16	13	23	33	23	25	28	26	26	21	32	41	26	22	52	29
Ba	260	215	815	208	250	320	1830	4090	4650	nd	3220	nd	849	928	1220	458
Ce	33	<30	75	122	nd	nd	nd	156	77	nd	135	nd	90	128	180	175
La	9	<30	25	50	nd	nd	nd	65	9	nd	42	nd	48	58	83	105
Cu	62	48	31	16	nd	nd	nd	26	3	nd	10	nd	17	13	17	<2
Ni	52	164	147	118	96	100	nd	18	<5	nd	<5	nd	22	20	8	<5
Zn	71	74	101	90	61	60	nd	98	71	nd	80	nd	97	75	94	43
Cr	342	88	271	87	355	237	nd	27	<20	nd	<20	nd	27	30	<20	<20
Trace-element concentration, in parts per million[4, 5]																
Co	43.6	52.9	nd	nd	35.8	40.0	17.0	14.8	3.18	nd	nd	nd	nd	nd	nd	nd
Cs	0.32	0.28	nd	nd	3.64	1.1	5.07	6.09	6.27	nd	nd	nd	nd	nd	nd	nd
Hf	1.3	1.7	nd	nd	1.71	2.0	12.0	9.05	15.5	nd	nd	nd	nd	nd	nd	nd

Table 4—Continued. Major-oxide and trace-element concentrations in Early Proterozoic gabbro and coarse-grained granite from the Poachie region.

	Small bodies of gabbro in coarse-grained granite, and Signal Granite						Coarse-grained granitic rocks									
Appendix No.	10	11	12	13	14	15	17	18	19	20	21	22	23	24	25	26
Field No.	450	907	W-61	W-307	1165	750	192	1137	W-301	1167	552a	749	1132a	212	713	680
Lab No.	D-3637772	D-568685	D-363771	D-363773	D-78412	D-259526	D-259527	D-363778	D-363777	D-278414	D-363781	D-259524	D-363779	D-363780	D-363784	D-363776
Job No.	UD76 WB47	WB23	UD76	UD76	SD65 WB47	SC97 RP40 WB47	RP40 SC97 WB47	UD76	UD76	SD65	UD76	RP40	UD76	UD76	UD76	UD76
Trace-element concentration, in parts per million[4, 5]—*Continued*																
Sb	<.08	<0.08	nd	nd	<0.18	0.15	0.14	0.16	<0.17	nd	nd	nd	nd	nd	nd	nd
Ta	0.25	0.50	nd	nd	0.60	0.32	0.90	0.62	0.804	nd	nd	nd	nd	nd	nd	nd
Sc	43.3	24.3	nd	nd	32.7	34.4	19.0	14.5	11.3	nd	nd	nd	nd	nd	nd	nd
Y	nd	nd	nd	nd	nd	19.9	31.8	nd	nd	nd	nd	40.6	nd	nd	nd	nd
La	11.2	10.7	nd	nd	16.4	11.7	67.3	75.0	31.4	99.4	nd	58.9	nd	nd	nd	nd
Ce	26	22.2	nd	nd	30.2	26.7	137	134	61.2	191	nd	144	nd	nd	nd	nd
Pr	nd	nd	nd	nd	3.7	2.5	15.3	nd	nd	21.9	nd	17.3	nd	nd	nd	nd
Nd	13	14	nd	nd	13.9	13.5	61.3	48	28	76.2	nd	72.3	nd	nd	nd	nd
Sm	2.8	3.83	nd	nd	2.93	3.0	10.8	8.83	6.73	12.3	nd	10.0	nd	nd	nd	nd
Eu	0.89	1.49	nd	nd	0.76	1.12	3.09	2.48	4.60	2.19	nd	2.76	nd	nd	nd	nd
Gd	nd	nd	nd	nd	2.66	3.8	9.2	nd	nd	7.46	nd	10.7	nd	nd	nd	nd
Tb	0.40	0.58	nd	nd	0.42	>0.5	1.2	0.90	0.78	1	nd	1.9	nd	nd	nd	nd
Dy	nd	nd	nd	nd	2.75	3.4	6.8	nd	nd	5.54	nd	8	nd	nd	nd	nd
Ho	nd	nd	nd	nd	0.55	0.73	1.27	nd	nd	0.89	nd	1.49	nd	nd	nd	nd
Er	nd	nd	nd	nd	1.62	2.1	3.0	nd	nd	1.97	nd	3.8	nd	nd	nd	nd
Tm	nd	nd	nd	nd	0.24	0.3	0.42	nd	nd	0.19	nd	0.53	nd	nd	nd	nd
Yb	1.3	1.6	nd	nd	1.54	2.2	2.6	2.1	2.2	0.85	nd	3.7	nd	nd	nd	nd
Lu	0.21	0.22	nd	nd	0.24	0.3	0.33	0.29	0.33	0.1	nd	0.52	nd	nd	nd	nd
[6]Th	1.1	0.89	3.1	1.8	<2.5	1.8	4.09	4.1	3.7	11.9	6.83	11.9	5.06	12.3	19.7	21.6
[6]U	0.13	0.19	0.67	0.52	2.41	0.69	1.56	1.13	2.91	2.02	1.14	2.74	1.58	1.53	3.24	2.72

[1]Major oxides determined by wavelength dispersive X-ray fluorescence spectroscopy: D.F. Siems, J.E. Taggart, A.J. Bartel, K. Stewart, E. Robb, J.S. Mee, analysts.

[2]FeO determined by potentiometric titration and F determined by ion-selective electrode potentiometry: E. Brandt, J. Sharkey, G. Mason, J.H. Christie, analysts

[3]Trace elements determined by energy-dispersive X-ray fluorescence: J.R. Evans, B.W. King, R. Johnson, S. Fleming, analysts. Ba, Ni, Zn, and Cr in samples 14, 15, and 17 determined by instrumental neutron activation analysis: C.A. Palmer, G.A. Wandless, analysts.

[4]Rare earths determined by inductively coupled plasma-mass spectrometry: J.G. Crock, K. Kennedy, A. Meir, analysts.

[5]Rare earths and trace elements in samples 10, 15, and 19 by instrumental neutron activation analysis: C.A. Palmer, G.A Wandless, analysts.

[6]Th and U determined by delayed neutron counting: E.J. Knight, R.B. Vaughn, D. McKown, analysts.

Table 5. Major-oxide and trace-element concentrations in Early Proterozoic fine-grained granite, granite of Thorn Peak, and gneissic tonalite and other Proterozoic granites of the Poachie region.

[nd, not determined; LOI, loss on ignition; FeTO3, total Fe as Fe_2O_3]

	Fine-grained granite	Granite of Thorn Peak					Gneissic tonalite			Other Proterozoic granitic rocks	
Appendix No.	27	31	32	33	34	35	36	37	38	39	40
Field No.	172b	636a	175b	A-10	A-21	1158	A-108	A-111	1163	A-85	A-152
Lab No.	D-363764	D-363770	D-363766	D-363767	D-363769	D-266705	D-366774	D-363775	D-278411	D-363768	D-327701
Job No.	UD76	UD76	UD76	UD76	UD76 WB47	RV13	UD76 WB47	UD76	SD65	UD76	TG29
Major-oxide concentration, in weight percent[1]											
SiO_2	74.7	68.7	68.7	69.7	71.6	73.8	52.6	53.4	61.0	65.9	66.5
Al_2O_3	13.5	14.1	14.1	14.0	14.0	13.5	16.7	15.1	16.0	13.6	14.9
FeTO3	1.06	4.64	4.7	4.08	2.09	1.51	8.66	10.3	6.22	6.47	4.83
MgO	0.19	1.1	1.08	0.96	0.45	0.48	4.61	5.81	2.93	1.4	1.12
CaO	0.93	2.00	1.85	1.81	1.32	1.20	5.68	7.55	3.52	3.27	2.66
Na_2O	3.39	2.32	2.14	2.45	2.96	2.67	4.3	3.0	2.72	2.44	3.09
K_2O	5.09	4.26	4.63	4.63	5.33	4.72	2.82	1.73	3.67	3.86	3.67
TiO_2	0.08	0.73	0.74	0.62	0.27	0.22	1.22	1.03	0.98	1.13	0.83
P_2O_5	<.05	0.27	0.3	0.23	0.13	0.14	0.91	0.32	0.59	0.54	0.53
MnO	0.03	0.13	0.12	0.1	0.06	0.07	0.12	0.14	0.09	0.14	0.08
LOI	0.55	1.05	1.00	0.89	0.72	0.89	1.55	1.39	1.80	0.66	0.92
Total	99.02	98.25	98.36	98.58	98.41	98.31	97.62	98.38	97.72	98.75	97.93
[2]FeO	nd	nd	nd	nd	nd	0.67	nd	nd	3.65	nd	2.05
[2]F	nd	nd	nd	nd	nd	0.05	nd	nd	0.09	nd	0.08
Trace-element concentration, in parts per million[3]											
Nb	21	30	25	21	20	15	>10	12	13	20	29
Rb	386	207	311	241	325	286	110	71	193	155	181
Sr	64	242	244	204	132	151	1380	694	635	286	312
Zr	74	296	286	241	171	93	294	102	261	282	354
Y	51	59	58	52	39	37	23	24	26	55	52
Ba	324	1020	1090	915	753	nd	1100	561	nd	1100	nd
Ce	74	175	172	157	122	nd	193	87	nd	172	nd
La	39	77	63	69	52	nd	106	31	nd	82	nd
Cu	4	33	16	21	7	nd	81	83	nd	18	nd
Ni	<5	7	<5	9	<5	nd	91	106	nd	6	nd
Zn	33	85	106	95	52	nd	108	81	nd	108	nd
Cr	<20	<20	<20	<20	<20	nd	140	155	nd	<20	nd
Trace-element concentration, in parts per million[4]											
Co	nd	nd	nd	nd	2.70	nd	49.6	nd	nd	nd	nd
Cs	nd	nd	nd	nd	18.9	nd	9.06	nd	nd	nd	nd
Hf	nd	nd	nd	nd	5.06	nd	7.05	nd	nd	nd	nd
Sb	nd	nd	nd	nd	0.12	nd	0.31	nd	nd	nd	nd
Ta	nd	nd	nd	nd	2.75	nd	0.83	nd	nd	nd	nd
Sc	nd	nd	nd	nd	5.93	nd	18.0	nd	nd	nd	nd
La	nd	nd	nd	nd	49.3	26.9	94.6	nd	41.1	nd	99
Ce	nd	nd	nd	nd	94.7	55.2	183	nd	86.4	nd	200
Pr	nd	nd	nd	nd	nd	7.2	nd	nd	10.8	nd	22
Nd	nd	nd	nd	nd	37.0	24.6	82.3	nd	42.0	nd	88
Sm	nd	nd	nd	nd	4.87	4.8	15.3	nd	8.21	nd	15
Eu	nd	nd	nd	nd	1.05	1.21	3.60	nd	2.26	nd	2.6

Table 5—Continued. Major-oxide and trace element concentrations in Early Proterozoic fine-grained granite, granite of Thorn Peak, and gneissic tonalite and other Proterozoic granites of the Poachie region.

	Fine-grained granite	Granite of Thorn Peak					Gneissic tonalite			Other Proterozoic granitic rocks	
Appendix No.	27	31	32	33	34	35	36	37	38	39	40
Field No.	172b	636a	175b	A-10	A-21	1158	A-108	A-111	1163	A-85	A-152
Lab No.	D-363764	D-363770	D-363766	D-363767	D-363769	D-266705	D-366774	D-363775	D-278411	D-363768	D-327701
Job No.	UD76	UD76	UD76	UD76	UD76 WB47	RV13	UD76 WB47	UD76	SD65	UD76	TG29
Trace-element concentration, in parts per million[4]—*Continued*											
Gd	nd	nd	nd	nd	nd	4.6	nd	nd	6.18	nd	11
Tb	nd	nd	nd	nd	0.978	0.6	1.4	nd	0.88	nd	1.7
Dy	nd	nd	nd	nd	nd	4.3	nd	nd	4.98	nd	10.0
Ho	nd	nd	nd	nd	nd	0.81	nd	nd	0.90	nd	1.8
Er	nd	nd	nd	nd	nd	2.3	nd	nd	2.36	nd	5.2
Tm	nd	nd	nd	nd	nd	0.34	nd	nd	0.28	nd	0.69
Yb	nd	nd	nd	nd	3.71	2.4	2.6	nd	1.04	nd	4.2
Lu	nd	nd	nd	nd	0.519	0.35	0.37	nd	0.12	nd	nd
[5]Th	30.2	16.1	17.5	20.8	23.9	9.34	11.9	3.2	2.5	<2.5	17.9
[5]U	5.03	3.04	3.93	3.63	3.78	1.81	2.90	1.13	2.78	3.94	3.3

[1]Major oxides determined by energy dispersive X-ray fluorescence: D.F. Siems, J.E. Taggart, A.J. Bartel, K. Stewart, analysts.
[2]FeO determined by potentiometric titration and F by ion-selective electrode potentiometry: E. Brandt, S. Roof, C. Papp, J. Sharkey, analysts.
[3]Minor elements determined by energy dispersive X-ray fluorescence: J.R. Evans, R.R. Larson, analysts.
[4]Rare earth determined by inductively coupled plasma–mass spectrometry: J.G. Crock, K. Kennedy, G. Riddle, analysts. Rare earths and minor elements determined by instrumental neuron activation analysis in Nos. 34 and 36: C.A. Palmer, analyst.
[5]Th and U determined by delayed neutron counting: E.J. Knight, R.B. Vaughn, D.M. McKown, analysts.

Granite of Thorn Peak

The granite of Thorn Peak has a distinctive chemical character, and analytical data for it form a cluster of points on the various chemical diagrams (table 5; figs. 19, 20). It has 70–75 weight percent SiO_2, is slightly Mg rich, and is generally calc-alkalic, somewhat more calcic than rocks of the coarse-grained granite unit having a similar SiO_2 concentration. The granite of Thorn Peak is more strongly peraluminous than rocks of the coarse-grained granite having a similar silica concentration and has high Rb and low Sr concentrations and high U concentration compared to most samples of the coarse-grained granite unit. Thorium concentrations are similar to those of the more Th-rich samples of the coarse-grained granite and range from 4.5 to 6.3. The granite of Thorn Peak shows a gently sloping chondrite-normalized REE pattern and a small negative europium anomaly (fig. 21*D*). Light-rare-earth element enrichment is less than that of the coarse-grained granite [(La/Yb)CN=7.5–8.9]. Total rare-earth element concentration in sample 1158 (appendix sample No. 35, fig. 21*D*) is 136 ppm. The fine-grained granite (Xg) that intrudes the coarse-grained granite at the east end of the Poachie Range is chemically similar to the granite of Thorn Peak in major-element concentration but is richer in Rb, Th, and U.

Gneissic Tonalite

The gneissic tonalite has SiO_2 concentrations of 52–62 percent and is slightly more alkalic and more potassic (fig. 19A, B) than rocks of the coarse-grained granite unit. It is magnesium-rich and metaluminous to peraluminous and has a low Th concentration (fig. 20*A*, *B*, and *D*). Th/U ratios range from 0.9 to 4. The most silicic, peraluminous gneissic tonalite sample is from a part of the pluton that contains numerous mica schist and gneiss inclusions. The gneissic tonalite is moderately enriched in LREE [(La/Yb)CN=24.4–26.6] (fig. 21*D*), and sample 1163 (appendix sample No. 38) has a rare-earth element concentration of 208 ppm.

The Early Proterozoic rocks of the Poachie region have normal K_2O concentrations for their SiO_2 concentrations (fig. 19*B*), similar to rocks in the Mojave province in California (Anderson and others, 1993). They differ from those in the Central Arizona province in north-central Arizona where many of the Early Proterozoic plutonic rocks are sodic and very sodic rocks (DeWitt, 1989; written commun., 1999).

Th/U ratios based on delayed neutron counting (tables 4 and 5; fig. 20*D*) in the Early Proterozoic plutonic rocks are similar to the ratios calculated on the basis of Pb-isotope data (table 8). They average about 4.6 if we ignore the two samples in which the Th concentration was below the limits of detection. If we include them and assume that they have Th concentrations not far below that limit, the average Th/U ratio of the Early Proterozoic plutonic rocks is 4.3; that figure would be lower if their Th content is lower. The Th/U ratios calculated from the whole-rock isotopic data for some of these rocks average about 2.8 (table 8; Wooden and DeWitt, 1991). This value is intermediate between that of the Central Arizona and Mojave crustal provinces (Wooden and DeWitt, 1991).

Zirconium concentrations (fig. 20*E*) form a trend with low values in rocks having silica concentrations of ≈75 weight percent SiO_2 to high values at 65 weight percent SiO_2 and lower values at lower SiO_2 contents. Some rocks with 62–67 percent SiO_2 have low Zr contents. The trend of Zr contents increasing with decreasing SiO_2 is best defined by analyses from the granite of Thorn Peak.

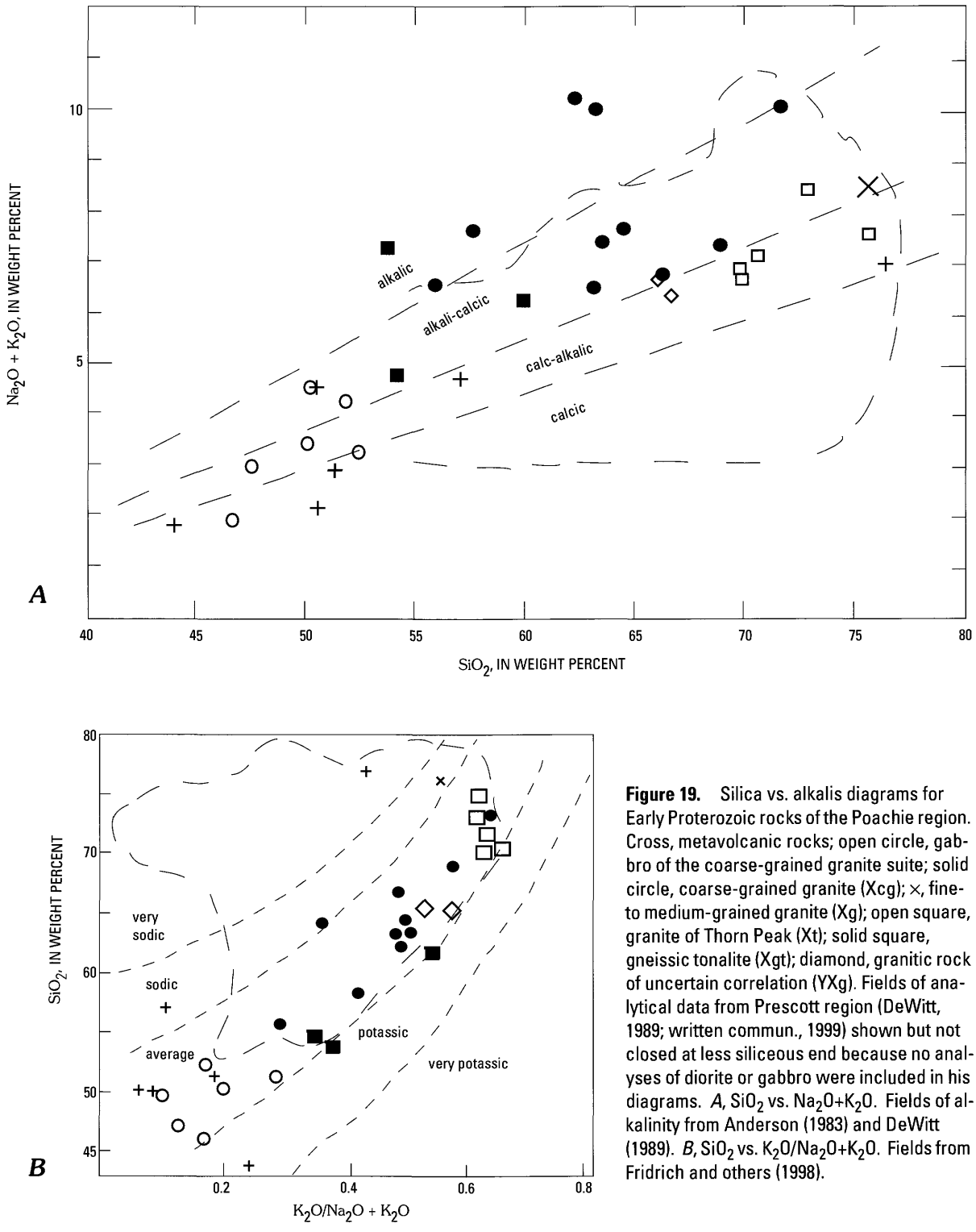

Figure 19. Silica vs. alkalis diagrams for Early Proterozoic rocks of the Poachie region. Cross, metavolcanic rocks; open circle, gabbro of the coarse-grained granite suite; solid circle, coarse-grained granite (Xcg); ×, fine- to medium-grained granite (Xg); open square, granite of Thorn Peak (Xt); solid square, gneissic tonalite (Xgt); diamond, granitic rock of uncertain correlation (YXg). Fields of analytical data from Prescott region (DeWitt, 1989; written commun., 1999) shown but not closed at less siliceous end because no analyses of diorite or gabbro were included in his diagrams. *A*, SiO_2 vs. Na_2O+K_2O. Fields of alkalinity from Anderson (1983) and DeWitt (1989). *B*, SiO_2 vs. K_2O/Na_2O+K_2O. Fields from Fridrich and others (1998).

In an Rb versus Nb+Y diagram, which has been suggested as a tectonic discrimination diagram (Pearce and others, 1984), the Early Proterozoic granitic rocks straddle the boundary between volcanic arc and within-plate granites (fig. 22). The younger, more evolved granite of Thorn Peak plots in the within-plate field, as does the fine-grained granite. Yet the youngest unit, the gneissic tonalite, plots in the volcanic arc field. The overall pattern of data points may reflect either magmatic processes, different source involvement, or an evolving tectonic setting.

Middle Proterozoic Plutonic Rocks

Middle Proterozoic rocks discussed herein are Signal Granite and mafic granodiorite, granite of Olea Ranch, granite of Joshua Tree Parkway, and granite of Grayback Mountain. The Middle Proterozoic plutonic rocks (tables 6 and 7) have some similarities to and some differences from the Early Proterozoic rocks. Other than the ≈1,150 Ma diabase, the Middle Proterozoic plutonic rocks are intermediate to silicic (60–76 percent SiO_2),

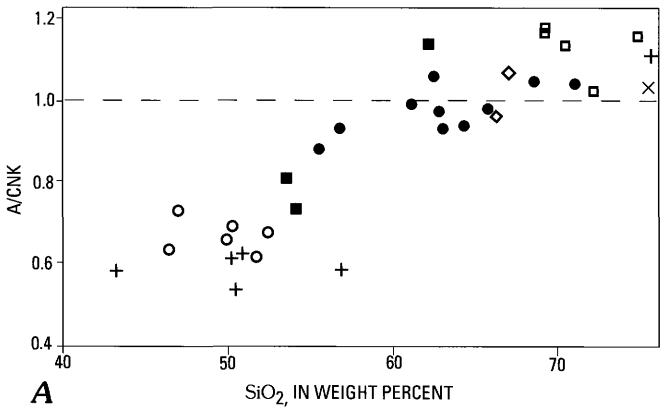

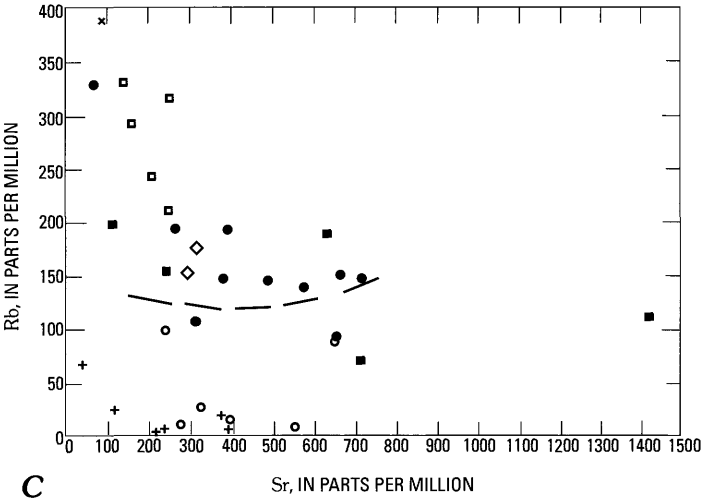

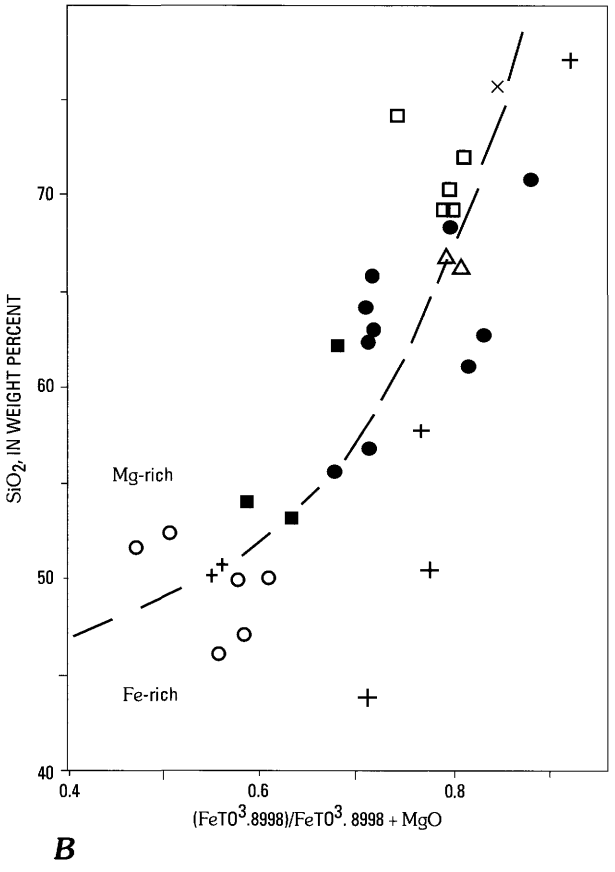

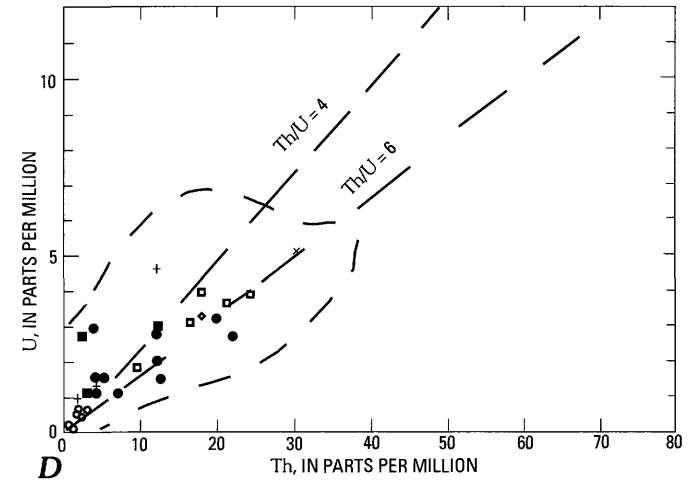

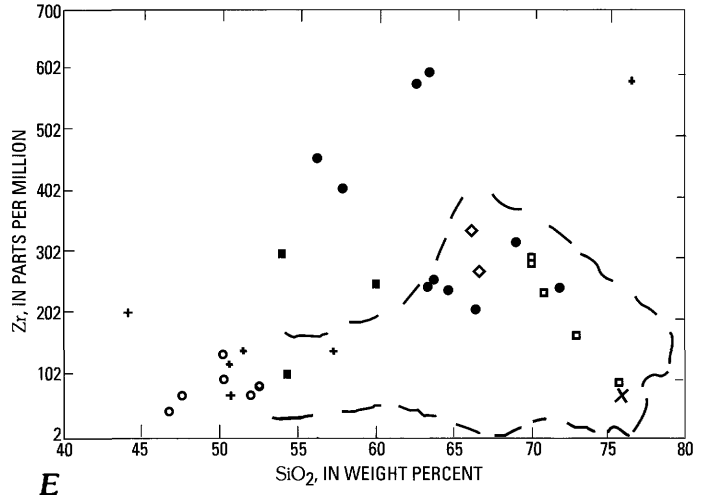

Figure 20. Chemical diagrams for Early Proterozoic rocks of the Poachie region. Cross, metavolcanic rock; open circle, gabbro of the coarse-grained granite suite; solid circle, coarse-grained granite (Xcg); ×, fine- to medium-grained granite (Xg); open square, granite of Thorn Peak (Xt); solid square, gneissic tonalite (Xgt); diamond, granitic rocks of uncertain correlation (Yxg). *A*, SiO_2 vs. A/CNK. *B*, SiO_2 vs. Fe/Fe+Mg. Mg-rich-Fe-rich field boundary from Anderson (1983). *C*, Sr vs. Rb. Line separates group 4 rocks of DeWitt (1989) above from his groups 1-3 below. *D*, Th/U. Dashed line is field of Early Proterozoic granitic rocks from the Prescott area in the Arizona crustal province (Ed DeWitt, written commun., 1999). *E*, SiO_2 vs. Zr. Dashed line outlines field of Early Proterozoic granitic rocks from the Prescott area (Ed DeWitt, written commun., 1999).

generally alkali calcic, and similar to the Early Proterozoic granitic rocks having similar silica concentrations, except for some alkalic rocks in the Early Proterozoic assemblage (fig. 23). The Middle Proterozoic granitic rocks range from average to potassic on the SiO_2 vs. K_2O/Na_2O+K_2O diagram and are more potassic than the Early Proterozoic granitic rocks. The Signal Granite in the western part of the area shows a full range of silica content, whereas the plutons to the east have silica >67 weight percent SiO_2. The Signal Granite and associate mafic granodiorite are

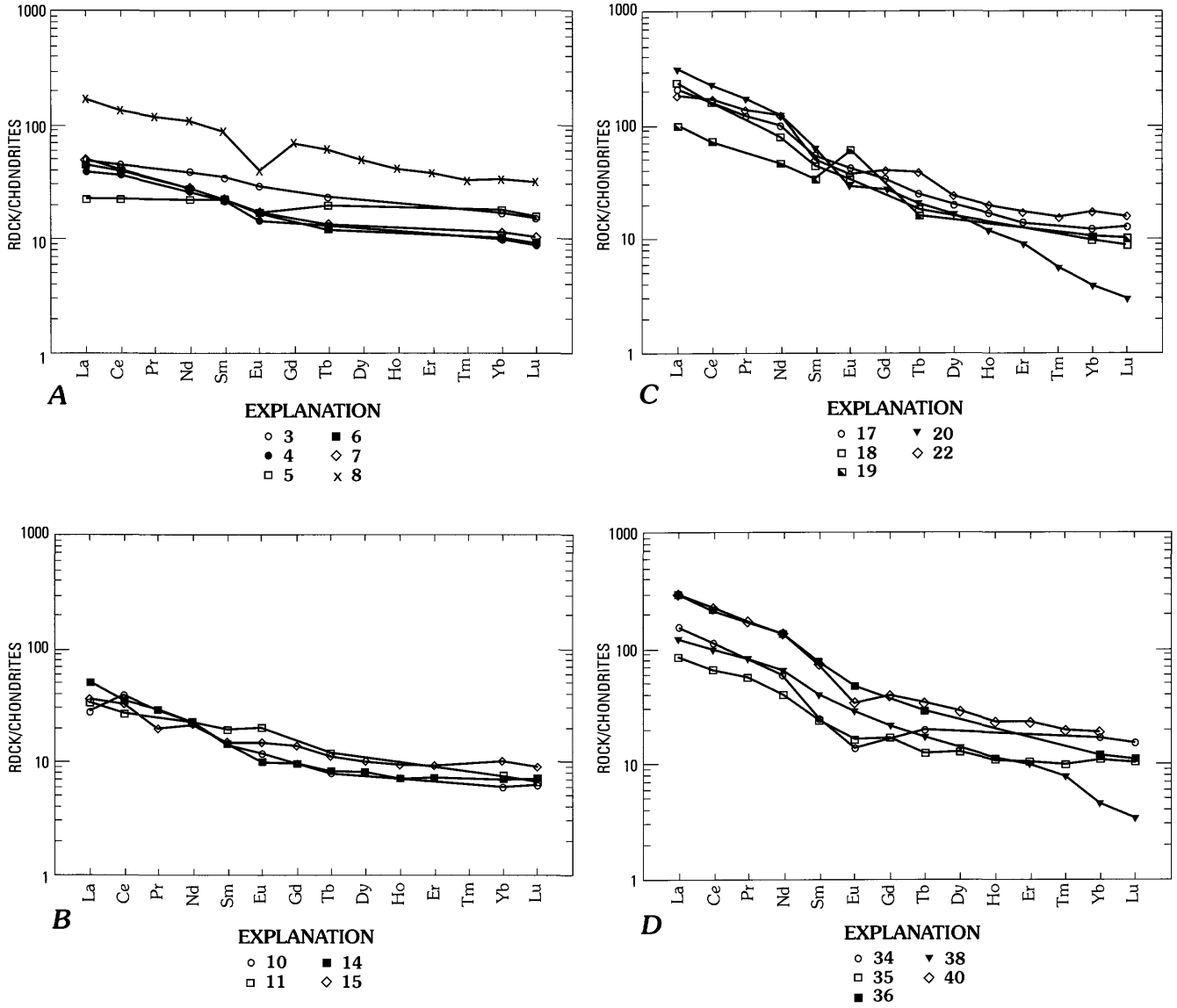

Figure 21. Chondrite-normalized rare-earth element contents of Early Proterozoic rocks. Numbers on symbols refer to appendix sample number. *A*, metavolcanic rocks; *B*, gabbros of the coarse-grained granitic suite; *C*, monzodiorite to granite of the coarse-grained granite suite; *D*, granite of Thorn Peak, gneissic tonalite, and other Proterozoic granite of undetermined age.

potassic, except for the felsic phase of the Signal, which is average. The Middle Proterozoic rocks range from metaluminous to peraluminous (fig. 24*A*). The Signal Granite is metaluminous except for its most silicic variant, whereas the plutons in the central and eastern part of the area are weakly metaluminous to peraluminous (fig. 24*A*). The Signal Granite is Fe-rich, whereas the granite of Joshua Tree Parkway is partly Fe-rich and partly Mg rich. The granites of Olea Ranch and of Grayback Mountain are Mg-rich. The Middle Proterozoic rocks have less Sr and more Rb than the Early Proterozoic rocks (fig. 24*C*).

Signal Granite and Mafic Granodiorite

The Signal Granite has the full range of SiO_2 concentration (61–76 percent) of the Middle Proterozoic granitic rocks. It is alkali-calcic and potassic and is metaluminous except for the most silicic variant (fig. 23*A*, *B*; fig. 24*A*). The Signal is Fe-rich except for its most silicic varieties, which have average Fe/FeO+MgO ratios (fig. 24*B*). Average Th/U ratio is 7.3, and it ranges from 4.3 for the mafic phase to 12.3 for the main phase. The main and mafic phases of the Signal Granite have high REE concentrations ranging from 559–682 ppm for the mafic phase to 479–530 ppm for the main phase (fig. 25*A*). The main phase shows moderate LREE/HREE enrichment patterns [(La/Yb)CN=10–18], and the mafic phase an LREE/HREE ratio of about 10. Both phases have small to moderate negative europium anomalies. Although the patterns for the main and mafic phases are parallel to that of the felsic phase of the Signal Granite, the felsic phase (sample 467B; appendix sample No. 46) has a much lower REE content (120 ppm) and a significantly less light REE enrichment [(La/Yb)CN=6] (fig. 25*A*). That rock has few minerals that contain those elements.

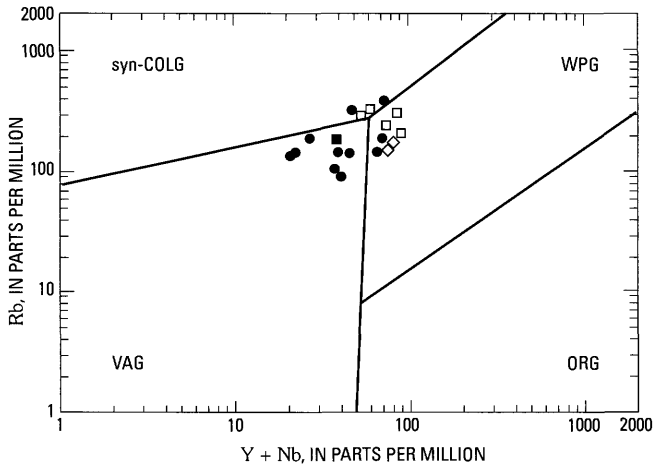

Figure 22. Rb vs. Y+Nb discriminant diagram (Pearce and others, 1984) for Early Proterozoic granitic rocks of the Poachie region. ORG, ocean ridge granites; VAG, volcanic arc granites; WPG, within plate granites; COLG, syn-collision granites. Solid circle, coarse-grained granite (Xcg); open square, granite of Thorn Peak (Xt); solid square, gneissic tonalite (Xgt); diamond, granitic rock of uncertain corrrelation (YXg).

The mafic granodiorite (60–62 percent SiO_2) chemically overlaps the mafic phase of the Signal. The mafic granodiorite is more Fe-rich and slightly more metaluminous than the mafic phase of the Signal and has a slightly lower Th/U ratio of 3.5. The mafic granodiorite has a somewhat smaller europium anomaly compared to the mafic and main phases of the Signal Granite, and it has rare-earth element concentrations of 504-550 ppm.

Granite of Olea Ranch

The granite of Olea Ranch has a range in SiO_2 concentration of 66–73 percent, is alkali-calcic, and is normally potassic for its SiO_2 concentrations (fig. 23*A*, *B*). It is weakly peraluminous and has somewhat Fe-rich to average FeO/FeO+MgO ratios (fig. 24*A*, *B*). Th/U ratios average 6.7. The granite of Olea Ranch shows moderate LREE/HREE enrichment patterns [(La/Yb)CN=10–13] and small to moderate negative europium anomalies (fig. 25*B*). The largest negative europium anomaly is from the fine-grained granite, which is the youngest phase of the granite of Olea Ranch. The porphyritic phase is somewhat richer in $FeTO_3$ and MgO and poorer in SiO_2 than the coarse-grained granite phase.

Granite of Joshua Tree Parkway

The granite of Joshua Tree Parkway has SiO_2 concentrations of 67–72 percent, is alkali-calcic, and has average K_2O concentrations (fig. 23*A*, *B*). It is mildly peraluminous (fig. 24*A*) and ranges from Mg-rich to Fe-rich (fig. 24*B*) and has Th/U ratios of 7.4 (fig. 24*D*). It shows moderate to strong LREE/HREE enrichment patterns [(La/Yb)CN=12] in the megacrystic phase and [(La/Yb)CN=52] in the fine-grained phase (fig. 25*C*). A positive europium anomaly in the megacrystic phase of the unit is consistent with feldspar accumulation in the magma that formed that phase, and a negative europium anomaly is consistent with feldspar depletion in the fine-grained phase. Total rare-earth element concentration is 258 ppm in the megacrystic phase and 355 ppm in the fine-grained granite phase.

Granite of Grayback Mountain

The granite of Grayback Mountain is alkali-calcic and has average K_2O concentrations for rock of its SiO_2 content (71–73 percent) (fig. 23*A*, *B*). It falls on the line between the metaluminous and peraluminous fields (fig. 24*A*) and is somewhat Mg-rich (fig. 24*B*). Th/U ratios average 5.2 (fig. 24*D*). The granite of Grayback Mountain is depleted in Ba, Zr, and Sr compared to the Signal Granite, the granite of Olea Ranch, and the granite of Joshua Tree Parkway. The one sample of this unit for which REE analyses are available is moderately LREE enriched [(La/Yb) CN=13], has a total rare-earth element concentration of 280 ppm, and shows a moderate negative europium anomaly (fig. 25*C*). The chondrite-normalized pattern for that sample resembles that of the megacrystic granite of Joshua Tree Parkway but has a greater negative europium anomaly.

Diabase

The diabases in the Poachie region are calc-alkalic to alkali-calcic and have normal K_2O concentrations for mafic rock (fig. 23*A*, *B*), and are metaluminous (fig. 24*A*), Fe-rich (fig. 24*B*), and Rb-poor (fig. 24*C*). Th/U ratios are 3.9 for the samples for which we have data. They show almost no LREE enrichment [(La/Yb)CN=2.8–4.8]. One has a small positive Eu anomaly that is consistent with plagioclase accumulation (fig. 26). Total rare-earth element concentrations are 60–79 ppm. These diabase samples are only slightly more enriched in LREE compared to the most primitive tholeiitic basalt from northeastern Minnesota (Arth and Hanson, 1975). The relatively flat REE patterns suggest that garnet was not involved in the generation of the diabase. The difference in LREE abundances between the two samples can be accounted for by olivine±clinopyroxene±plagioclase fractionation or by different degrees of partial melting of mantle peridotite. Other potentially important interpretations cannot be made with the limited amount of data.

In a regional study of the chemistry of diabase in the southwestern United States, Hammond (1990) found differences in the composition of samples of diabase from Death Valley, the Colorado River trough, and central Arizona. On a P/Zr vs. Ba/Zr diagram, the diabases fall into two groups, but the samples in each group come from more than one of the three areas just mentioned. One sample from the Poachie region falls into each of the two groups. The two groups were attributed to two separate but similar parental magmas forming the source for the diabase bodies. Sample suites from the Colorado River trough are generally tholeiitic, whereas those from Death Valley and central Arizona are generally alkalic. The Poachie region diabases are tholeiitic as indicated by their Fe-rich composition (fig. 24*B*), and they plot in the field of Colorado River trough diabases, which are tholeiitic (Hammond, 1990, fig. 2). They also fall within the field of Colorado River trough samples on several geochemical diagrams, including total alkali versus silica, TiO_2 vs. MgO/(MgO+FeO), SiO_2 vs. MgO/(MgO+FeO), and TiO_2 vs. P_2O_5, perhaps due to similarities in source regions in the upper mantle.

Table 6. Major-oxide and trace-element concentrations in Middle Proterozoic Signal Granite and associated mafic granodiorite.

[nd, not determined; LOI, loss on ignition; FeTO3, total Fe as Fe_2O_3]

	Mafic phase		Main phase granite			Felsic phase	Mafic granodiorite	
Sample No.	41	42	43	44	45	46	47	48
Field No.	NAP154	876	1168	1164	49a	467b	390	1144
Lab No.	D-266702	D-266701	D-278416	D-278415	D-259525	D-266703	D-259523	D-266704
Job No.	RV13	RV13	SD65,WB47	SD65	RP40	RV13	RP40,WB47	RV13
Major-oxide composition, in weight percent[1]								
SiO_2	61.3	64	64.3	65.4	69.1	74.6	59.6	61.7
Al_2O_3	13.3	13.7	13.9	13.4	14	13.1	12.7	12.7
FeTO3	9.09	7.18	6.79	5.95	3.17	1.14	10.7	9.73
MgO	1.76	1.29	1.14	1.01	0.62	0.18	1.69	1.42
CaO	4.19	3.64	3.04	2.76	2.26	1.05	4.76	3.93
Na_2O	2.71	2.91	2.83	2.75	2.91	2.54	2.52	2.5
K_2O	3.89	4.08	5.06	4.91	5.24	6.07	3.76	3.88
TiO_2	1.47	1.21	1.06	0.93	0.54	0.16	1.76	1.61
P_2O_5	0.58	0.5	0.4	0.37	0.19	0.05	1.07	0.96
MnO	0.13	0.1	0.1	0.09	0.05	0.02	0.16	0.13
LOI	0.55	0.52	0.4	0.49	1.33	0.46	0.63	1.04
Total	98.42	98.61	98.62	97.57	98.08	98.91	98.72	98.56
[2]FeO	3.66	3.76	3.2	3.15	1.74	0.37	6.08	4.52
[2]F	0.24	0.25	0.11	0.11	0.17	0.04	0.18	0.16
Trace-element concentration, in parts per million[3]								
Nb	28	31	21	24	24	11	17	22
Rb	124	183	203	175	221	248	100	107
Sr	426	287	252	243	240	52	339	338
Zr	495	444	378	382	300	126	595	567
Y	82	86	71	69	61	28	85	77
Trece-element concentration, in parts per million[4]								
Ba	nd	nd	1280	nd	nd	nd	1500	nd
Co	nd	nd	10.1	nd	nd	nd	17.4	nd
Cr	nd	nd	7.4	nd	nd	nd	<12.20	nd
Cs	nd	nd	2	nd	nd	nd	1.9	nd
Hf	nd	nd	12.3	nd	nd	nd	15.5	nd
Sb	nd	nd	<0.100	nd	nd	nd	0.15	nd
Ta	nd	nd	1.77	nd	nd	nd	1.41	nd
Zn	nd	nd	96	nd	nd	nd	150	nd
Sc	nd	nd	14.9	nd	nd	nd	21.6	nd
La	107	123	94.9	111	126	23.7	96.8	105
Ce	228	209	199	232	241	45.6	201	219
Pr	28.9	30.7	25.5	27.4	25.1	5.6	26.1	29.7
Nd	111	114	87.5	95.9	89.3	21.1	98.3	115
Sm	20.8	21.5	18.8	13.3	10	5	21.4	22.2
Eu	3.68	3.21	2.48	2.62	2.39	1.06	4.25	4.92

Comparison of Middle Proterozoic Plutonic Rocks with Early Proterozoic and Other Middle Proterozoic Plutonic Rocks in Region

As mentioned previously, the Middle Proterozoic plutonic rocks are more potassic than the Early Proterozoic rocks, although their alkalinity is similar to that of the Early Proterozoic rocks at similar SiO_2 contents. However, the concentrations of some minor elements differ.

Zirconium concentrations increase with decreasing SiO_2 within the 60–75 percent range of SiO_2 concentrations of the Middle Proterozoic granitic rocks, as they do in the Early Proterozoic granite of Thorn Peak. The Middle Proterozoic rocks have less Sr and more Rb than the Early Proterozoic rocks (fig. 24*C*).

Overall the Middle Proterozoic rocks have higher total REE concentrations but lower LREE/HREE ratios than do the Early Proterozoic rocks (figs. 25 and 21). The Middle Proterozoic rocks give patterns with well-developed negative europium anomalies, indicating that differentiation of plagioclase played a greater role in their genesis than it did in the Early Proterozoic rocks.

The Middle Proterozoic rocks have higher Th and U concentrations and Th/U ratios than the Early Proterozoic rocks (figs. 24*D* and 20*D*). U/Th ratios average 6.4. Our data show a

Table 6—Continued. Major-oxide and trace-element concentrations in Middle Proterozoic Signal Granite and associated mafic granodiorite.

	Mafic phase		Main phase granite			Felsic phase	Mafic granodiorite	
Sample No.	41	42	43	44	45	46	47	48
Field No.	NAP154	876	1168	1164	49a	467b	390	1144
Lab No.	D-266702	D-266701	D-278416	D-278415	D-259525	D-266703	D-259523	D-266704
Job No.	RV13	RV13	SD65,WB47	SD65	RP40	RV13	RP40,WB47	RV13
Trace-element concentration, in parts per million[4]—*Continued*								
Gd	17.4	18.2	13.5	13.7	12.0	5.0	20.2	20.2
Tb	2.30	2.40	2.22	2.23	2.10	.80	2.48	3.00
Dy	14.4	15.6	13.3	13.6	10	4.9	16.0	16.1
Ho	2.74	3.00	2.50	2.62	1.90	.99	3.00	3.05
Er	7.3	8.1	6.93	6.96	4.8	2.8	7.6	8.6
Tm	1.00	1.2	1.03	1.04	0.68	.41	.99	1.1
Yb	7.00	8.30	6.5	6.24	4.52	2.7	6.5	6.8
Lu	0.94	1.11	0.91	.82	.64	.35	0.926	1.01
As	nd	nd	4.2	nd	nd	nd	<1.60	nd
[5]Th	12	32.2	22	37	43	52.1	7.05	3.8
[5]U	3.26	6.53	3.3	3.38	4.23	7.05	1.25	2.49

[1]Major oxides determined by wavelength dispersive X-ray fluorescence: J.E. Taggart, A.J. Bartel, K. Stewart, E. Robb, analysts.
[2]FeO determined by potentiometric titration and F by ion-selective electrode potentiometry: E.L. Brandt, J. Starkey, S. Roof, G. Mason, J.H. Christie, analysts.
[3]Trace elements determined by energy dispersive X-ray fluorescence: R.R. Larson, R. Johnson, S. Fleming, J. Evans, analysts.
[4]Rare earths determined by inductively coupled plasma–mass spectrometry: J.G. Crock, P.H. Briggs, D. Frey, A. Meier, analysts. Rare earths and other trace elements in samples 1168 and 390 determined by instrumental neutron activation analysis: G.A. Wandless, analyst.
[5]Th and U determined by delayed neutron counting: R.B. Vaughn, D.M. McKown, analysts.

westward increase from an average of 5.2 for the granites of Grayback Mountain and Joshua Tree Parkway to 7.3 for the Signal Granite (tables 6 and 7). Th/U ratios of 1.4 Ga granitic rocks averaged by plutons are 12.6 in the Mojave province in southeastern California and 6.7 in the Central Arizona province, east of the Poachie region (Anderson and Bender, 1989). Thus the average Th/U ratio of 1.4 Ga rocks in the Poachie region closely resembles that of 1.4 Ga rocks in the Central Arizona province.

The high Th and U concentrations in the 1,400 Ma rocks in the Poachie region are well shown by the distribution of anomalies on aerorad maps produced during the NURE (National Uranium Resource Evaluation) program. Uranium deposits in the Date Creek basin south of the Poachie Range are in carbonaceous tuffaceous siltstone and mudstone and were deposited in early Miocene inter-fan lakes (Otton, 1985). Streams draining into the basin before the formation of the Poachie Range 13 Ma or later probably were carrying detritus from the Signal Granite and the granite of Olea Ranch. Altered and silicified ash in the lacustrine rocks is also enriched in uranium, but whether the volcanic rocks originally contained anomalous concentrations of uranium or whether uranium was added from another source during alteration is not known (Otton, 1985). Lower Miocene silicic volcanic rocks from the Poachie region have low U (1–3 ppm) and Th (4–10 ppm) concentrations (Bryant, unpub. data, 1985–87). Certainly the Middle Proterozoic plutonic rocks could have contributed to the uranium deposits in the Date Creek basin through leaching of uranium from those rocks by ground water and by leaching of uranium from detritus derived from them by surface water and, after deposition of that detritus in the basin, by ground water.

In a regional overview of the chemistry of the Middle Proterozoic rocks in the southwestern United States, Anderson (1989) defined a boundary between metaluminous rocks to the west and peraluminous rocks to the east bisecting the Poachie Range. The Signal Granite, except for the leucocratic phase, and the mafic granodiorite are definitely metaluminous. The granite of Olea Ranch, on the other hand, is slightly peraluminous, the fine-grained phase of the granite of Joshua Tree Parkway is weakly peraluminous, and the coarse-grained granite and the porphyritic granite of Grayback Mountain are on the boundary between the metaluminous and peraluminous fields (table 7; fig. 24*A*). The change in chemistry of these Middle Proterozoic plutonic rocks from metaluminous on the west to weakly peraluminous to neutral on the east may be related to a change in composition of the underlying crust from which they probably were at least partly derived, or a change in the level in the crust which was melted or partly melted to produce the granitic magmas (Anderson, 1989). Many of the Early Proterozoic plutonic rocks are peraluminous, and overall for a given SiO_2 concentration the Early Proterozoic plutonic rocks are more peraluminous or less metaluminous than the Middle Proterozoic rocks (figs. 20*A*, 24*A*). The Early Proterozoic peraluminous rocks generally have pelitic schist and gneiss country rock or (and) inclusions. They also have $^{207}Pb/^{204}Pb$ to $^{206}Pb/^{204}Pb$ ratios like those of the pelitic schist (table 8, appendix sample Nos. 1 and 2 compared to Nos. 35 and 38). Those ratios resemble those to the west in the main area of the Mojave crustal province (Wooden and Miller, 1990; Wooden and DeWitt, 1991).

Middle Proterozoic granites show more of a within-plate tectonic signature than the Early Proterozoic granites (figs. 27, 22). All samples of the Signal Granite and associated mafic granodiorite and of the granite of Olea Ranch plot in the within-plate granite field. The granites of Joshua Tree Parkway and Grayback Mountain show more of a volcanic arc geochemical signature.

Table 7. Major-oxide and trace-element concentrations in the Middle Proterozoic granites of Olea Ranch, of Joshua Tree Parkway, and of Grayback Mountain, and diabase.

[nd, not determined; LOI, loss on ignition; $FeTO_3$, total Fe as Fe_2O_3]

	Granite of Olea Ranch					Granite of Joshua Tree Parkway		Granite of Grayback Mountain		Diabase			
	Porphyritic granite		Coarse-grained granite		Fine-grained granite	Mega-crystic granite	Fine-grained granite	Porphyrit-ic granite	Coarse-grained granite				
Appendix No.	49	50	51	52	53	54	55	56	57	60	61	62	63
Field No.	666	752	753	M72	1160	A-151a	A-151b	A-107b	A-153	1052	A-91	G-38	852
Lab No.	D-363783	D-259528	D-259529	D-363782	D-266705	D-327699	D-327700	D-367765	D-327702	D-266700	D-568683	D-568684	D-266699
Job No.	UD76	RP40	RP40 WB47	UD76	RV13 SC97	TG29	TG29	UD76	TG29 WB47	RV13 SC97	WB23	WB23	RV13 SC97
Major-oxide composition, in weight percent[1]													
SiO_2	66.1	68.2	69.2	69.6	73.0	67.3	72.1	71.4	73.3	46.3	48.6	49.1	49.1
Al_2O_3	14.6	14.3	13.7	13.7	13.5	15.7	13.9	13 5	13.2	17.1	16.8	16.5	15.6
$FeTO_3$	5.35	4.44	3.75	3.82	1.79	3.05	1.98	2.68	1.78	12.5	13.7	12.5	13.0
MgO	1.36	1.18	.78	.81	.28	.53	.43	.85	.38	6.97	6.83	6.75	7.13
CaO	2.27	2.49	2.46	2.13	1.2	2.68	1.31	1.77	1.65	9.73	9.54	9.48	10.9
Na_2O	2.65	2.74	2.91	2.87	2.98	3.19	2.73	2.88	2.91	2.67	2.73	2.82	2.26
K_2O	5.01	4.06	4.55	4.68	5.55	5.4	6.04	619	5.03	.67	.66	.85	.51
TiO_2	.76	.66	.64	57	.22	.50	.23	.28	.25	1.83	1.29	1.19	1.22
P_2O_5	.35	.25	.29	.24	.05	.19	.08	.08	.10	.58	.24	.26	.17
MnO	.09	.07	.07	.07	.04	.06	.03	.05	.03	.19	.19	.18	.19
LOI	.94	.71	.88	.41	.75	.54	.52	.56	.56	1.51	<.01	.11	.39
Total	98.54	98.39	98.35	98.49	98.61	98.6	98.83	98.68	98.63	98.54	100.54	99.74	100.08
[2]FeO	nd	2.45	1.77	nd	.77	1.46	1.01	nd	.94	nd	nd	nd	nd
[2]F	nd	.16	.15	nd	.05	.03	.01	nd	.08	nd	nd	nd	nd
Trace-element concentration, in parts per million[3]													
Nb	24	25	30	20	34	16	15	16	16	10	<10	<10	<10
Rb	286	259	270	218	412	111	162	207	170	30	<10	10	15
Sr	239	229	294	243	95	332	231	133	166	437	355	320	178
Zr	311	364	265	330	166	363	213	176	156	75	98	112	90
Y	49	62	73	212	59	34	17	30	38	21	18	16	22
Ba	1270	nd	nd	1110	nd	nd	nd	636	nd	nd	255	320	nd
Ce	209	nd	nd	207	nd	nd	nd	131	nd	nd	<30	<30	nd
La	112	nd	nd	96	nd	nd	nd	64	nd	nd	<30	<30	nd
Cu	16	nd	nd	4	nd	nd	nd	10	nd	nd	120	86	nd
Ni	<5	nd	nd	<5	nd	nd	nd	6	nd	nd	128	142	nd
Zn	75	nd	nd	62	nd	nd	nd	52	nd	nd	76	58	nd
Trace-element concentration, in parts per million[4]													
Ba	nd	nd	776	nd	nd	nd	nd	nd	642	nd	260	330	nd
Co	nd	nd	5.25	nd	nd	nd	nd	nd	2.66	nd	56.1	51.9	nd
Ni	nd	nd	<17	nd	nd	nd	nd	nd	>12	nd	160	180	nd
Cr	nd	nd	2.1	nd	nd	nd	nd	nd	2.9	nd	105	62.7	nd
Cs	nd	nd	11.4	nd	nd	nd	nd	nd	7.74	nd	0.20	1.4	nd
Hf	nd	nd	9.06	nd	nd	nd	nd	nd	4.66	nd	2.46	2.68	nd
Sb	nd	nd	<0.220	nd	nd	nd	nd	nd	0.13	nd	0.11	<.09	nd
Ta	nd	nd	3.80	nd	nd	nd	nd	nd	1.60	nd	0.34	0.38	nd
Zn	nd	nd	64	nd	nd	nd	nd	nd	32	nd	93	88	nd
Sc	nd	nd	9.12	nd	nd	nd	nd	nd	2.83	nd	24.8	25.2	nd
La	nd	102	102	nd	88.2	61	92	nd	63	11.7	10.7	13.3	7.5
Ce	nd	204	204	nd	181	110	170	nd	120	27.7	24.3	28.8	20.2
Pr	nd	23.3	22.6	nd	19.0	12.0	16.0	nd	13	3.2	nd	nd	2.3
Nd	nd	85.4	83.7	nd	64.2	45	56	nd	48	17.2	14	17	12.7

Table 7—Continued. Major-oxide and trace-element concentrations in the Middle Proterozoic granites of Olea Ranch, of Joshua Tree Parkway, and of Grayback Mountain and diabase.

	Granite of Olea Ranch					Granite of Joshua Tree Parkway		Granite of Grayback Mountain		Diabase			
	Porphyritic granite		Coarse-grained granite		Fine-grained granite	Mega-crystic granite	Fine-grained granite	Porphyrit-ic granite	Coarse-grained granite				
Appendix No.	49	50	51	52	53	54	55	56	57	60	61	62	63
Field No.	666	752	753	M72	1160	A-151a	A-151b	A-107b	A-153	1052	A-91	G-38	852
Lab No.	D-363783	D-259528	D-259529	D-363782	D-266705	D-327699	D-327700	D-367765	D-327702	D-266700	D-568683	D-568684	D-266699
Job No.	UD76	RP40	RP40 WB47	UD76	RV13 SC97	TG29	TG29	UD76	TG29 WB47	RV13 SC97	WB23	WB23	RV13 SC97
Trace-element concentration, in parts per million[4]—*Continued*													
Sm	nd	1.7	10.6	nd	11.3	7.4	7.3	nd	9.2	4.1	4.09	4.34	3.3
Eu	nd	2.31	2.34	nd	.96	2.90	1.20	nd	1.2	1.79	1.26	1.40	1.26
Gd	nd	12.3	12.4	nd	9.1	5.9	4.7	nd	7.9	4.3	nd	nd	4.1
Tb	nd	2.20	2.3	nd	1.40	.96	.76	nd	1.4	.5	.64	.66	.5
Dy	nd	11.0	11.0	nd	8.1	5.2	3.3	nd	7.6	3.6	nd	nd	3.6
Ho	nd	1.99	2.18	nd	1.61	1.0	.60	nd	1.4	.67	nd	nd	.68
Er	nd	5.4	6.0	nd	4.5	3.1	1.7	nd	4.0	1.8	nd	nd	1.9
Tm	nd	.76	0.86	nd	.76	.44	.24	nd	0.47	.27	nd	nd	.26
Yb	nd	5.38	6.04	nd	5.40	3.30	1.16	nd	3.3	1.6	2.06	2.2	1.8
Lu	nd	.76	0.82	nd	.79	nd	nd	nd	0.41	.21	.29	.29	.24
[5]Th	31.60	30.4	36.00	25.20	75.80	9.94	29.50	25.40	18.90	<1.9	.67	.86	<2.0
[5]U	4.13	3.61	6.02	6.38	11.30	1.84	3.07	4.35	4.04	<.22	.25	.21	.32

[1]Major oxides determined by wavelength dispersive X-ray fluorescence: D.F Siems, J.E. Taggart, A.J. Bartel, K. Stewart, analysts.

[2]FeO determined by potentiometric titration and F by ion-selective potentiometry: C. Papp, J. Sharkey, E. Brandt, S. Roof, J.H. Christie, analysts.

[3]Trace elements determined by energy dispersive X-ray fluorescence: J.R. Evans, R.R. Larson, R. Johnson, S. Fleming, analysts.

[4]Rare earths determined by inductively coupled plasma–mass spectrometry: J.G. Crock, K. Kennedy, G. Riddle, analysts; sample Nos. 51, 57, 61, and 62 rare earths and other minor elements by instrumental neutron activation analysis: G.A. Wandless, analyst.

[5]Th and U determined by delayed neutron activation except for sample Nos. 61 and 62: R.J. Knight, R.B. Vaughn, D.M. McKown, analysts.

The general similarity in the chemical characteristics of the 1.7 Ga and 1.4 Ga plutonic suites in the Mojave crustal province has been discussed by Anderson and Bender (1989) and Anderson and others (1993), and comparison of figures 19 and 23, 20 and 24, 21 and 25 shows that those similarities exist in the Poachie region. In both suites, melting of similar crustal material was probably an important process in magma production. For instance, the 1.4 Ga granite of Olea Ranch and the 1.7 Ga granite of Thorn Peak are adjacent to each other, and they have many chemical similarities: high Rb, within-plate classification on the discriminant diagram, normal K, and both peraluminous and somewhat enriched in Mg. One difference is that the granite of Olea Ranch is more U- and Th-rich than the granite of Thorn Peak, and the granite of Thorn Peak is calc-alkalic, whereas the granite of Olea Ranch is alkali-calcic.

The Parker Dam granite and the Bowmans Wash quartz monzodiorite in the upper plate rocks above the Whipple Mountains detachment fault east of the Whipple Mountains (fig. 1) near the Colorado River, about 60 km west of the Signal Granite in the Poachie region, resemble the Signal Granite and the mafic granodiorite, respectively. However, the Parker Dam is, and the Bowmans Wash may be, slightly younger than the Signal Granite; and the Parker Dam granite is a few million years younger than the Bowmans Wash quartz monzodiorite (Anderson and Bender, 1989). The Parker Dam does not have as wide a range of silica content as the Signal Granite. Silica for the Parker Dam (Anderson and Bender, 1989) ranges from 64.6 to 69.9 weight percent SiO_2, and the rocks have a color index ranging from 2 to 18. Silica for the Signal Granite ranges from 61.3 to 74.6 percent, and the color index ranges from 1 to 28. Taken together, the Signal and mafic granodiorite compared to the Parker Dam and Bowmans Wash are remarkably similar in chemical composition, except that the Parker Dam granite has a higher potassium concentration at high silica concentrations (fig. 28*A*) and the Th/U ratios of the Parker Dam and Bowmans Wash are greater than those of the Signal because they contain much less uranium (fig. 28*B*). The average Th/U is about 16 for the Parker Dam and 28 for Bowmans Wash (Anderson and Bender, 1989) compared to 9.2 for the main phase of the Signal Granite, which has the same range of silica content as the Parker Dam granite, and 3.5 for the mafic granodiorite. The Th/U ratio in the Parker Dam and Bowmans Wash is higher than the average for 1.4 Ga granitic rocks in the Mojave crustal province west of the Poachie region, whereas the Th/U ratio in the Signal Granite and other 1.4 Ga plutons in the Poachie region is similar to that of 1.4 Ga plutons in the Central Arizona province (Anderson and Bender, 1989).

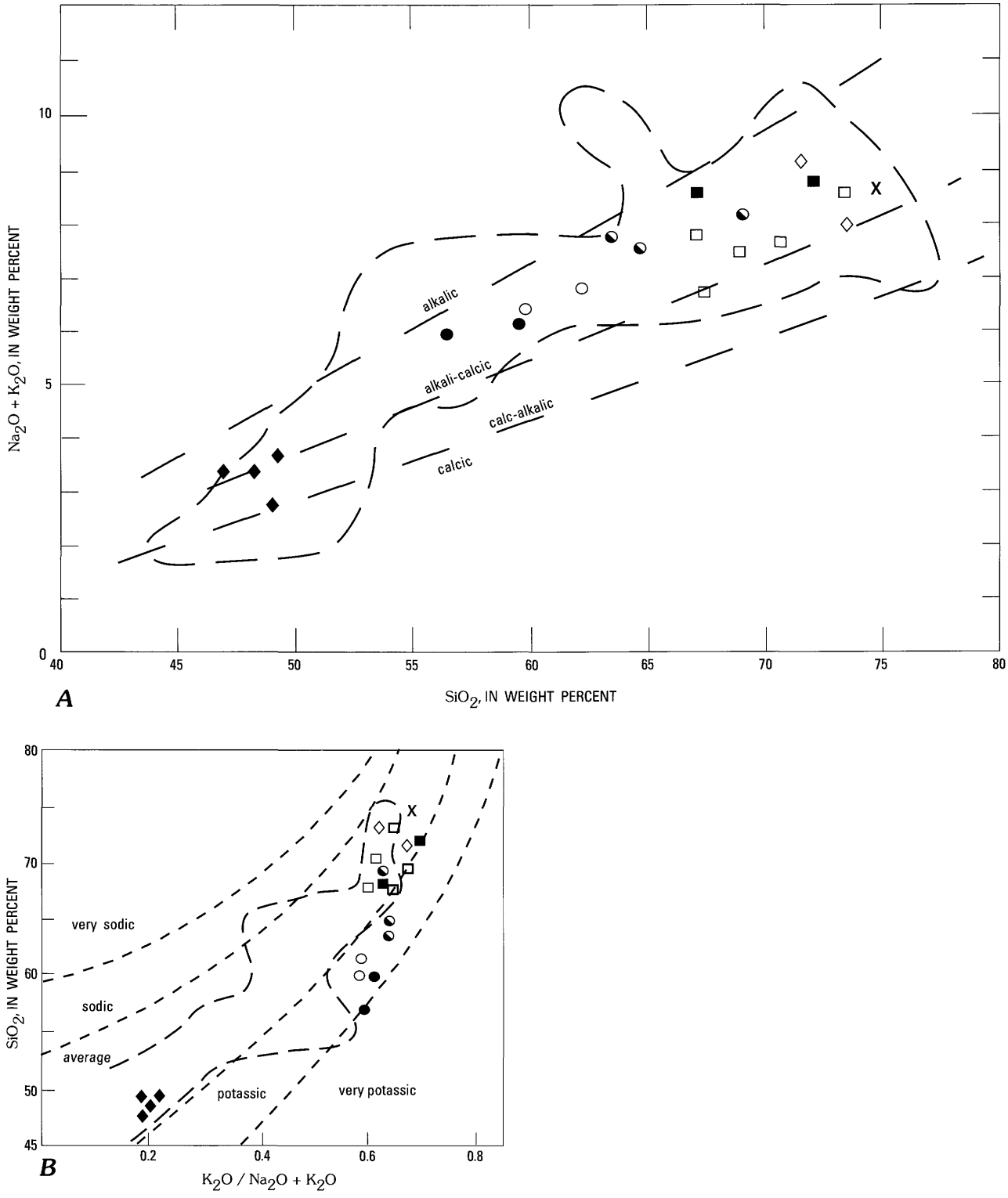

Figure 23. Silica vs. alkalis diagrams for Middle Proterozoic granitic rocks and diabase. Fields of Early Proterozoic igneous rocks from figure 19 outlined. *A*, SiO_2 vs. Na_2O+K_2O. Fields of alkalinity from Anderson (1983) and DeWitt (1989). *B*, SiO_2 vs. K_2O/Na_2O+K_2O. Fields from Fridrich and others (1998). Open circle, Signal Granite (Ys), mafic phase; half-filled circle, main phase; ×, felsic phase; solid circle, mafic granodiorite (Ygd); open square, granite of Olea Ranch (Yo); solid square, granite of Joshua Tree Parkway (Yj); open diamond, granite of Grayback Mountain (Yb); solid diamond, diabase.

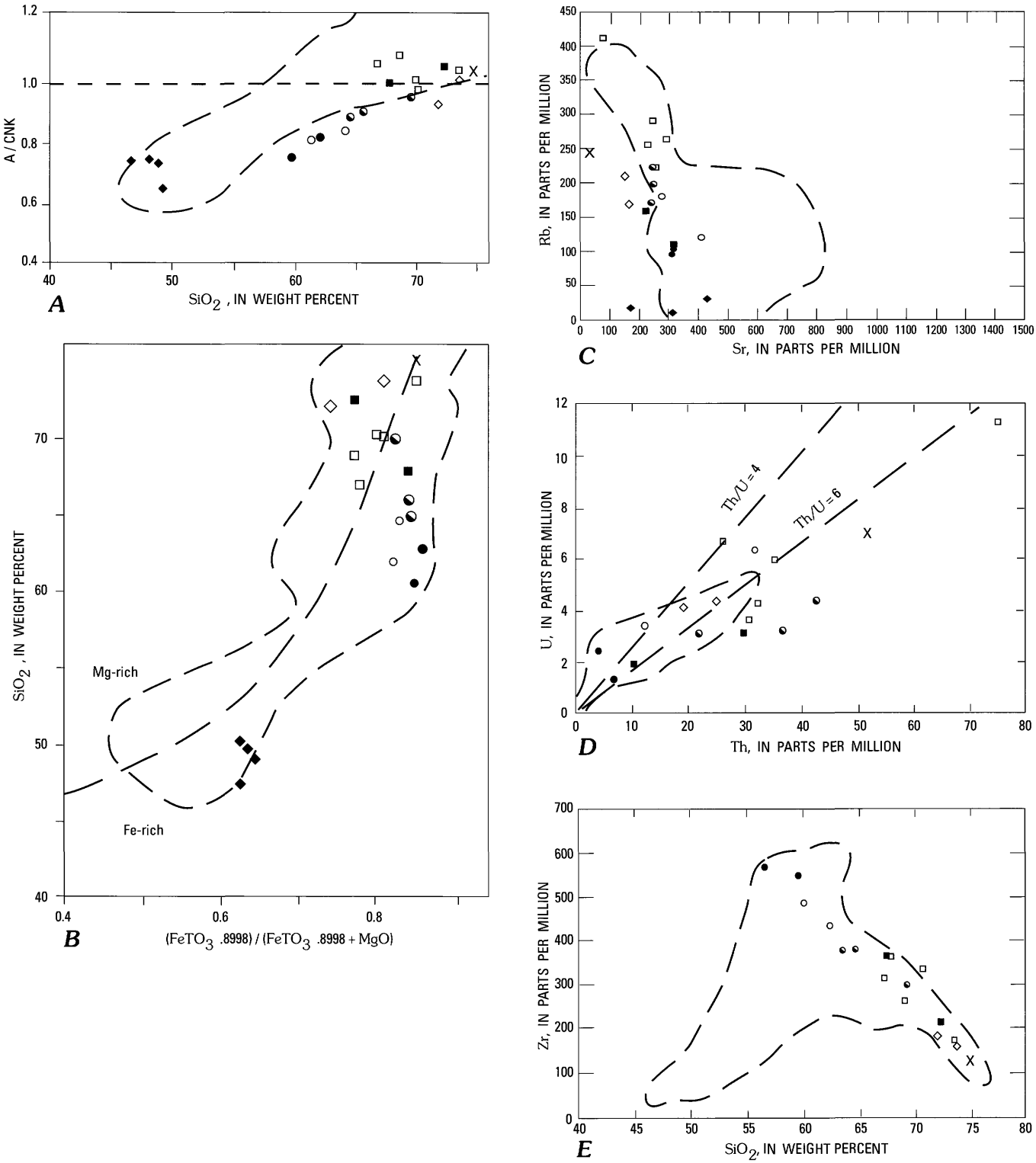

Figure 24. Chemical diagrams for Middle Proterozoic granitic rocks and diabase. Fields of Early Proterozoic rocks from figure 20 outlined. *A*, SiO_2 vs. A/CNK. *B*, SiO_2 vs. Fe/Fe+Mg. Mg-rich-Fe-rich field boundary from Anderson (1983). *C*, Sr vs. Rb. *D*, Th vs. U (diabase not shown). *E*, SiO_2 vs. Zr (diabase not shown). Open circle, Signal Granite (Ys), mafic phase; half-filled circle, main phase; ×, felsic phase; solid circle, mafic granodiorite (Ygd); open square, granite of Olea Ranch (Yo); solid square, granite of Joshua Tree Parkway (Yj); open diamond, granite of Grayback Mountain (Yb); solid diamond, diabase.

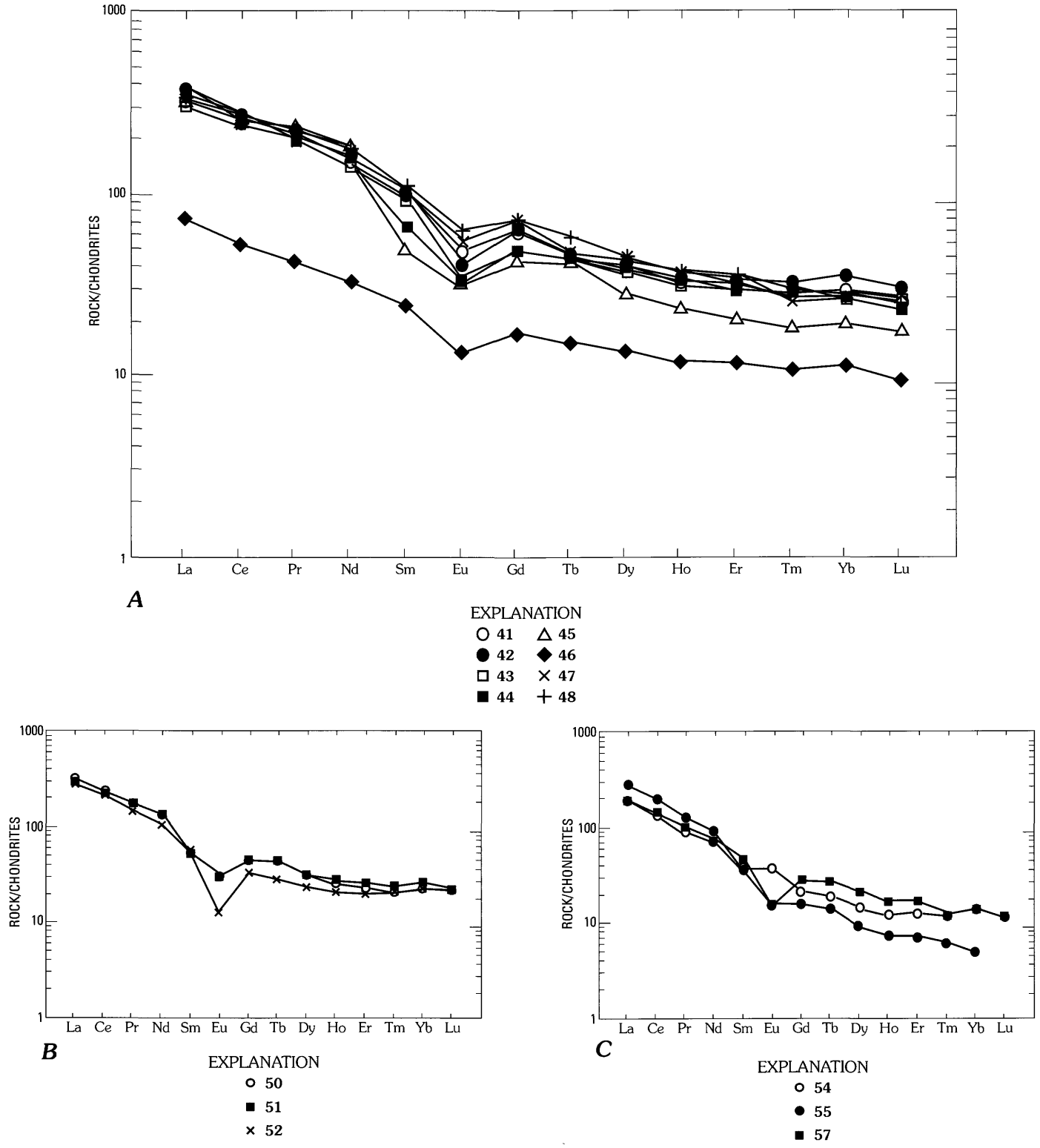

Figure 25. Chondrite-normalized rare-earth contents of Middle Proterozoic granitic rocks. *A*, Signal Granite and related mafic granodiorite; *B*, granite of Olea Ranch; *C*, granite of Joshua Tree Parkway and granite of Grayback Mountain. Numbers by symbols refer to appendix sample numbers.

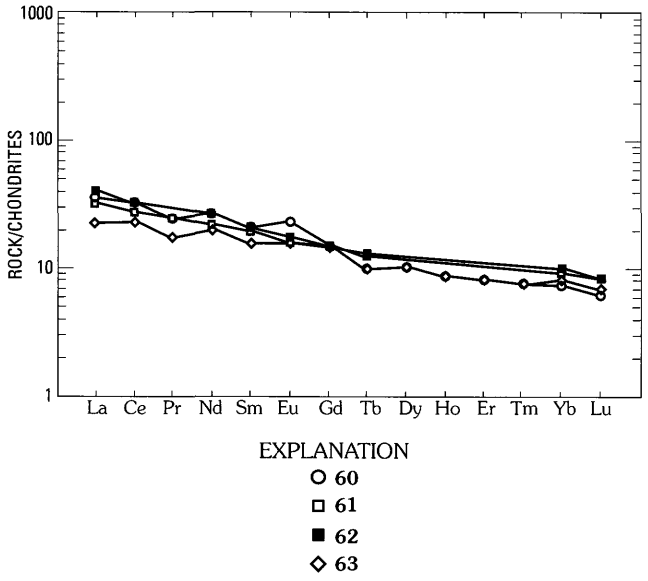

Figure 26. Chondrite-normalized rare-earth contents of diabase.

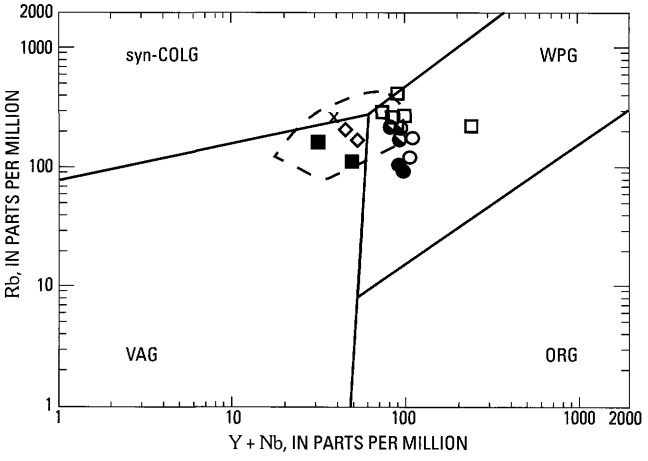

Figure 27. Rb vs. Y+Nb discriminant diagram (Pearce and others, 1984) for Middle Proterozoic granitic rocks of the Poachie region. ORG, ocean ridge granites; VAG, volcanic arc granites; WPG, within-plate granites; synCOLG, syn-collision granites. Distribution of Early Proterozoic plutonic rocks (fig. 22) shown by dashed outline. Open circle, Signal Granite, mafic phase; half-filled circle, main phase; ×, felsic phase; solid circle, mafic granodiorite; open square, granite of Olea Ranch; solid square, granite of Joshua Tree Parkway; open diamond, granite of Grayback Mountain.

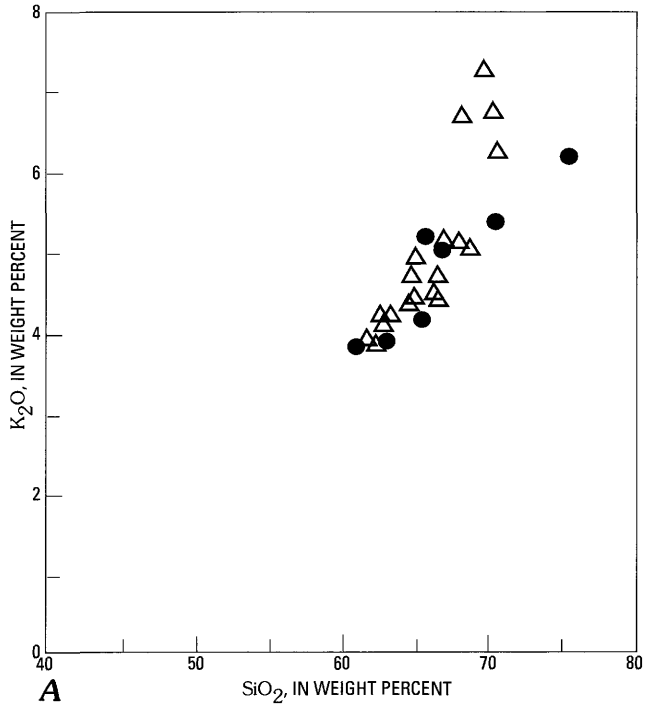

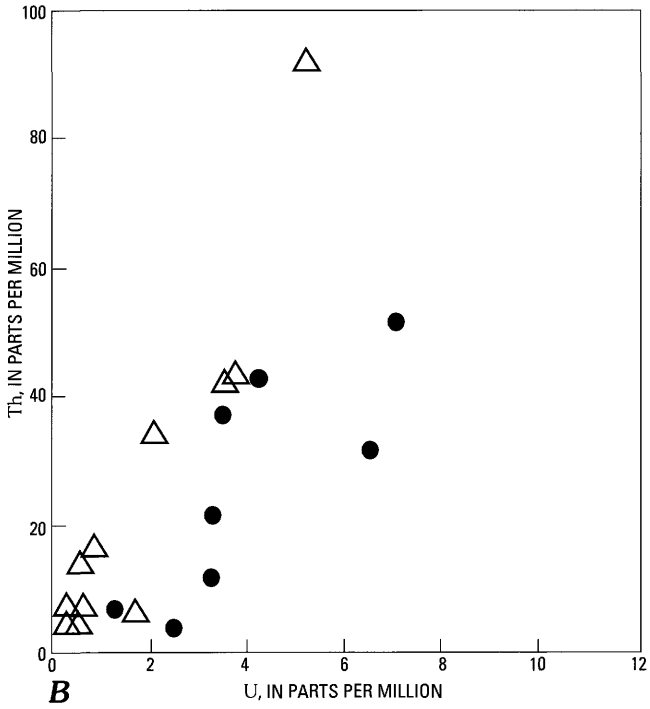

EXPLANATION

△ Parker Dam granite and Bowmans Wash quartz monzodiorite

● Signal Granite and mafic granodiorite

Figure 28. Chemical diagrams comparing the Signal Granite, including the mafic granodiorite, with the granite of Parker Dam and the quartz monzodiorite of Bowmans Wash. Data for the Parker Dam granite and the Bowmans Wash quartz monzodiorite from Anderson and Bender (1989). *A*, SiO_2 vs. K_2O. *B*, Th vs. U.

Other Proterozoic Plutonic Rocks

Granitic rocks of uncertain correlation are alkali-calcic to calc-akalic, have average K and Fe concentrations, are peraluminous to weakly metaluminous, and have Th/U ratios averaging 5.4 (table 5; figs. 19*A*, *B*, 20*A*, *B*, *D*). One sample (A-152; appendix sample No. 40) has moderate LREE enrichment [(La/Yb) CN=15.8] and has total rare-earth element concentration of 452 ppm and a small negative europium anomaly. We interpret these rocks to be of Middle Proterozoic age because of the high rare-earth element concentration and negative europium anomaly (fig. 21*D*) in the sample for which we have those data. In many respects they resemble the Early Proterozoic granite of Thorn Peak, but the Thorn Peak rocks have less LREE enrichment and lower total rare-earth element concentrations.

Whole-Rock and Feldspar Pb-Isotopic Compositions

Whole-rock and feldspar Pb-isotopic analyses of rocks from the Poachie region were made as part of a regional study of Proterozoic Pb-isotopic crustal provinces (Wooden and Miller, 1990; Wooden and DeWitt, 1991, table 2; unpublished data by J.L. Wooden; table 8, fig. 29).

On a $^{207}Pb/^{204}Pb$ vs. $^{206}Pb/^{204}Pb$ diagram, whole-rock samples from rocks of the Mojave and Central Arizona crustal provinces fall on two distinct lines (Wooden and Miller, 1990; Wooden and DeWitt, 1991). In order to better illustrate the differences between $^{207}Pb/^{204}Pb$ ratios of different rocks, we normalize the data in reference to the analytical results from an ore lead from the United Verde mine at Jerome in the Central Arizona province (Wooden and DeWitt, 1991). A model 1.7 Ga $^{207}Pb/^{204}Pb$ vs. $^{206}Pb/^{204}Pb$ isochron passing through the data from that sample was calculated. For any $^{206}Pb/^{204}Pb$ ratio measured for a sample, a $^{207}Pb/^{204}Pb$ ratio can be calculated that falls on the model isochron. The $^{206}Pb/^{204}Pb$ measured for the sample is compared to the calculated value by subtracting the model value from the sample value and multiplying by 100. This value is expressed as $\Delta\ ^{207}Pb/^{204}Pb$. Analytical error in this derived value is ±1.5 units, so small differences between samples are not significant.

The high $^{207}Pb/^{204}Pb$ relative to $^{206}Pb/^{204}Pb$ and high but variable Th/U ratios obtained from Early Proterozoic plutonic rocks of the Poachie region are much more similar to those from the Mojave crustal province than those from the Central Arizona crustal province. However, both those parameters are also more variable than those from the Mojave province (fig. 29*A*). The Poachie region apparently lies in the Mojave crustal province but near its eastern margin where magmas had some variable, but usually minor, input from central Arizona mantle and (or) aesthenosphere. Single crystal zircon studies of samples from the gneissic tonalite and similar studies of the Butte Falls Tuff, a unit in the Bagdad metamorphic belt north of the Poachie region, indicate that the source region for the magmas which crystallized to form those units was Mojave crust containing some Archean

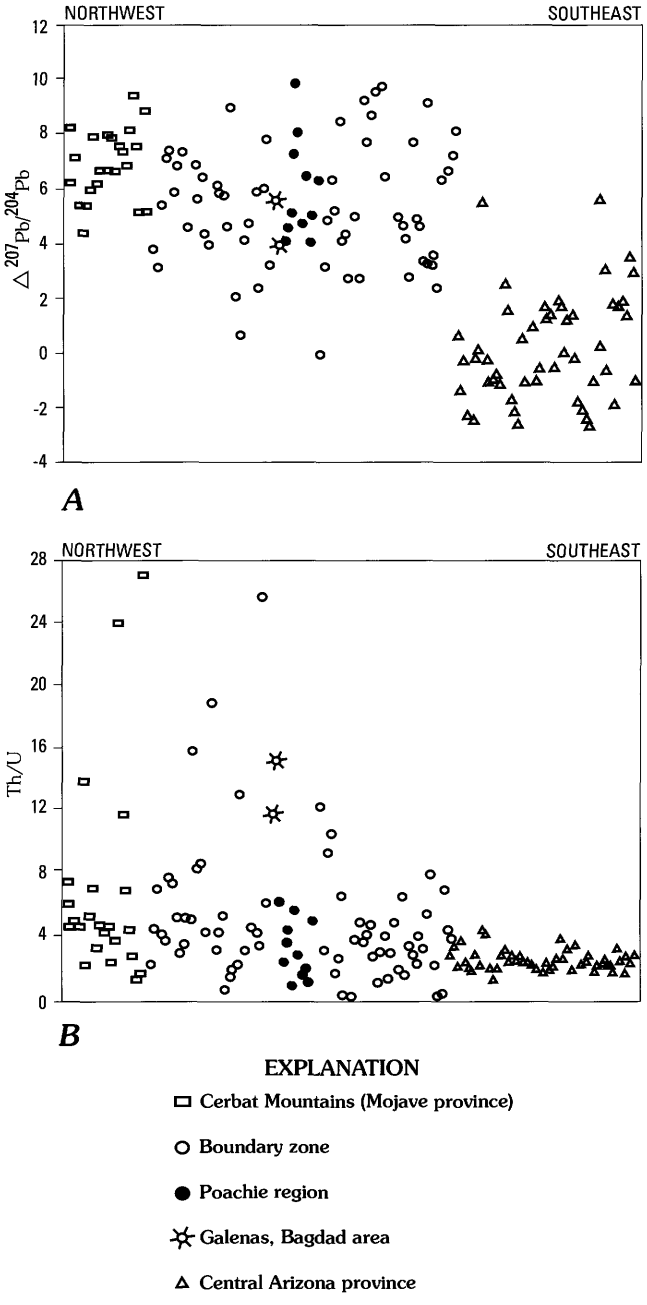

Figure 29. $\Delta\ ^{207}Pb/^{204}Pb$ values and calculated Th/U ratios of Early Proterozoic rocks of the Poachie region in a data array across the Mojave-Central Arizona Pb-isotopic crustal boundary plotted against a curved transect from the Cerbat Mountains in the Mojave province in the northwest to the Bradshaw Mountains in the Central Arizona province in the southeast. No distance scale. Data from the Poachie region in table 8. *A*, $\Delta\ ^{207}Pb/^{204}Pb$. See text for explanation. *B*, Th/U calculated from Pb-isotopic analysis.

zircon (Wooden and others, 1994). Differences in the lithospheric mantle beneath the Mojave and Central Arizona crustal provinces are suggested by a regional Pb, Sr, and Nd study of 1.15 Ga diabase bodies (Hammond and Wooden, 1990). However, none of the samples in their study come from in or near the Poachie region so that we might relate their data to our Pb-isotopic data on the granitic rocks.

Table 8. Pb-isotopic compositions of whole rocks and feldspars from the Poachie region.

[U/Pb, Th/Pb, and Th/U calculated using 206/204, 207/204, 208/204 values of 15.8, 15.31, 35.4, and 16.5, 15.42, 36.0 for 1.7 and 1.4 Ga samples respectively. △207/204 calculated for a 1.71 Ga Pb-Pb isochron through the Jerome, Ariz., galena (See text; Wooden and DeWitt, 1991)]

		Measured			Calculated				△
Appendix sample No.	Field sample No.	$^{206}Pb/^{204}Pb$	$^{207}Pb/^{204}Pb$	$^{208}Pb/^{204}Pb$	$^{238}U/^{204}Pb$	$^{235}U/^{204}Pb$	$^{232}Th/^{204}Pb$	Th/U	$^{207}Pb/^{204}Pb$
				Galena					
	Bagdad	15.818	15.336	35.461	0.1	0.8	0.7	11.7	5.6
	Bruce mine[1]	15.805	15.318	35.422	0.0	0.2	0.2	15.2	4.0
				1.7-Ga rock and feldspar (F) samples					
1	1154	17.797	15.568	35.658	6.5	7.9	36.5	5.6	8.2
2	1166	16.884	15.496	36.787	3.5	5.7	15.5	4.4	10.5
8	1161	25.402	16.330	43.300	31.2	31.3	88.4	2.8	4.9
8	1161(F)	20.214	15.817	37.719	14.3	15.6	25.9	1.8	7.8
15	750(JW-84-11)	17.968	15.51	36.854	7.0	7.4	16.3	2.3	4.7
15	750(F)	16.737	15.437	35.891	3.0	3.9	5.5	1.8	6.1
16	751(JW-84-12)	17.126	15.468	36.785	4.3	4.8	15.5	3.6	5.2
16	751(F)	16.342	15.386	35.808	1.8	2.3	4.6	2.6	5.2
22	749(JW-84-9)	18.040	15.553	39.392	7.3	7.5	44.7	6.1	4.1
22	749(F)	16.292	15.403	35.912	1.6	2.9	5.7	3.6	7.4
28	B-95	23.219	16.094	39.597	24.1	24.0	47.0	1.9	4.1
28	B-95(F)	21.006	15.93	36.997	16.9	19.0	17.9	1.1	10.8
29	W-325	24.899	16.280	38.381	29.6	29.8	33.4	1.1	5.1
29	325(F)	20.469	15.903	36.643	15.2	18.2	13.9	0.9	13.7
30	317	19.372	15.715	40.563	11.6	12.4	57.8	5.0	6.4
30	317(F)	17.868	15.595	37.737	6.7	8.7	26.2	3.9	10.1
35	1158	19.105	15.689	36.855	10.7	11.6	16.3	1.5	6.6
35	1158(F)	17.153	15.502	35.895	4.4	5.9	5.5	1.3	8.3
38	1163(JW-85-63)	19.231	15.710	36.306	11.1	12.3	10.1	0.9	7.4
38	1163(F)	16.974	15.494	35.621	3.8	5.6	2.5	0.6	9.4
				1.4-Ga rock and feldspar (F) samples					
43	1168	18.413	15.613	40.771	7.8	8.7	65.6	8.4	6.2
43	1168(F)	16.606	15.450	37.392	0.4	1.4	19.1	44.5	8.8
44	1164F(JW-85-64)	16.527	15.428	36.962	0.1	0.4	13.2	120.6	7.4
47	390(JW-84-10)	17.146	15.467	37.358	2.6	2.1	18.7	7.1	4.9
47	390(F)	16.642	15.449	36.517	0.6	1.3	7.1	12.3	8.3
50	752(JW-84-13)	19.117	15.678	39.427	10.6	11.7	47.1	4.4	5.4
50	752(F)	16.841	15.475	36.105	1.4	2.5	1.4	1.0	8.8
51	753(JW-84-15)	21.079	15.845	41.041	18.6	19.2	69.3	3.7	1.6
51	753(F)	16.907	15.481	36.260	1.7	2.8	3.6	2.2	8.8
54	A-151a(F)	17.079	15.472	36.586	2.4	2.3	8.1	3.4	6.0
57	A-153(F)	16.677	15.417	36.032	0.7	0.1	0.4	0.6	4.7
58	W-295	23.200	16.015	42.490	27.2	26.9	89.2	3.3	3.6
58	W-295(F)	18.290	15.597	37.227	7.3	8.0	16.9	2.3	5.9
59	W-322	19.628	15.696	42.329	12.7	12.5	87.0	6.9	1.8
59	W-322(F)	17.588	15.524	37.841	4.4	4.7	25.3	5.7	5.9

[1]Stacey and others (1976). Massive sulfide deposit in the Bagdad metamorphic belt 5 km north of the Poachie region.

Summary and Interpretation

The Poachie region consists of Early and Middle Proterozoic plutonic rocks in about equal amounts. Plutons are separated by screens of, and contain inclusions of, amphibolite-facies metamorphosed sedimentary and volcanic rock. No basement to the metamorphic sequence has been identified, but inherited zircons in some of the metamorphic and plutonic rocks indicate that earliest Late Archean and Proterozoic crustal material forms some part of the lower crust.

Metamorphic rocks are not well dated but are probably 1.74 to 1.72 Ga. The oldest plutonic rocks may be of similar age, but most of them are 1.71–1.68 Ga. Deformation and metamorphism probably reached a peak about 1.71–1.70 Ga but continued at least locally to <1.69 Ga. Local faulting and formation of mylonite zones occurred at least as late as 1.68 Ga and at least locally as late as ≈1.4 Ga. The main deformation, metamorphism, and plutonism occurred at about the same time as the Ivanpah orogeny in the Mojave province in southeastern California (Wooden and Miller, 1990) and destroyed evidence of older crustal rocks at

levels now exposed in the region. Similar metamorphism and plutonism were associated with the Ivanpah orogeny in southeastern California.

Early Proterozoic mafic metavolcanic rocks are more primitive than the gabbros emplaced during the regional metamorphism. They are more Fe-rich and contain less Sr. The gabbros show more LREE/HREE enrichment and have higher Th/U ratios than the metavolcanic rocks. These metavolcanic rocks may represent contributions from the aesthenosphere and (or) Central Arizona province mantle to volcanic arcs built on Mojave province lithosphere.

Early Proterozoic plutonic rocks range from gabbro to granite and from calcic to alkalic and show metaluminous to peraluminous signatures. No evidence of changing composition with time has been detected, except our data do indicate that the gabbros are older than all the other granitic rocks. The peraluminous rocks have higher whole-rock $^{207}Pb/^{204}Pb$ relative to $^{206}Pb/^{204}Pb$ ratios than the metaluminous plutonic rocks, and those ratios are similar to ones from the metasedimentary rocks. Pb-isotopic ratios indicate that the metasedimentary rocks were derived from crust having the Mojave Pb-isotopic signature. The peraluminous chemistry of some of the Early Proterozoic plutonic rocks appears to be related, at least in part, to contamination by aluminous metasedimentary rocks. For both metaluminous and peraluminous rock the Pb-isotopic compositions range from transitional to about equal to those in the Mojave crustal province. Variable Pb-isotopic ratios in Early Proterozoic whole-rock samples and feldspars indicate that these rocks were derived in various degrees from a combination of Mojave crust and a younger, central Arizona, mantle component.

Large volumes of alkali-calcic magma invaded the crust in Middle Proterozoic time, about 1.42–1.41 Ga. The mostly metaluminous Signal Granite was emplaced 1,410 Ma. Farther east the granites of Olea Ranch crystallized at 1,418 Ma and were followed about 1,415 Ma by the granites of Joshua Tree Parkway and Grayback Mountain. Middle Proterozoic granites east of the Signal Granite are weakly peraluminous to weakly metaluminous. These rocks may have originated in part by crustal anatexis involving Early Proterozoic peraluminous material, which crops out extensively in the region. Emplacement and cooling of these rocks were locally accompanied by movement along shear zones.

Whole-rock Pb-isotopic studies indicate that the Poachie region lies at the east edge of the Mojave crustal province where some magmas may have had input from subducted Central Arizona mantle or from the aesthenosphere (Wooden and DeWitt, 1991; Bryant and others, 1994). Moreover, chemical similarities between the Early and Middle Proterozoic granitic rocks in the Mojave crustal province suggest that magmas of both ages may have shared sources in preexisting crust at the edge of the Mojave crustal block, and differences may reflect the addition of some juvenile components into melts that formed the 1.7 Ga rock suite.

References Cited

Aldrich, L.T., Wetherill, G.W., and Davis, G.L., 1957, Occurrence of 1350 million-year-old granitic rocks in the western United States: Geological Society of America Bulletin, v. 68, p. 655–656.

Anderson, C.A., Blacet, P.M., Silver, L.T., and Stern, T.W., 1971, Revision of the Precambrian stratigraphy in the Prescott-Jerome area, Yavapai County, Arizona: U.S. Geological Survey Bulletin 1324-C, p. C1–C16.

Anderson, C.A., Scholz, E.A., and Strobell, J.D., Jr., 1955, Geology and ore deposits of the Bagdad area, Yavapai County, Arizona: U.S. Geological Survey Professional Paper 278, 103 p.

Anderson, J.L.,1983, Proterozoic anorogenic granite plutonism in North America, *in* Medaris, L.G., Jr., Byers, C.W., Mickelson, D.M., and Shanks, W.C., eds., Proterozoic Geology—Selected papers from an international Proterozoic symposium: Geological Society of America Memoir 161, p. 133–154.

———1989, Proterozoic anorogenic granites of the southwestern United States, *in* Jenney, J.P., and Reynolds, S.J., eds., Geologic evolution of Arizona: Arizona Geological Society Digest, v. 17, p. 211–238.

Anderson, J.L., and Bender, E.E., 1989, Nature and origin of Proterozoic A-type granite magmatism in the southwestern United States of America: Lithos, v. 23, p. 19–52.

Anderson, J.L., Wooden, J.L., and Bender, E.E., 1993, Mojave province of southern California and vicinity, *in* Van Schmus, W.R., and others, eds., Transcontinental Proterozoic provinces, *in* Reed, J.C., Jr., and others, eds., Precambrian—Conterminous U.S.: Geological Society of America, The Geology of North America, v. C-2, p. 176–188.

Anderson, Philip, 1989a, Proterozoic plate tectonic evolution of Arizona, *in* Jenney, J.P. and Reynolds, S.J., eds., Geologic evolution of Arizona: Arizona Geological Society Digest, v. 17, p. 17–55.

———1989b, Stratigraphic framework, volcanic-plutonic evolution, and vertical deformation of the Proterozoic volcanic belts of central Arizona, *in* Jenney, J.P., and Reynolds, S.J., eds., Geologic evolution of Arizona: Arizona Geological Society Digest, v. 17, p. 57–147.

Arth, J.G., and Hanson, G.N., 1975, Geochemistry and origin of the Early Proterozoic crust of northeastern Minnesota: Geochimica et Cosmochimica Acta, v. 39, no. 3, p. 325–362.

Baedecker, P.A., and McKown, D.M., 1987, Instrumental neutron activation analysis of geochemical materials, *in* Baedecker, P.A., ed., Methods for geochemical analysis: U.S. Geological Survey Bulletin 1770, p. H1-H14.

Banks, N.G., Cornwall, H.R., Silberman, M.L., Creasey, S.C., and Marvin, R.F., 1972, Age of intrusion and ore deposition at Ray, Arizona—Part 1, K-Ar ages: Economic Geology, v. 67, p. 864-878.

Bennett, V.C., and DePaolo, D.J., 1987, Proterozoic crustal history of the western United States as determined by neodymium isotope mapping: Geological Society of America Bulletin, v. 99, p. 674–685.

Bryant, Bruce, 1992, Geologic map of the Poachie Range, Mohave and Yavapai Counties, Arizona: U.S. Geological Survey Miscellaneous Geologic Investigations Map I-2198, scale 1:25,000.

———1995, Geologic map, cross sections, isotopic dates, and mineral deposits of the Alamo Lake 30 × 60-minute quadrangle, west-central Arizona: U.S. Geological Miscellaneous Geologic Investigations Map I-2489, scale 1:100,000.

Bryant, Bruce, DeWitt, Ed, Wooden, J.L., and Conway, C.M., 1994, The boundary between the Early Proterozoic Mojave and central Arizona crustal provinces, western Arizona: Geological Society of America Abstracts with Programs, v. 26, p. 6–7.

Bryant, Bruce, Naeser, C.W., and Fryxell, J.F., 1991, Implications of low-temperature cooling history across the Colorado Plateau–Basin and Range boundary, west-central Arizona: Journal of Geophysical Research, v. 96, no. B7, p. 12376–12388.

Bryant, Bruce, and Wooden, J.L., 1986, Early and Middle Proterozoic crustal history of the Poachie Range, Arizona: Geological Society of America Abstracts with Programs, v. 18, no. 4, p. 344.

———1991a, Chemical and Pb isotopic composition of Proterozoic plutonic rocks in the transition zone between the Mojave and Arizona crustal provinces, Poachie region, west-central Arizona: Geological Society of America Abstracts with Programs, v. 23, no. 4, p. 8.

———1991b, Proterozoic geology of the Poachie Range and vicinity, west-central Arizona, *in* Karlstrom, K.E., ed., Proterozoic ore deposits, stratigraphy, and tectonics of Arizona: Arizona Geological Society Digest, v. 19, p. 85–95.

Bryant, Bruce, Wooden, J.L., Gehrels, G.E., and Spencer, J.E., 1996, Plutonic and metamorphic history, northern part of the Harcuvar metamorphic complex, Buckskin and eastern Harcuvar Mountains, Arizona: Geological Society of America Abstracts with Programs, v. 28, no. 5, p. 51.

Chamberlain, Kevin, and Bowring, Sam, 1990, Proterozoic geochronologic and isotopic boundary in NW Arizona: Journal of Geology, v. 98, p. 399–416.

Conway, C.M., Connelly, T.J., and Robison, L.C., 1986, An Early Proterozoic volcanic-hydrothermal-exhalative system at Bagdad, Arizona, *in* Beatty, Barbara, and Wilkinson, P.A.K., eds., Frontiers in geology and ore deposits of Arizona and the southwest: Arizona Geological Society Digest, v. 16, p. 24–34.

Creasey, S.C., 1980, Chronology of intrusion and deposition of porphyry copper ores, Globe-Miami district, Arizona: Economic Geology, v. 75, p. 830–844.

Damon, P.E., Livingston, D.E., and Erickson, R.C., 1962, New K-Ar dates for the Precambrian of Pinal, Gila, Yavapai, and Coconino Counties, Arizona, *in* Weber, R.H., and Pierce, H.W., eds., Guidebook of the Mogollon Rim region, east-central Arizona: New Mexico Geological Society Guidebook, 13th Field Conference, p. 56–57.

DeWitt, Ed, 1989, Geochemistry and tectonic polarity of Early Proterozoic (1700–1750 Ma) plutonic rocks, north-central Arizona, *in* Jenny, J.P., and Reynolds, S.J., eds., Geologic evolution of Arizona: Arizona Geological Society Digest 17, p. 149–163.

Duebendorfer, Ernie, and Chamberlain, Kevin, 1994, The Cerbat Mountains, Arizona—Implications for the boundary between the Mojave and Yavapai Proterozoic provinces: Geological Society of America Abstracts with Programs, v. 26, no. 6, p. 12.

Duebendorfer, E.M., Nyman, M.W., Chamberlain, K.R., and Jones, C.S., 1998, Proterozoic rocks within the Mojave-Yavapai boundary zone, northwestern Arizona—Comparison of metamorphic and structural evolution across a major lithospheric(?) structure, *in* Duebendorfer, E.M., ed., Geologic excursions in northern and central Arizona: Field trip guidebook for Geological Society of America Rocky Mountain Section meeting Northern Arizona University, Flagstaff, Ariz., May 1998, p. 127–148.

Elston, D.P., and McKee, E.H., 1982, Age and correlation of the late Proterozoic Grand Canyon disturbance, northern Arizona: Geological Society of America Bulletin, v. 93, p. 681–699.

Floyd, L.D., and Winchester, J.A., 1978, Identification and discrimination of altered and metamorphosed volcanic rocks using immobile elements: Chemical Geology, v. 21, p. 291–306.

Fridrich, C.J., DeWitt, Ed, Bryant, Bruce, Richard, Steve, and Smith, R.P., 1998, Geologic map of the Collegiate Peaks wilderness area and the Grizzly Peak caldera, Sawatch Range, central Colorado: U.S. Geological Survey Map I-2565, scale 1:50,000, 29 p.

Hammond, J.G., 1990, Middle Proterozoic diabase intrusions in the southwestern U.S.A. as indicators of limited extensional tectonism, *in* Gower, C.F., Rivers, T., and Ryan, B., eds., Mid-Proterozoic Laurentia-Baltica: Geological Association of Canada Special Paper 38, p. 517–531.

Hammond, J.G., and Wooden, J.L., 1990, Isotopic constraints on the petrogenesis of Proterozoic diabase in southwestern USA, *in* Parker, A.J., Rickwood, P.C., and Tucker, D.H., eds., Mafic dykes and emplacement mechanisms: Rotterdam, Balkema, p. 145–156.

Hanson, G.N., 1980, Rare-earth elements in petrogenetic studies of igneous systems: Annual Review of Earth and Planetary Sciences, v. 8, p. 371–406.

Hawkins, D.P, Bowring, S.A., Ilg, B.R., Karlstrom, K.E., and Williams, M.L., 1996, U-Pb geochronologic constraints on the Paleoproterozoic crustal evolution of the Upper Granite Gorge, Grand Canyon, Arizona: Geological Society of America Bulletin, v. 108, no. 9, p. 1167–1181.

Karlstrom, K.E., and Bowring, S.A., 1988, Early Proterozoic assembly of tectonostratigraphic terranes in southwestern North America: Journal of Geology, v. 96, p. 561–576.

———1991, Styles and timing of Early Proterozoic deformation in Arizona—Constraints on tectonic models, *in* Karlstrom, K.E., ed., Proterozoic geology and ore deposits of Arizona: Arizona Geological Society Digest, v. 19, p. 1–10.

———1993, Proterozoic orogenic history of Arizona, *in* Van Schmus, W.R., and Bickford, M.E., eds., Transcontinental Proterozoic provinces, *in* Reed, J.C., Jr., Bickford, M.E., Houston, R.S., Link, P.K., Rankin, D.W., Sims, P.K., and Van Schmus, W.R., eds., Precambrian—Conterminous U.S.: The geology of North America, v. C-2, Geological Society of America, p. 188–211.

Karlstrom, K.E., Bowring, S.A., and Conway, C.M., 1987, Tectonic significance of an Early Proterozoic two-province boundary in central Arizona: Geological Society of America Bulletin, v. 99, p. 529–538.

King, Bi-Shia, and Lindsay, J., 1990, Determination of 12 selected trace elements in geologic materials by energy-dispersive X-ray fluorescence spectrometry, *in* Arbogast, B.F., ed., Quality assurance manual for the Branch of Geochemistry, U.S. Geological Survey: U.S. Geological Survey Open-File Report 90-668, p. 161–165.

Le Bas, M.J., Le Maitre, R.W., Streckeisen, A.L., and Zanettin, B., 1986, A chemical classification of volcanic rocks based on the total alkali-silica diagram: Journal of Petrology, v. 27, p. 745–750.

Lichte, F.E., Meier, A.L., and Crock, J.G., 1987, Determination of the rare-earth elements in geological materials by inductively coupled plasma mass spectrometry: Analytical Chemistry, v. 59, no. 8, p. 1150–1157.

Lucchitta, Ivo, and Suneson, Neil, 1982, Signal Granite (Precambrian), west-central Arizona: U.S. Geological Survey Bulletin 1529-H, p. H87–H90.

———1994, Geologic map of the Signal quadrangle, Mohave County, Arizona: U.S. Geological Survey Geologic Quadrangle Map GQ-1709, scale 1:24,000.

McKown, D.M., and Knight, R.J., 1990, Determination of uranium and thorium in geologic materials by delayed neutron counting, *in* Arbogast, B.F., ed., Quality assurance manual for the Branch of Geochemistry, U.S. Geological Survey: U.S. Geological Survey Open-File Report 90-668, p. 146–150.

Nyman, M.W., Karlstrom, K.E., Kirby, E., and Graubard, C.M. 1994, Mesoproterozoic contractional orogeny in western North America—Evidence from 1.4 Ga plutons: Geology, v. 22, p. 901–904.

Otton, J.K., 1985, Geologic environment of uranium in lacustrine host rocks in the western United States, *in* Finch, W.I., and Davis, J.F., eds., Geological environments of sandstone-type uranium deposits: International Atomic Energy Agency Technical Document 328, p. 229–241.

Papp, C.S.E., Aruscavage, P.J., and Brandt, E.L, 1990, Determination of ferrous oxide in geologic materials by potentiometric titration, *in* Arbogast, B.F., ed., Quality assurance manual for the Branch of Geochemistry, U.S. Geological Survey: U.S. Geological Survey Open-File Report 90-668, p. 139–145.

Pearce, J.A., Harris, N.B.W., and Tindle, A.G., 1984, Trace element discrimination diagrams for the tectonic interpretation of granitic rocks: Journal of Petrology, v. 25, pt. 4, p. 956–983.

Pribble, S.T., 1990, Determination of fluoride in silicates by ion-selective electrode following $LiBO_4$ fusion and HNO_3 dissolution, *in* Arbogast, B.F., ed., Quality assurance manual for the Branch of Geochemistry, U.S. Geological Survey: U.S. Geological Survey Open-File Report 90-668, p. 123–126.

Reynolds, S.J., 1988, Geologic map of Arizona: Arizona Geological Survey Map 26, scale 1:1,000,000.

Reynolds, S.J., Florence, F.P., Welty, J.W., Roddy, M.S., Currier, D.A., Anderson, A.V., and Keith, S.B., 1986, Compilation of radiometric age determinations in Arizona: Arizona Bureau of Geology and Mineral Technology Bulletin 197, 258 p.

Shafiqullah, Muhammad, Damon, P.E., Lynch, R.J., Reynolds, S.J., Rehrig, W.A., and Raymond, R.H., 1980, K-Ar geochronology and geologic history of southwestern Arizona and adjacent areas, *in* Jenny, J.P., and Stone, Claudia, eds., Studies in western Arizona: Arizona Geological Society Digest, v. 12, p. 201–260.

Shastri, L.L., Chamberlain, K.R., and Bowering, S.A., 1991, Inherited zircon from CA. 1.1 Ma mafic dikes, NW Arizona: Geological Society of America Abstracts with Programs, v. 23, no. 4, p. 93.

Silver, L.T., 1960, Age determinations on a Precambrian diabase differentiate in the Sierra Ancha, Gila County, Arizona [abs.]: Geological Society of America Bulletin, v. 71, p. 1973–1974.

———1968, U-Pb isotope relations and their historical implications in Precambrian zircon from Bagdad, Arizona [abs.]: Geological Society of America Special Paper 101, p. 420.

———1978, Precambrian formations and Precambrian history in Cochise County, southeastern Arizona, *in* Callender, J.F., and others, eds., Land of Cochise—Southeastern Arizona: New Mexico Geological Association Guidebook, 29th Field Conference, p. 157–163.

Silver, L.T., Williams, I.S., and Woodhead, J.A., 1980, Uranium in granite from the southwestern United States—Actinide parent-daughter systems, sites, and mobilization, first year report: U.S. Department of Energy Open File Report GJBX-45-81, 380 p.

Stacey, J.S., Doe, B.R., Silver, L.T., and Zartman, R.E., 1976, Plumbotectonics IIA, Precambrian massive sulfide deposits: U.S. Geological Survey Open-File Report: OF 76-0476, 26 p.

Stacey, J.S., and Kramers, J.D., 1975, Approximation of terrestrial lead isotope evolution by a two-stage model: Earth and Planetary Science Letters, v. 26, p. 207–221.

Streckeisen, A.L., 1973, Plutonic rocks, classification and nomenclature recommended by the IUGS Subcommittee on the systematics of igneous rocks: Geotimes, v. 18, no. 10, p. 25–29.

Taggart, J.E., Jr., Bartel, A.J., and Siems, D.F., 1990, High precision major element analysis of rocks and minerals by wavelength dispersive X-ray fluorescence spectroscopy, *in* Arbogast, B.F., ed., Quality assurance manual for the Branch of Geochemistry, U.S. Geological Survey: U.S. Geological Survey Open-File Report 90-668, p. 166–172.

Taylor, S.R., and McLennan, S.M., 1981, The composition and evolution of the continental crust—Rare earth element evidence from sedimentary rocks: Philosophical Transactions of the Royal Society of London, v. A301, p. 381–399.

Wasserberg, G.J., and Lanphere, M.A., 1965, Age determinations in the Precambrian of Arizona and Nevada: Geological Society of America Bulletin, v. 76, p. 735–758.

Wilson, E.D., Moore, R.T., and Cooper, J.R., 1969, Geologic map of Arizona: Arizona Bureau of Mines, scale 1:500,000.

Wooden, J.L., and DeWitt, Ed, 1991, Pb isotope evidence for the boundary between the Early Proterozoic Mojave and Central Arizona crustal provinces in western Arizona, *in* Karlstrom, K.E., ed., Proterozoic ore deposits, stratigraphy, and tectonics of Arizona: Arizona Geological Society Digest, v. 19, p. 27–50.

Wooden, J.L., and Miller, D.M., 1990, Chronologic and isotopic framework for Early Proterozoic crustal evolution in the eastern Mojave Desert region: Journal of Geophysical Research, v. 95, no. B12, p. 20133–20146.

Wooden, J.L., Nutman, A.P., Miller, D.M., Howard, K.A., Bryant, Bruce, and DeWitt, Ed, 1994, SHRIMP U-Pb zircon evidence for late Archean and Early Proterozoic crustal evolution in the Mojave and Arizona crustal provinces: Geological Society of America Abstracts with Programs, v. 26, no. 6, p. 69.

Wooden, J.L., Stacey, J.S., Doe, B.R., Howard, K.A. and Miller, D.M., 1988, Pb isotopic evidence for the formation of Proterozoic crust in the southwestern United States, *in* Ernst, W.G., ed., Metamorphism and crustal evolution of the western United States: Englewood Cliffs, N.J., Prentice Hall, Rubey Volume VII, p. 68–86.

Appendix. Location and Description of Chemically and (or) Isotopically Analyzed Samples

1. Andalusite-bearing garnet-plagioclase-quartz-muscovite gneiss from large angular block slumped into wash from 3 m above. Sec. 14, T. 13 N., R. 10 W. 760 m N. 84° W. from BM 2906, lat 34°28'02" N., long 113°16'40" W., Arrastra Mtn NE 7½' quadrangle, Yavapai County. Unit of mica gneiss in the Bagdad metamorphic belt probably equivalent to the Hillside Mica Schist of the Bagdad area. Anhedral quartz 0.1–0.3 mm in diameter. Muscovite in synkinematic to postkinematic flakes 0.1–0.3 mm long and in postkinematic porphyroblasts as much as 1.1 mm long. Euhedral to subhedral garnet as much as 0.3 m in diameter. Andalusite mostly altered to muscovite. Secondary chlorite, probably from biotite. Accessory zircon, tourmaline, and opaque minerals. Major-oxide and trace-element concentrations, table 3. Whole-rock Pb-isotopic analysis, table 8. Field No. 1154.
2. Garnet-biotite-microcline-plagioclase-quartz gneiss from layered schist and gneiss containing lenses and stringers of pegmatite as much as 1 cm thick. From outcrop on north side of wash and about 2 m above its floor in E. part sec. 7, T. 13 N., R. 12 W. 800 m N. 46° W. from spot elevation 2730 and 150 m west of east line of sec. 7, lat 34°28' N., long 113°32'51" W., Signal Mountain 7½' quadrangle, Mohave County. Granoblastic to mosaic texture. Anhedral quartz as much as 1 mm in diameter, except 4 mm in a segregation; plagioclase (An_{32}) as much as 0.7 mm in diameter; microcline as much as 7 mm in diameter; synkinematic and postkinematic biotite as much as 0.3 mm long; garnet in skeletal crystals as much as 3 mm in diameter and as smaller anhedral to euhedral grains as much as 0.3 mm in diameter. Accessory zircon. Major-oxide and trace-element concentrations, table 3. Feldspar Pb-isotope analysis, table 8. Field Nos. 1166 and JW-85-66.
3. Garnet-bearing amphibolite layer 7 m thick from Bagdad metamorphic belt in mica gneiss and schist unit (Xmg of Bryant, 1992). In wash 300 m S. 67° W. from summit hill 3283. NW corner sec. 23, T. 13 N., R. 10 W., lat 34°27'31" N., long 113°15'11" W., Arrastra Mtn NE 7½' quadrangle, Yavapai County. Synkinematic to postkinematic green hornblende as much as 2 mm long, anhedral plagioclase 0.3 mm in diameter, subhedral garnet 2 mm in diameter, and accessory opaque minerals and apatite. Major-oxide and trace-element concentrations, table 3. Field No. 1159a.
4. Quartz-bearing amphibolite from Bagdad metamorphic belt in mica schist and gneiss unit (Xsg of Bryant, 1992). SW¼SE¼ sec. 6, T. 12 N., R. 10 W., lat 34°24'27" N., long 113°20'14" W., Arrastra Mtn NE 7½' quadrangle, Yavapai County. Anhedral to subhedral synkinematic to postkinematic green hornblende as much as 1.2 mm long, locally grades to colorless amphibole having the same extinction. Anhedral plagioclase (An_{35-28}) as much as 1 mm in diameter and quartz as much as 3 mm in diameter in segregation lens. Accessory opaque minerals, apatite, and sphene. Major-oxide and trace-element concentrations, table 3. Field No. W-419.
5. Fine-grained amphibolite from outlier of Bagdad metamorphic belt (Xa in Bryant, 1992) included in the granite of Thorn Peak and cut by numerous bodies of pegmatite and leucogranite as much as 20 m thick. In wash 200 m N. 9.5° W. from Negro Ben Spring NE¼SW¼ sec. 12, T. 12 N., R. 10 W., lat 34°23'11" N., long 113°15'11" W., Arrastra Mtn NE 7½' quadrangle, Yavapai County. Untwinned plagioclase 0.1 mm in diameter interstitial to euhedral to anhedral synkinematic to postkinematic green hornblende 0.3–0.6 mm long. Accessory opaque minerals and sphene. Cut by epidote veinlet 0.1 mm thick. Major-oxide and trace-element concentrations, table 3. Field No. 633.
6. Amphibolite from unit 20–40 m thick used as a marker for the west boundary of the interlayered gneiss unit (Xl) of Bryant (1992) in the Bagdad metamorphic belt. In wash 250 m S. 21°E. from 3324 spot elevation. N. 30° E. from center sec. 11, T. 13 N., R. 10 W., lat 34°28'52" N., long 113°16'29" W. Arrastra Mountain NE 7½' quadrangle, Yavapai County. Anhedral to subhedral synkinematic to postkinematic green hornblende as much as 0.6 mm long, anhedral to subhedral plagioclase (An_{25-45}) 0.05–0.2 mm in diameter. Sparse biotite and accessory sphene. Major-oxide and trace-element concentrations, table 3. Field No. M-96.
7. Quartz-bearing amphibolite from Bagdad metamorphic belt from interlayered gneiss unit (Xl) of Bryant (1992). South line of sec. 1, T. 13 N., R. 10 W. 320 m east of SE corner of sec. and triangulation point 3390, lat 34°29'18" N., long 113°29'17" W., Arrastra Mtn NE 7½' quadrangle, Yavapai County. Green hornblende as much as 0.7 mm long in aggregates, quartz and untwinned plagioclase 0.05–0.3 mm in diameter, and accessory sphene and opaque mineral. Major-oxide and trace-element concentrations, table 3. Field No. M-81.
8. Biotite-quartz-feldspar gneiss from outcrop in wash in NW¼ sec. 11, T. 13 N., R. 10 W., 660 m S. 75° E. from BM 3104; lat 34°28'59" N., long 113°16'51" W., Arrastra Mtn NE 7½' quadrangle, Yavapai County. Southward extension of unit mapped as Dick Rhyolite by Anderson and others (1955) and Conway and others (1986). Scattered quartz phenocrysts to 1 mm in diameter in nonlayered biotite-quartz-feldspar gneiss. Some streaky biotite concentrations, quartz segregations, and quartz-potassic feldspar-tourmaline pegmatites. Quartz in polycrystalline aggregates to 1 mm and in mosaic-textured groundmass with plagioclase (An_{32}) and microcline with a grain size of 0.1 mm, synkinematic and postkinematic biotite 0.1–0.3 mm long, sparse muscovite, accessory sphene and zircon, and secondary chlorite (fig. 3). U-Pb zircon age determination, figure 12. Major-oxide and trace-element concentrations, table 3. Whole-rock and feldspar Pb-isotopic analyses, table 8. Field No. 1161.
9. Biotite-muscovite-quartz schist from outcrop in wash at sharp bend 160 m N. 11° E. from center of sec. 11, T. 13 N., R. 10 W., lat 34°28'57" N., long 113°16'31"W., Arrastra Mtn

NE 7½' quadrangle, Yavapai County. Quartz in sparsely scattered roundish grains and aggregates as much as 0.8 mm in diameter and in a mosaic-textured matrix with a grain size of 0.1–0.2 mm. Synkinematic muscovite and biotite as much as 0.5 mm long, accessory opaque minerals and zircon, and secondary chlorite from biotite. U-Pb zircon age determination, figure 12. Field No. P-93-1.

10. Metagabbro from small body foliated and cut by pegmatite in Signal Granite (Bryant, 1992). Interpreted to be a roof pendant or inclusion in the granite. Sec. 28, T. 13 N., R. 12 W. 550 m S. 45° W. from Arrowhead Spring. Lat 34°26'27" N., long 113°30'45" W., Signal Mountain 7½' quadrangle, Mohave County. Anhedral to subhedral greenish-brown hornblende as much as 2 mm long, anhedral plagioclase (An_{55-65}) as much as 1 mm in diameter, accessory apatite and opaque minerals, and secondary chlorite and epidote. Major-oxide and trace-element concentrations, table 4. Field No. 450.
11. Diabase cut by sparse quartz-feldspar pegmatites. 125 m N. 85° W. from spot elevation 1854. South-central sec. 19, T. 13 N., R. 12 W., lat 34°26'55" N., long 113°33'20" W., Signal Mountain 7½' quadrangle, Mohave County. Plagioclase laths (An_{58-65}) as much as 2 mm long; monoclinic pyroxene as much as 3 mm in diameter encloses the plagioclase laths. Accessory opaque minerals and apatite; secondary amphibole, chlorite, and epidote. Major-oxide and trace-element concentrations, table 4. Field No. 907.
12. Biotite-hornblende gabbro from outcrop in wash 680 m N. 22° E. of center sec. 19, T. 13 N., R. 11 W., lat 24°27'25" N., long 113°26'50" W., Arrastra Mtn 7½' quadrangle, Mohave County. In unit of mixed plutonic and metamorphic rocks rich in gabbro and diorite shown on Poachie Range map (Bryant, 1992). Included in coarse-grained granite unit (Xcg) in figure 2. Intrudes hornblende and biotite schist and gneiss. Locally saussuritized, anhedral to subhedral, normally zoned plagioclase (An_{30-38}); anhedral to subhedral green hornblende as much as 1.5 mm long in aggregates locally accompanied by biotite; anhedral biotite as much as 1.5 mm long in aggregates with or without hornblende; accessory opaque minerals and sphene, and secondary epidote and carbonate minerals. Major-oxide and trace-element concentrations, table 4. Field No. W-61.
13. Hornblende gabbro from outcrop on top of hill 170 m S. 20° E. from NW corner of sec. 5, T. 12 N., R. 11 W., lat 34°24'52" N., long 113°25'57" W., Arrastra Mtn 7½' quadrangle, Mohave County. Forms a 150×400 m body shown on the Poachie Range map (Bryant, 1992) in coarse-grained granite unit (Xcg) and is cut by leucocratic granite. Anhedral to subhedral green hornblende as much as 3 mm long having sieve texture with plagioclase and opaque mineral; subhedral normally zoned, weakly saussuritized plagioclase (An_{40-47}) as much as 4 mm long; opaque minerals, minor quartz, accessory apatite and allanite, and secondary epidote and chlorite. Major-oxide and trace-element concentrations, table 4. Field No W-307.
14. Metagabbro from small body on north side of wash up drainage from crossing on county road, E center sec. 7, T. 13 N., R. 12 W.; 1,580 m N. 41½° W. of spot elevation 2730; lat 34°28'54" N., long 113°32'48" W., Signal Mountain 7½' quadrangle, Mohave County. Biotite-hornblende-plagioclase granofels with a grain size of 0.3–0.5 mm and a few hornblende grains as long as 1 mm. Plagioclase (An_{45}), green hornblende, biotite, and sparse monoclinic pyroxene and accessory apatite. Pyroxene is partly altered to hornblende in places. Cut by a sheared and altered zone rich in epidote. Major-oxide and trace-element concentrations, table 4. Field No. 1165.
15. Biotite-hornblende gabbro from outcrop on northwest side of wash, 220 m S. 32° W. of center sec. 17, T. 13 N., R. 11 W.; 420 m S. 20° E. from spot elevation 2952; lat 34°27'52" N., long 113°26'04" W., Arrastra Mtn 7½' quadrangle, Mohave County. Typical of the small bodies that form the oldest rock type in the complex of generally foliated plutonic rocks underlying much of the Poachie Range. In area of mixed plutonic and metamorphic rocks shown on the Poachie Range map (Bryant, 1992) but included in coarse-grained granite unit (Xcg) in figure 2. Anhedral to subhedral grains of plagioclase (An_{47}) to 3 mm in diameter with weak normal zoning and locally partly saussuritized, anhedral green hornblende to 1 mm but mostly 0.2–0.4 mm in diameter as aggregates between the plagioclase grains, anhedral brown biotite to 1.5 mm long, and accessory sphene and opaque minerals. U-Pb zircon age determination, figure 13. Major-oxide and trace-element concentrations, table 4. Whole-rock and feldspar Pb-isotopic analysis, table 8. Field Nos. 750 and JW-84-11.
16. Gneissic biotite diorite from 1.5 m long boulder in wash where this rock type forms numerous outcrops. Northwest corner of outcrop area of Early Proterozoic plutonic rocks forming the central and eastern parts of the Poachie Range. 580 m S. 33° E. from center sec. 17, T. 13 N., R. 11 W., 1,350 m S. 83° W. from Colorado Spring; lat 34°27'43" N., long 113°25'47" W., Arrastra Mtn 7½' quadrangle, Mohave County. Rock fairly typical texturally but somewhat more mafic than foliated plutonic rock typical of this part of large heterogeneous unit underlying much of the Poachie Range. Anhedral to subhedral variously saussuritized grains of plagioclase (An_{30}) as much as 4 mm in diameter, dark-brown synkinematic to postkinematic biotite as much as 2 mm long, accessory sphene, apatite, zircon, and secondary epidote, chlorite, and carbonate minerals. Chemical analysis was made of quartz monzodiorite 130 m up wash (appendix sample No. 17; field No. 192, following) containing much less secondary epidote than this sample. U-Pb zircon age determination, figure 13. Whole-rock and feldspar Pb-isotopic analysis, table 8. Field Nos. JW-84-12 and 751.
17. Gneissose hornblende-biotite quartz monzodiorite from northwest corner of area underlain by Early Proterozoic rocks in the Poachie Range. Outcrop in wash. 540 m N. 69½° W. from SE corner sec. 17, T. 13 N., R. 11 W., lat 34°27'40" N., long 113°25'48" W., Arrastra Mtn 7½' quadrangle, Mohave County. Anhedral to subhedral plagioclase (An_{28}) to 4 mm long; anhedral quartz to 2 mm diameter; anhedral locally strained and bent potassic

feldspar to 4 mm diameter; sieve-textured green hornblende to 3 mm long; weakly aligned biotite as much as 1.5 mm long; sparse myrmekite, accessory sphene, apatite, opaque minerals, and epidote. Major-oxide and trace-element concentrations, table 4. Field No. 192.

18. Hornblende-bearing biotite quartz monzodiorite from outcrop in wash 330 m S. 10° W. from center sec. 27, T. 13 N., R. 11 W., lat 34°26'03" N., long 113°23'56" W., Arrastra Mtn 7½' quadrangle, Mohave County. Anhedral to subhedral plagioclase (An_{28}) as much as 4 mm in diameter; biotite as much as 2 mm long in aggregates with sphene and opaque minerals; anhedral quartz as much as 3 mm in diameter; and anhedral microcline as much as 1.2 cm long, sparse myrmekite and hornblende, accessory sphene, hornblende, apatite, zircon, opaque minerals, epidote containing cores of allanite, and secondary chlorite. One glob of sphene grains has inclusions of opaque mineral and interstitial allanite and epidote. Major-oxide and trace-element concentrations, table 4. Field No. 1137.
19. Coarse-grained leucomonzonite from outcrop in wash 100 m N. 32° W. from center sec. 33, T. 13 N., R. 11 W., lat 34°25'29" N., long 113°24'58" W., Arrastra Mtn 7½' quadrangle, Mohave County. At contact with granodiorite. Biotite in clots. Anhedral microcline as much as 8 mm in diameter; anhedral to subhedral plagioclase (An_{38}) as much as 1 mm in diameter; anhedral to subhedral biotite as much as 2 mm long in single grains and in clots; interstitial quartz as much as 1 mm in diameter; sparse myrmekite, accessory opaque minerals, sphene, and zircon, and secondary epidote. Major-oxide and trace-element concentrations, table 4. Field No. W-301.
20. Porphyritic microcline-bearing biotite tonalite gneiss typical of the porphyritic granodiorite containing large equant feldspar phenocryst phase of the coarse-grained granite unit shown on the Poachie Range map (Bryant, 1992), but not shown in figure 2. This sample is from a sill(?) about 15 m thick in metamorphic rocks east of the Signal batholith. Outcrop in wash in north part sec. 18, T. 13 N., R. 11 W.; 1,320 m S. 55° W. from NE corner sec. 18; lat 34°28'11" N., long 113°26'51" W., Arrastra Mtn 7½' quadrangle, Mohave County. Anhedral, strongly strained quartz as much as 3 mm in diameter between plagioclase grains; anhedral to subhedral plagioclase (An_{34}) as much as 6 mm long; synkinematic and postkinematic biotite as much as 1.3 mm long in aggregates between larger plagioclase grains; microcline as much as 4 mm in diameter; sparse myrmekite, accessory opaque minerals, apatite, and zircon, and secondary epidote and chlorite. Major-oxide and trace-element concentrations, table 4. Field No. 1167.
21. Hornblende-biotite granite from outcrop on ridge 690 m S. 21° W. from center sec. 15, T. 12 N., R. 12 W., lat 34°22'37" N., long 113°29'50" W., Arrastra Mtn 7½' quadrangle, Mohave County. Well-foliated, migmatitic granite containing potassic feldspars as much as 3 cm in diameter in coarser grained layers. Biotite concentrated in clots 1–2 cm long. Locally clots outline swirly structure. Anhedral to subhedral plagioclase (An_{24}) as much as 8 mm long; anhedral microcline as much as 2 mm in diameter; anhedral quartz; anhedral to subhedral biotite as much as 0.5 mm long; dark-green anhedral hornblende as much as 2 mm long; sparse myrmekite and accessory opaque minerals and sphene. Major-oxide and trace-element concentrations, table 4. Field No. 552a.
22. Biotite granite from boulder associated with large outcrops in channel of Burro Creek. Possibly part of the Early Proterozoic plutonic suite of the Poachie Range. Middle of S½ sec. 9, T. 14 N., R. 12 W.; 230 m downstream from NNW.-trending tributary of Burro Creek fed by warm spring; 1,450 m S. 33° W. from triangulation point 2272. Lat 34°33'51" N., long 113°31'10" W., Greenwood Peak 7½' quadrangle, Mohave County. Porphyritic biotite granite containing equant potassic feldspar phenocrysts as much as 2 cm in diameter; subhedral normally zoned plagioclase (An_{27-17}) as much as 4 mm long; perthitic microcline; greenish-brown anhedral biotite as much as 2 mm long in aggregates; anhedral to euhedral epidote as much as 1 mm long; sparse myrmekite, accessory sphene, apatite, and zircon, and secondary chlorite from biotite. Compared to the Signal Granite the potassic feldspars in this rock are equant as opposed to elongate and the mafic clots are longer and more irregular. U-Pb zircon age determination, figure 14. Major-oxide and trace-element concentrations, table 4. Whole-rock and feldspar Pb-isotopic analysis, table 8. Field Nos. JW-84-9 and 749.
23. Hornblende-bearing biotite granodiorite from outcrop in wash 460 m S. 25° W. from center sec. 16, T. 13 N., R. 11 W., lat 34°27'50" N., long 113°25'05" W., Arrastra Mtn 7½' quadrangle, Mohave County. Intruded by coarse-grained granite nearby. Anhedral quartz as much as 3.5 mm in diameter; plagioclase (An_{23}) as much as 4 mm in diameter; anhedral to subhedral perthitic microcline as much as 6 mm in diameter; biotite as much as 1 mm long in aggregates; epidote in mafic clots with biotite and hornblende; accessory opaque minerals, zircon, apatite, and green hornblende in mafic clots with biotite and epidote. Major-oxide and trace-element concentrations, table 4. Field No. 1132a.
24. Biotite granite from outcrop in wash on line between secs. 30 and 31, 450 m E. of township line T. 13 N., R. 11 W., lat 34°25'50" N., long 113°27'13" W., Arrastra Mtn 7½' quadrangle, Mohave County. Foliated porphyritic biotite granite cut by dike of leucogranite containing faint foliation parallel to that in granite. Anhedral to subhedral microcline phenocrysts as much as 2.5 cm long; anhedral to subhedral plagioclase (An_{33}) as much as 3 mm long; anhedral quartz as much as 2 mm in diameter partly in mosaic-textured aggregates as much as 5 mm in diameter; anhedral biotite as much as 2 mm long; sparse hornblende and accessory sphene, opaque minerals, and apatite. Major-oxide and trace-element concentrations, table 4. Field No. 212.
25. Biotite granite from outcrop in wash 100 m N. 85° W. from SE corner sec. 16, T. 11 N., R. 10 W., lat 34°22'33" N., long 113°17'44" W., Arrastra Mtn NE 7½' quadrangle, Yavapai County. In outcrop porphyritic granite contains

a few xenoliths of biotite schist and gneiss. Anhedral to subhedral microcline as much as 3.5 mm in diameter; anhedral partly saussuritized and normally zoned plagioclase (An_{30}) as much as 6 mm long; anhedral to subhedral biotite as much as 2 mm long; and accessory opaque minerals, zircon, and apatite. Major-oxide and trace-element concentrations, table 4. Field No. 713.

26. Biotite granite gneiss from outcrop in wash 600 m east of center sec. 18, T. 12 N., R. 10 W., lat 34°22'59" N., long 113°19'52" W., Arrastra Mtn NE 7½' quadrangle, Yavapai County. Rock typical of unit Xcg in vicinity. Anhedral quartz as much as 6 mm in diameter; partly saussuritized anhedral plagioclase (An_{12}) as much as 1.5 mm in diameter; anhedral microcline as much as 4 mm in diameter; synkinematic to postkinematic biotite as much as 0.5 mm long; accessory allanite, apatite, zircon, and opaque minerals; secondary chlorite and epidote. Major-oxide and trace-element concentrations, table 4. Field No. 680.
27. Biotite granite gneiss from pluton of finer grained granite at the east end of the high crest of the Poachie Range (Xg of Bryant, 1992). Outcrop about 15 m above and east of wash at east margin of Arrastra Mtn 7½' quadrangle, 650 m S. 49° E. from center sec. 26, T. 13 N., R. 11 W., lat 34°26'00" N., long 113°22'31" W., Mohave County. Foliated medium-grained, rather leucocratic granite. Anhedral to subhedral plagioclase (An_{28}) as much as 2 mm in diameter; anhedral microcline as much as 2 mm in diameter; anhedral quartz as much as 3 mm long; synkinematic and postkinematic biotite as much as 1 mm long; accessory opaque minerals and zircon; secondary muscovite and epidote. Major-oxide and trace-element concentrations, table 5. Field No. 172b.
28. Leucocratic medium-grained granite (Xg) from pluton at the east end of the Poachie Range. From triangulation station Poachie at spot elevation 4807 in south-central sec. 35, T. 13 N., R. 11 W., lat 34°25'16" N., long 113°22'53" W., Arrastra Mtn 7½' quadrangle, Mohave County. Anhedral quartz and plagioclase (An_{23}) as much as 2 mm in diameter; microcline and biotite as much as 1.5 mm in diameter; accessory muscovite at least partly contemporaneous with biotite, zircon, allanite, apatite, and opaque minerals. Whole-rock and feldspar Pb-isotopic analysis, table 8. Field No. B-95.
29. Subhorizontal sheet of weakly foliated leucocratic granite intruding coarse-grained granite in SW¼SW¼ sec. 7, T. 12 N., R. 11 W., on south side of wash 330 m N. 82° W. from spot hilltop 3199; lat 34°23'43" N., long 113°26'47" W., Arrastra Mtn 7½' quadrangle, Mohave County. Anhedral quartz as much as 2.3 mm in diameter; anhedral saussuritized plagioclase and microcline as much as 1.5 mm long; sparse aligned biotite, accessory allanite, zircon, and opaque minerals, and secondary sericite from feldspar. Whole-rock and feldspar Pb-isotopic analyses, table 8. Field No. W-325.
30. Leucocratic biotite granite from small pluton mapped as YXg (Bryant, 1992). In wash in SW¼ sec. 2, T. 12 N., R. 11 W., 480 m N. 40° W. from spot elevation 3580, lat 34°24'21" N., long 113°22'10" W., Arrastra Mtn NE 7½' quadrangle, Mohave County. Anhedral quartz 0.1–0.6 mm but locally as much as 1.3 mm in diameter; anhedral, partly saussuritized plagioclase (about An_{20}) as much as 1 mm in diameter; anhedral microcline mainly 1 mm, but locally as much as 2 mm in diameter; well-aligned biotite as much as 0.7 mm in diameter; sparse myrmekite and muscovite partly contemporaneous and partly later than the biotite; accessory zircon, apatite, sphene, and opaque minerals; secondary epidote and chlorite. Whole-rock and feldspar Pb-isotopic analysis, table 8. Field No. 317.
31. Biotite-muscovite granite from outcrop in wash 570 m S. 5° W. from Negro Ben Spring in sec. 13, T. 12 N., R. 10 W., lat 34°23'14" N., long 113°15'12" W., Arrastra Mtn NE 7½ quadrangle, Yavapai County. Weakly developed foliation shown best in outcrop by aligned inclusions of mica gneiss. Plagioclase (An_{30}) as much as 2 mm in diameter. Potassic feldspar as much as 3 mm in diameter; muscovite as much as 1.3 mm long, some in aggregates; biotite as much as 1.3 mm long; accessory opaque minerals, apatite, and zircon. Major-oxide and trace-element concentrations, table 5. Field No. 636a.
32. Muscovite-biotite granite from outcrop south side of wash in sec. 9, T. 13 N., R. 9 W., 350 m N. 23° E. of Quail Spring; lat 34°28'47" N., long 113°11'55" W., Thorn Peak 7½ quadrangle, Yavapai County. Intrudes and includes xenoliths of hornblende-biotite-plagioclase gneiss and contains some zones of pegmatite dikes. Anhedral quartz as much as 1.5 mm in diameter mostly in granoblastic textured aggregates between feldspar grains; subhedral saussuritized plagioclase (An_{32}); anhedral to subhedral strained microcline as much as 4 mm in diameter; anhedral, locally bent, biotite and muscovite as much as 1 mm long—muscovite partly contemporaneous with biotite and partly younger; accessory opaque minerals, apatite, and zircon, and secondary sphene and epidote. A few zones of mortar structure cut the rock. Major-oxide and trace-element concentrations, table 5. Field No. 175b.
33. Biotite-muscovite granite gneiss from outcrop in wash 700 m N. 78° W. from center sec. 20, T. 12 N., R. 9 W., lat 34°22'11" N., long 113°13'24" W., Ives Peak 7½' quadrangle, Yavapai County. Granite in outcrop has numerous inclusions of fine-grained muscovite gneiss. Subhedral sericitized plagioclase as much as 6 mm long; subhedral microcline as much as 6 mm long; anhedral quartz as much as 0.6 mm in diameter in aggregates with mosaic texture; anhedral to subhedral, synkinematic to postkinematic biotite and muscovite as much as 1 mm long; accessory opaque minerals, apatite, allanite, zircon, and sphene; and secondary chlorite. Major-oxide and trace-element concentrations, table 4. Field No. A-10.
34. Biotite-muscovite granite from outcrop in wash 250 m S. 23° W. from center sec. 28, T. 13 N., R. 9 W., lat 34°26'07" N., long 113°12'25" W., Thorn Peak 7½' quadrangle, Yavapai County. Anhedral quartz as much as 0.5 mm in diameter in mosaic-textured areas interstitial to the feldspars; sericitized subhedral plagioclase as much as 5 mm in diameter; subhedral microcline as much as 9 mm long; anhedral muscovite as much as 1 mm long and anhedral biotite as much as 1.5 mm long in aggregates; accessory zircon, allanite rimmed by epidote, and

secondary epidote. Major-oxide and trace-element concentrations, table 5. Field No. A-21.

35. Muscovite-biotite granite from large roadcut in granite of Thorn Peak on U.S. Highway 93 in SW¼ sec. 5, T. 12 N., R. 9 W.; 690 m S. 19° E. from Bridge triangulation point. Sample from first bench in cut about 8 m above highway; lat 34°24'24" N., long 113°13'19" W., Thorn Peak 7½' quadrangle, Yavapai County. Rock in roadcut somewhat sheared and fractured, and unweathered rock is scarce. A few pegmatite dikes and one gently dipping diabase sheet cut the granite. Quartz in mosaic-textured aggregates with a grain size as much as 1 mm; anhedral to subhedral plagioclase to 2.3 mm in diameter; euhedral phenocrysts of microcline to 5 mm in diameter; anhedral muscovite and biotite to 1 mm long intergrown; accessory garnet, apatite, zircon, and opaque minerals and secondary epidote and chlorite. U-Pb zircon age determination, figure 14. Whole-rock and feldspar Pb-isotopic analysis, table 8. Major-oxide and trace-element concentrations, table 5. Field No. 1158.
36. Biotite monzodiorite from outcrop on east side of wash in Skunk Canyon 200 m north of section line, sec. 8, T. 13 N., R. 9 W., lat 34°28'32" N., long 113°14'52" W., Thorn Peak 7½' quadrangle, Yavapai County. Medium-grained granodiorite to diorite containing inclusions of fine-grained diorite or granodiorite and cut by some pegmatite. Locally foliated. Anhedral to subhedral saussuritized, locally antiperthitic plagioclase; anhedral to subhedral biotite as much as 2 mm long; anhedral microcline; anhedral sphene as much as 1.5 mm in diameter; accessory quartz, green hornblende, apatite, allanite, and secondary epidote. Major-oxide and trace-element concentrations, table 5. Field No. A-108.
37. Biotite-hornblende diorite from outcrop on east side of wash in Skunk Canyon 50 m north of section line, sec. 5, T. 13 N., R. 9 W., lat 34°29'19" N., long 113°14'51" W., Thorn Peak 7½' quadrangle, Yavapai County. Saussuritized anhedral to subhedral plagioclase (An_{32}) partly having normal zoning; anhedral to subhedral dark-green hornblende as much as 2 mm long; anhedral to subhedral biotite as much as 2 mm long; accessory opaque minerals and apatite; secondary sphene, epidote, and chlorite. Major-oxide and trace-element concentrations, table 5. Field No. A-111.
38. Gneissic biotite tonalite from pluton on east side of Bagdad metamorphic belt. Numerous inclusions of amphibolite and muscovite-biotite gneiss and some of biotite-quartz-feldspar gneiss 1 cm to 10 cm long in outcrop but not in sample. Outcrop in bottom of wash near west edge of the center of sec. 13, T. 13 N., R. 10 W., 530 m N. 74° E. from BM 2906; lat 34°28'06" N., long 113°15'05" W., Arrastra Mtn NE 7½' quadrangle, Yavapai County. Plagioclase (An_{32}) in locally bent and broken grains as much as 4 mm in diameter and in mosaic-textured areas with quartz; quartz as much as 1.5 mm in diameter but mostly in mosaic-textured aggregates; microcline as much as 2 mm in diameter and in mosaic-textured aggregates with quartz and plagioclase; synkinematic and postkinematic biotite as much as 2 mm long in aggregates—a few of the larger biotite grains are bent, and a minor amount of muscovite is intergrown with the biotite and is locally bent. Accessory opaque minerals, sphene, apatite, and zircon, and secondary chlorite from biotite. U-Pb zircon age determination, figure 15. Major-oxide and trace-element concentrations, table 5. Whole-rock and feldspar Pb-isotopic analysis, table 8. Field Nos. JW-85-63 and 1163.
39. Somewhat gneissose biotite granodiorite from outcrop in wash on section line 130 m west of SE corner sec. 23, T. 13 N., R. 8 W., lat 34°26'41" N., long 113°03'31" W., Malpais Mesa NE 7½' quadrangle, Yavapai County. Locally saussuritized plagioclase (An_{32}) as much as 2.7 mm in diameter; quartz 0.2–0.5 mm in diameter in mosaic-textured aggregates; anhedral microcline as much as 1 mm in diameter; synkinematic to postkinematic biotite as much as 2 mm long in aggregates; sparse muscovite, accessory allanite, opaque minerals, apatite, zircon, and sphene, and secondary epidote. Muscovite is partly contemporaneous with biotite and partly younger. Major-oxide and trace-element concentrations, table 5. Field No. A-85.
40. Muscovite-biotite granite from east-facing outcrop on Black Canyon Wash in SW¼ sec. 35, T. 12 N., R. 8 W., 760 m S. 27½° W. from spot elevation 2903; lat 34°20'08" N., long 113°04'20" W., Malpais Mesa 7½' quadrangle, Yavapai County. Coarser grained porphyritic granite phase in mixed unit containing fine-grained granite and migmatite. Potassic feldspars as much as 2 cm long in outcrop. Strained and locally broken grains of perthitic microcline as much as 1 cm long; anhedral to subhedral, slightly altered plagioclase (An_{27}) as much as 3.5 mm long; anhedral quartz as much as 2 mm in diameter; muscovite and biotite as much as 1.5 mm long; sparse myrmekite, accessory apatite, zircon, and opaque minerals, and secondary carbonate and chlorite. Major-oxide and trace-element concentrations, table 5. Field No. A-152.
41. Biotite-hornblende granodiorite from mafic phase of the Signal Granite. From outcrop in gully 700 m N. 24° W. from Signal triangulation point on Signal Mountain. SE¼ sec. 15, T. 13 N., R. 13 W., lat 34°27'58" N., long 113°36'11" W., Signal Mountain 7½' quadrangle, Mohave County. Anhedral quartz as much as 1.2 mm in diameter; anhedral to subhedral plagioclase (An_{32}) as much as 2.5 mm in diameter; anhedral microcline as much as 1.6 mm in diameter; anhedral green hornblende as much as 2.2 mm long; opaque minerals as much as 1 mm in diameter; anhedral biotite as much as 2.2 mm long; accessory sphene. Major-oxide and trace-element concentrations, table 6. Field No. NAP154.
42. Porphyritic hornblende-biotite granite from mafic phase of the Signal Granite on south side of Government Wash, 30 m east of fault contact with Tertiary arkosic sandstone and conglomerate. 520 m S. 33° E. of spot elevation 1792; NW¼NW¼ sec. 1, T. 12 N., R. 13 W., lat 34°24'51" N., long 113°34'19" W., Signal Mountain 7½' quadrangle, Mohave County. Anhedral quartz as much as 6 mm in diameter; anhedral to subhedral plagioclase (An_{29}) as much as 1 cm in diameter; anhedral to

subhedral microcline as much as 2 cm in diameter; anhedral biotite as much as 3 mm long in aggregates; anhedral green hornblende intergrown with biotite; accessory allanite, sphene, apatite, zircon, and opaque minerals. Major-oxide and trace-element concentrations, table 6. Field No. 876.

43. Hornblende-biotite granite from near the type locality of the Signal Granite. Outcrop on south side of wash, 200 m west of Big Sandy River; lat 34°27'17" N., long 113°37'38" W., Signal 7½' quadrangle, Mohave County. Anhedral quartz as much as 1 cm in diameter; anhedral to subhedral plagioclase (An_{38}) as much as 4 mm long; well-aligned subhedral to euhedral perthitic microcline as much as 6 cm long and 2 cm wide; biotite as much as 3 mm long as aggregates with hornblende; anhedral green hornblende as much as 3 mm long, sphene rimming opaque minerals and in anhedral to subhedral grains as much as 1.3 mm in diameter; accessory opaque minerals, apatite, and zircon. U-Pb zircon age determination, figure 16. Major-oxide and trace-element concentrations, table 6. Whole-rock and feldspar Pb-isotopic analysis, table 8. Field No. 1168.
44. Biotite granite from block on slope below outcrop. At contact of Signal Granite in NW¼ sec. 9, T. 13 N., R. 12 W.; 220 m N. 25° E. from Big Sandy Spring; lat 34°29'03" N., long 113°31'20" W., Signal Mountain 7½' quadrangle, Mohave County. Anhedral quartz as much as 3 mm diameter in aggregates that tend to surround feldspars; anhedral to subhedral plagioclase (An_{28}); perthitic potassic feldspar in grains as much as 2 cm in diameter; biotite as much as 1 mm long in aggregates as much as 4 mm long with or without hornblende; anhedral to subhedral dark-green hornblende as much as 2.5 mm long locally surrounded by biotite; sparse myrmekite and accessory allanite, zircon, sphene, apatite, and opaque minerals. U-Pb zircon age determination, figure 16. Major-oxide and trace-element concentrations, table 6. Feldspar Pb-isotopic analysis, table 8. Field Nos. JW-85-64 and 1164.
45. Coarse-grained porphyritic biotite granite containing phenocrysts of potassic feldspar 1–4 cm long from Signal Granite from 1,950' altitude in gully in SW½ sec. 10, T. 12 N., R. 13 W.; 750 m S. 82° W. of spot elevation 2278; lat 34°23'32" N., long 113°36'26" W., Signal Mountain 7½' quadrangle, Mohave County. Anhedral quartz as much as 5 mm long; anhedral plagioclase (An_{17}) as much as 6 mm long; subhedral microcline, anhedral brown biotite as much as 2 mm long, partly in aggregates; sparse dark olive-green hornblende and myrmekite, accessory sphene rimming opaque minerals, sphene, apatite, and zircon, and secondary sericite, carbonate minerals, and chlorite. Major-oxide and trace-element concentrations, table 6. Field No. 49a.
46. Coarse-grained leucocratic granite cutting the main phase of the Signal Granite. Outcrop at junction of two washes. SW¼ sec. 18, T. 13 N., R. 12 W.; 330 m S. 14° E. from spot elevation 2530, lat 34°27'50" N., long 113°33'30" W., Signal Mountain 7½' quadrangle, Mohave County. Anhedral quartz as much as 3 mm in diameter; anhedral to subhedral plagioclase (An_{33}) as much as 4 mm in diameter; anhedral perthitic microcline as much as 1 cm in diameter; anhedral biotite as much as 2 mm long in aggregates; accessory apatite, zircon, and opaque minerals. Major-oxide and trace-element concentrations, table 6. Field No. 467b.
47. Pyroxene-hornblende-biotite granodiorite (Ygd). From dump of adit NW¼ sec. 9, T. 13 N., R. 12 W. at adit symbol on Signal Mountain 7½' quadrangle. 470 m N. 35° W. from Big Sandy Spring; lat 34°29'08" N., long 113°31'33" W., Mohave County. Quartz in granophyric intergrowths with potassic feldspar; anhedral to euhedral, normally zoned plagioclase (An_{27-42}) as much as 2 mm long; very finely perthitic potassic feldspar; anhedral brown hornblende as much as 1.5 mm long; opaque mineral as much as 0.2 mm in diameter; monoclinic pyroxene mantled by hornblende; accessory zircon and apatite and secondary carbonate minerals. U-Pb zircon age determination, figure 16. Major-oxide and trace-element concentrations, table 6. Whole-rock and feldspar Pb-isotopic analysis, table 8. Field Nos. JW-84-10 and 390.
48. Hornblende-biotite granodiorite (Ygd). In wash 390 m S. 19½° W. from Big Sandy Spring. SW¼ sec. 9, T. 13 N., R. 12 W., lat 34°28'52" N., long 113°31'30" W., Signal Mountain 7½' quadrangle, Mohave County. Quartz as a 6.6-mm-diameter xenocryst and as round grains 0.02–0.05 mm in diameter in a matrix of alkali feldspar; euhedral to subhedral phenocrysts of normally zoned plagioclase (An_{23-32}) as much as 1 mm in diameter; anhedral biotite to 0.3 mm long; anhedral to subhedral green hornblende as much as 0.3 mm long; accessory epidote, allanite, apatite, sphene, and opaque minerals, and secondary carbonate minerals. Epidote apparently contemporaneous with biotite and hornblende. Major-oxide and trace-element concentrations, table 6. Field No. 1144.
49. Porphyritic biotite granite from the porphyritic granite phase of the granite of Olea Ranch. Outcrop by wash in Cottonwood Canyon, 320 m S. 43° W. of center sec. 35, T. 13 N., R. 10 W., lat 34°25'15" N., long 113°16'40" W., Arrastra Mtn NE 7½' quadrangle, Yavapai County. In outcrop granite contains a few lenses of pegmatite a few centimeters thick. Microcline as phenocrysts as much as 2 cm long; subhedral to anhedral, locally saussuritized and sericitized plagioclase (An_{30}) as much as 1.5 mm in diameter; anhedral quartz as much as 4 mm in diameter; anhedral to subhedral biotite as much as 1.2 mm long in aggregates; accessory apatite, allanite, opaque minerals, and zircon, and secondary epidote. Major-oxide and trace-element concentrations, table 7. Field No. 666.
50. Porphyritic biotite granite from the porphyritic granite phase of the granite of Olea Ranch containing potassic feldspar phenocrysts as much as 4 cm long in a medium-grained matrix. From large boulder in Cottonwood Wash, 720 m from E edge of Arrastra Mountain NE 7½' quadrangle, Yavapai County. 620 m S. 7° E. from spot elevation 3078; NW¼ sec. 1, T. 12 N., R. 10 W., lat 34°24'46" N., long 113°15'12" W. Anhedral quartz generally 0.3 mm in diameter but a few larger ones as much as 3 mm; anhedral to euhedral locally saussuritized plagioclase (An_{30})

as much as 2 mm in diameter; anhedral to euhedral perthitic microcline as much as 2 cm long; anhedral to subhedral biotite as much as 1.3 mm long aligned parallel to the potassic feldspar; sparse myrmekite, accessory allanite, zircon, apatite, and opaque minerals, and secondary epidote and chlorite. U-Pb zircon age determination, figure 16. Major-oxide and trace-element concentrations, table 7. Whole-rock and feldspar Pb-isotopic analysis, table 8. Field Nos. JW-84-13 and 752.

51. Coarse-grained biotite granite of the granite of Olea Ranch. Sample from unweathered remnant in roadcut on U.S. Highway 93, S edge sec. 8, T. 13 N., R. 10 W. 270 m W. of triangulation point 3376; lat 34°28'24" N., long 113°19'22" W., Arrastra Mtn NE 7½' quadrangle, Yavapai County. Mosaic-textured quartz with a grain size as much as 1 mm interstitial to feldspars; subhedral, partly saussuritized plagioclase (An_{17}) as much as 3 mm long; anhedral, somewhat perthitic microcline as much as 1 cm in diameter; green to brownish-green anhedral to subhedral biotite as much as 2 mm long; accessory sphene, apatite, and zircon, and secondary epidote, muscovite, and sericite. U-Pb zircon age determination, figure 16. Major-oxide and trace-element concentrations, table 7. Whole-rock and feldspar Pb-isotopic analysis, table 8. Field Nos. JW-84-15 and 753.
52. Porphyritic biotite granite from coarse-grained granite phase of the granite of Olea Ranch. Sample of spoil from excavation for power line tower site on crest of shoulder in west part of sec. 15, T. 13 N., R. 10 W.; 270 m N. 89° E. of spot elevation 3258, lat 34°27'57" N., long 113°17'59" W., Arrastra Mtn NE 7½' quadrangle, Yavapai County. Subhedral perthitic microcline as much as 2 cm long; anhedral to subhedral partly saussuritized and sericitized plagioclase (An_{27}) as much as 2 mm in diameter; anhedral quartz as much as 2 mm in diameter in mosaic-textured aggregates between feldspar grains; anhedral greenish-brown biotite in aggregates; sparse muscovite, accessory sphene, zircon, allanite, apatite, and opaque minerals, and secondary epidote. Major-oxide and trace-element concentrations, table 7. Field No. M72.
53. Porphyritic medium-grained biotite granite in the fine-grained phase of the granite of Olea Ranch from outcrop in wash in NE¼ sec. 16, T. 13 N., R. 11 W.; 170 m N. 31° W. of spot elevation 3183; lat 34°28'21" N., long 113°21'32" W., Arrastra Mtn NE 7½' quadrangle, Mohave County. From pluton of finer grained granite intruding coarse-grained granite. Anhedral quartz as much as 3 mm in diameter; subhedral to anhedral saussuritized plagioclase as much as 2 mm long; euhedral to anhedral microcline as much as 1 cm long; anhedral, partly chloritized biotite as much as 1.3 mm long; accessory opaque minerals, primary and secondary muscovite, and secondary epidote. Major-oxide and trace-element concentrations, table 7. Field No. 1160.
54. Megacrystic phase of the granite of Joshua Tree Parkway from a 2-m-diameter block in wash near windmill about 30 m down wash from location 55. SW¼ sec. 19, T. 11 N., R. 7 W., 300 m S. 53° E. of hill 3267; lat 34°16'45" N., long 113°02'13" W., Malpais Mesa 7½' quadrangle, Yavapai County. Quartz in mosaic-textured aggregates with a grain size of 1–3 mm between feldspar grains; anhedral to subhedral plagioclase (An_{25}) as much as 5 mm long; somewhat perthitic microcline as much as 4 cm long; anhedral dark-green hornblende as much as 2 mm long; anhedral biotite as much as 3.5 mm long; accessory sphene, apatite, allanite, zircon, and opaque minerals, and secondary chlorite from biotite. Mafic minerals are concentrated in clots as much as 1 cm long. U-Pb zircon age determination, figure 17. Major-oxide and trace-element concentrations, table 7. Feldspar Pb-isotopic analysis, table 8. Field No. A-151a.
55. Fine-grained biotite granite from the granite of Joshua Tree Parkway from outcrop containing a 0.2-m-long inclusion of megacrystic granite. SW¼ sec. 19, T. 11 N., R. 7 W.; 300 m S. 53° E. of hill 3267; lat 34°16'45" N., long 113°02'13" W., Malpais Mesa 7½' quadrangle, Yavapai County. Anhedral quartz as much as 1.5 mm in diameter; anhedral, locally saussuritized plagioclase as much as 1 mm in diameter; anhedral, weakly perthitic microcline as much as 2 mm in diameter; anhedral biotite as much as 1 mm long; accessory sphene, allanite, zircon, and opaque minerals and secondary chlorite from biotite. Major-oxide and trace-element concentrations, table 7. Field No. A-151b.
56. Medium-grained porphyritic biotite granite from float in wash 480 m N. 25° E. from center sec. 32, T. 13 N., R. 7 W., lat 34°25'40" N., long 113°00'45" W., Malpais Mesa NE 7½' quadrangle, Yavapai County. Typical of finer grained, porphyritic phase of the granite of Grayback Mountain. Anhedral microcline as much as 1 cm in diameter, anhedral quartz as much as 1.3 mm in diameter; anhedral to subhedral, locally saussuritized plagioclase (An_{15-20}) as much as 6 mm in diameter; anhedral biotite as much as 1.3 mm long; accessory sphene, opaque minerals, and allanite, and secondary epidote. Major-oxide and trace-element concentrations, table 7. Field No. A-107b.
57. Coarse-grained biotite granite from the granite of Grayback Mountain from roadcut on south side of where Arizona Highway 96 crosses Tank Wash. N. 9° E. of center sec. 22, T. 13 N., R. 7 W., lat 34°27'15" N., long 112°58'44" W., Hillside 7½' quadrangle, Yavapai County. Cut by sparse quartz-feldspar and biotite-quartz-feldspar pegmatites. Anhedral quartz as much as 2 mm but mostly about 1 mm in diameter in mosaic-textured masses interstitial to feldspars; subhedral, partly saussuritized plagioclase as much as 3.5 mm in diameter; perthitic microcline as much as 3 mm in diameter; anhedral biotite as much as 2 mm long in aggregates; accessory opaque minerals, allanite, apatite, and zircon, and secondary epidote and sericite from plagioclase and chlorite from biotite. Cut by a few thin shear zones containing sericite and epidote. U-Pb zircon age determination, figure 17. Major-oxide and trace-element concentrations, table 7. Feldspar Pb-isotopic analysis, table 8. Field No. A-153.
58. Medium-grained porphyritic granite intruding the coarse-grained granite unit east of the Signal batholith, in gully in NE¼ sec. 5, T. 12 N., R. 11 W., 1,070 m N. 4° E. from

spot elevation 3555; lat 34°24'53" N., long 113°25'21" W., Arrastra Mtn 7½' quadrangle, Mohave County. In outcrop contains microcline phenocrysts as much as 2 cm in diameter. In thin section anhedral quartz as much as 5 mm in diameter; anhedral to subhedral plagioclase (about An_{25}) as much as 2 mm in diameter; anhedral to subhedral microcline as much as 3 mm in diameter; anhedral biotite as much as 1 mm in diameter; sparse myrmekite and accessory sphene, zircon, and apatite. Whole-rock and feldspar Pb-isotopic analyses, table 8. Field No. W-295.

59. Coarse-grained porphyritic granite containing phenocrysts of potassic feldspar as much as 2 cm long in an elongate pluton in the coarse-grained granite east of the Signal batholith. From wash in NE¼ sec. 7, T. 12 N., R. 11 W., 1,020 m S. 67° W. from spot elevation 3555, lat 34°24'06" N., long 113°26'01 W., Arrastra Mtn 7½' quadrangle, Mohave County. No thin section available. Whole-rock and feldspar Pb-isotopic analyses, table 8. Field No. W-322.

60. Diabase in flat-lying sheet 2–3 m thick from wash NW¼ sec. 22, T. 13 N., R. 10 W., 210 m N. 37° W. from spot elevation 3168, lat 34°27'25" N., long 113°17'42" W., Arrastra Mtn NE 7½' quadrangle, Yavapai County. Plagioclase (An_{55-60}) with some normal zoning as nonoriented laths as much as 4 mm long; anhedral monoclinic pyroxene as much as 3.5 mm in diameter between the plagioclase laths; light-green actinolite and green chlorite from pyroxene; biotite to 0.6 mm long; opaque minerals as much as 1 mm in diameter. Major-oxide and trace-element concentrations, table 7. Field No. 1052.

61. Coarse-grained diabase from small plug not shown on published map (Bryant, 1995). From 70 m S. 81° W. from top of hill 3124, SW¼NW¼ sec. 14, T. 12 N., R. 8 W., lat 34°23'19" N., long 113°04'13" W., Malpais Mesa NE 7½' quadrangle, Yavapai County. Euhedral laths of plagioclase (An_{55-75}) as much as 3 mm long, anhedral to subhedral olivine as much as 2 mm in diameter, monoclinic pyroxene as much as 5 mm in diameter includes plagioclase laths. Accessory opaque minerals and secondary actinolite and biotite. Major-oxide and trace-element concentrations, table 7. Field No. A-91.

62. Diabase forming sill 2–3 m thick in coarse-grained granite. In wash east part sec. 1, T. 13 N., R. 13 W., 760 m S. 84° W. from spot elevation 3124; lat 34°29'31" N., long 113°34'08" W., Signal Mountain 7½' quadrangle, Mohave County. Thin section not available. Major-oxide and trace-element concentrations, table 7. Field No. G-38.

63. Diabase sheet 3–4 m thick dipping 10° SW. in wash southwest side of the Big Sandy River in Signal Canyon, NW¼ sec. 27, T. 13 N., R. 13 W., lat 34°26'22" N., long 113°36'32" W., Signal Mountain 7½' quadrangle, Mohave County. Plagioclase (An_{60}) in laths as much as 3 mm long; anhedral monoclinic pyroxene as much as 1 mm in diameter between the laths; amphibole and biotite from pyroxene, and opaque minerals. Major-oxide and trace-element concentrations, table 7. Field No. 852.

☆ U.S. GOVERNMENT PRINTING OFFICE: 2001 — 673-049 / 30049 Region No. 8

Selected Series of U.S. Geological Survey Publications

Books and Other Publications

Professional Papers report scientific data and interpretations of lasting scientific interest that cover all facets of USGS investigations and research.

Bulletins contain significant data and interpretations that are of lasting scientific interest but are generally more limited in scope or geographic coverage than Professional Papers.

Water-Supply Papers are comprehensive reports that present significant interpretative results of hydrologic investigations of wide interest to professional geologists, hydrologists, and engineers. The series covers investigations in all phases of hydrology, including hydrogeology, availability of water, quality of water, and use of water.

Circulars are reports of programmatic or scientific information of an ephemeral nature; many present important scientific information of wide popular interest. Circulars are distributed at no cost to the public.

Fact Sheets communicate a wide variety of timely information on USGS programs, projects, and research. They commonly address issues of public interest. Fact Sheets are generally two or four pages long and are distributed at no cost to the public.

Reports in the **Digital Data Series (DDS)** distribute large amounts of data through digital media, including compact disc read-only memory (CD-ROM). They are high-quality, interpretative publications designed as self-contained packages for viewing and interpreting data and typically contain data sets, software to view the data, and explanatory text.

Water-Resources Investigations Reports are papers of an interpretative nature made available to the public outside the formal USGS publications series. Copies are produced on request (unlike formal USGS publications) and are also available for public inspection at depositories indicated in USGS catalogs.

Open-File Reports can consist of basic data, preliminary reports, and a wide range of scientific documents on USGS investigations. Open-File Reports are designed for fast release and are available for public consultation at depositories.

Maps

Geologic Quadrangle Maps (GQ's) are multicolor geologic maps on topographic bases in 7.5- or 15-minute quadrangle formats (scales mainly 1:24,000 or 1:62,500) showing bedrock, surficial, or engineering geology. Maps generally include brief texts; some maps include structure and columnar sections only.

Geophysical Investigations Maps (GP's) are on topographic or planimetric bases at various scales. They show results of geophysical investigations using gravity, magnetic, seismic, or radioactivity surveys, which provide data on subsurface structures that are of economic or geologic significance.

Miscellaneous Investigations Series Maps or **Geologic Investigations Series (I's)** are on planimetric or topographic bases at various scales; they present a wide variety of format and subject matter. The series also includes 7.5-minute quadrangle photogeologic maps on planimetric bases and planetary maps.

Information Periodicals

Metal Industry Indicators (MII's) is a free monthly newsletter that analyzes and forecasts the economic health of five metal industries with composite leading and coincident indexes: primary metals, steel, copper, primary and secondary aluminum, and aluminum mill products.

Mineral Industry Surveys (MIS's) are free periodic statistical and economic reports designed to provide timely statistical data on production, distribution, stocks, and consumption of significant mineral commodities. The surveys are issued monthly, quarterly, annually, or at other regular intervals, depending on the need for current data. The MIS's are published by commodity as well as by State. A series of international MIS's is also available.

Published on an annual basis, **Mineral Commodity Summaries** is the earliest Government publication to furnish estimates covering nonfuel mineral industry data. Data sheets contain information on the domestic industry structure, Government programs, tariffs, and 5-year salient statistics for more than 90 individual minerals and materials.

The Minerals Yearbook discusses the performance of the worldwide minerals and materials industry during a calendar year, and it provides background information to assist in interpreting that performance. The Minerals Yearbook consists of three volumes. Volume I, Metals and Minerals, contains chapters about virtually all metallic and industrial mineral commodities important to the U.S. economy. Volume II, Area Reports: Domestic, contains a chapter on the minerals industry of each of the 50 States and Puerto Rico and the Administered Islands. Volume III, Area Reports: International, is published as four separate reports. These reports collectively contain the latest available mineral data on more than 190 foreign countries and discuss the importance of minerals to the economies of these nations and the United States.

Permanent Catalogs

"Publications of the U.S. Geological Survey, 1879–1961" and "Publications of the U.S. Geological Survey, 1962–1970" are available in paperback book form and as a set of microfiche.

"Publications of the U.S. Geological Survey, 1971–1981" is available in paperback book form (two volumes, publications listing and index) and as a set of microfiche.

Annual supplements for 1982, 1983, 1984, 1985, 1986, and subsequent years are available in paperback book form.

ISBN 0-607-96229-1